ENZYMATIC DEGRADATION OF PETROLEUM HYDROCARBONS (C_{10}-C_{50}) IN SALINE WATER ENVIRONMENTS

JEAN CARLOS VICCARI PEREIRA

A THESIS SUBMITTED TO
THE FACULTY OF GRADUATE STUDIES
IN PARTIAL FULFILMENT OF THE REQUIREMENTS
FOR THE DEGREE OF
MASTER OF APPLIED SCIENCE

GRADUATE PROGRAM IN CIVIL ENGINEERING
YORK UNIVERSITY
TORONTO, ONTARIO

AUGUST, 2024

© Jean Carlos Viccari Pereira, 2024

ABSTRACT

Along with the increasing exploration of oil and gas, the contamination of marine environments (0.6 M NaCl) with petroleum hydrocarbons has emerged as a significant environmental concern. Saline and hypersaline environments are linked to oil exploration and active petroleum seeps. These environments are considered the largest and ultimate sink for petroleum hydrocarbon pollution due to the nearby human activities. Among the technologies available for the remediation of such contaminants, the use of microorganisms or enzymes has been suggested as a viable approach for efficient and affordable removal from saline environments. This thesis investigates the enzymatic degradation of petroleum hydrocarbons (C10-C50) in saline water environments using *Alcanivorax borkumensis*. The first objective explores the production of alkane hydroxylase, esterase, and lipase by *A. borkumensis* under various salinities (0.3 M, 0.6 M, and 1.2 M NaCl) with diesel as the sole energy source. Results indicate effective degradation of short-chain alkenes and large-chain alkanes at specific salinities, although further research is needed to enhance enzyme stability and activity in high salinity conditions. The second objective evaluates the use of chitosan scaffolds for immobilizing *A. borkumensis* cells and enzymes to improve petroleum hydrocarbon degradation under brine (7% w/v NaCl) conditions of salinity. Scaffolds with a high degree of deacetylation produced by the freeze-casting method, when cross-linked with glutaraldehyde, showed enhanced stability and reduced protein release, achieving over 61% diesel degradation in brine conditions. The present thesis helped understand strategies for decontaminating diesel fuel at elevated salinities.

DEDICATION

This thesis is dedicated to my family for being there and for always supporting me and loving me.

"We have always defined ourselves by the ability to move beyond what is possible"

Interstellar

ACKNOWLEDGEMENTS

I would like to express my deepest gratitude to my supervisor, **Dr. Satinder Kaur Brar,** and my co-supervisor, **Dr. Siu Ning Leung**, for their unwavering support, insightful guidance, and invaluable expertise throughout this research. Their encouragement and mentorship have been instrumental in the completion of this thesis.

I am also deeply thankful to my mentor, **Dr. Carlos S. Osorio-González**, for the close guidance provided in the lab and for the friendship we developed throughout the program. Your constant support, both academically and personally, has significantly shaped my research and made this journey an enriching and memorable experience.

I wish to extend my sincere appreciation to the members of my revision committee, **Dr. Magdalena Krol** and **Dr. Luz Adriana Puentes Jácome** for their thorough evaluation, constructive feedback, and valuable insights. Their careful review and suggestions have greatly contributed to the refinement and quality of this thesis.

I am profoundly thankful to my family for their endless love, patience, and encouragement. Their belief in me has been a constant source of strength and motivation, especially during the most challenging moments of this journey.

I also wish to extend my sincere appreciation to my lab mates on the **Inzymes** team, especially my "hermano" **Diego Ospina**, for the camaraderie, intellectual discussions, and collaboration. The shared experiences and teamwork have made this journey both rewarding and enjoyable.

Special thanks go to the technicians, **Dr. Magdalena Jaklewicz** and **Dr. Stéphane Moïse**, for their technical support and assistance. Their expertise and dedication were essential in ensuring the smooth progress of my experiments.

Lastly, I am grateful to the Natural Sciences and Engineering Research Council (NSERC) of Canada Discovery Grants, Alliance Mission, and the James and Joanne Love Chair in Environmental Engineering for providing the financial support and resources necessary to carry out this research. Without their assistance, this work would not have been possible. To everyone who has contributed in some way to the success of this thesis, thank you!

TABLE OF CONTENTS

ABSTRACT ii
DEDICATION iii
ACKNOWLEDGEMENTS iv
TABLE OF CONTENTS v
LIST OF TABLES vii
LIST OF FIGURES viii
ABBREVIATIONS ix
PUBLICATIONS WITHIN THIS THESIS x
PUBLICATIONS OUTSIDE OF THIS THESIS xi
CONFERENCES xii
CHAPTER ONE: BACKGROUND 1
1. INTRODUCTION 2
CHAPTER TWO: LITERATURE REVIEW 6
2. REVIEW OF LITERATURE 7
2.1. Sources and diversity of halophilic microorganisms used for PHCs degradation 7
2.2. Degradation of PHCs by haloenzymes 15
2.3. Effect of salinity on PHCs biodegradation 20
2.3.1. Slightly halophilic enzymes (2-5% NaCl) 20
2.3.2. Moderate and extreme halophilic enzymes (5-30% NaCl) 20
2.4 Fundamental challenges and future research needs 22
2.4.1 Expression of functional genes and enzyme activity 22
2.4.2. Enhanced bioremediation through biotechnological advances 24
2.5 RESEARCH GAPS 27
2.6 HYPOTHESES 27
2.7 OBJECTIVES 28
2.8 ORIGINALITY 28
CHAPTER THREE: SALINITY EFFECT ON THE ENZYMATIC ACTIVITY AND DIESEL FUEL DEGRADATION BY *Alcanivorax borkumensis* SK2 29
3.1 Salinity effect on enzymatic activities and diesel fuel degradation by *Alcanivorax borkumensis* SK2 30
Abstract 30
Introduction 31

Materials and methods.....32

Results and discussion.....35

Conclusion.....48

CHAPTER FOUR: IMMOBILIZATION OF ENZYMES FOR THE BIODEGRADATION OF PETROLEUM HYDROCARBONS IN SALINE WATER ENVIRONMENT.....50

4.1 Chitosan-based scaffold for improvement of *A. borkumensis* activity and biodegradation of diesel fuel at brine conditions.....51

Abstract.....51

Introduction.....52

Material and methods.....53

Results and discussion.....58

Conclusion.....71

5. CONCLUSIONS.....72

6. RECOMMENDATIONS.....72

BIBLIOGRAPHY.....74

APPENDICES.....86

APPENDIX A. Supplementary information of section 3.....86

APPENDIX B - Supplementary information of section 4.....101

LIST OF TABLES

Table 2: Solubilities of PHCs present in crude oil and adverse health effects from exposure. Adapted from [21]. 7
Table 2.1: Examples of halophilic bacteria with hydrocarbon-degrading ability 13
Table 3: Analysis of metabolites formed due to diesel fuel biodegradation by *A. borkumensis* SK2 at different salinities 44
Table 3.1: Analysis of metabolites produced in response to salinity 48

LIST OF FIGURES

Figure 2: The distribution of halophiles exhibits a wide range of diversity across the three domains of life. Adapted from [35]. Groups highlighted in red contain a minimum of one halophilic representative shown in different colours. 9
Figure 2.1: Mechanism of alkanes oxidation by alkane hydroxylase. 16
Figure 2.2.: Transformation of aromatic compounds by catechol 1,2 and 2,3-dioxygenases. 17
Figure 3: Performance of *A. borkumensis* under high salinity conditions. (a) Microbial growth; (b) total protein content. Brackish: 1.9% w/v NaCl; Saline: 3.5% w/v NaCl; Brine: 7% w/v NaCl. 37
Figure 3.1: Maximum enzyme activity at different salinities concentrations and respective time to achieve it. Brackish: 1.9% w/v NaCl (positive control); Saline: 3.5% w/v NaCl; Brine: 7% w/v NaCl. 39
Figure 4: Top view of chitosan scaffolds produced at different degree of deacetylations and freezing temperatures 59
Figure 4.1: Thermogravimetry curves 30-800 ºC. (a) 85%, (b) 95% and (c) 95.6% degree of deacetylation 60
Figure 4.2: Thermogravimetry curves 30-100 ºC. (d) 85% DD, (e) 95% DD and (f) 95.6% DD. 60
Figure 4.3: SEM images of cross-section and longitudinal section of (a, b and c) Ch80 scaffold, (e, f, and g) Ch20 scaffold and (g) Ch196 scaffold (with details of fractured material). 62
Figure 4.4: Brunauer-Emmett-Teller (BET) surface area and pore diameter for Ch20 and Ch80. 64
Figure 4.5: Total protein released at t = 48h and T = 168h. T1: scaffold-immobilized enzyme; T2: scaffold-immobilized enzyme cross-linked with 0.02% GTA; T3: scaffold-immobilized bacteria; T4: scaffold-immobilized bacteria cross-linked with 0.02% GTA and T5= free *A. borkumensis* cells. 65
Figure 4.6: Maximum enzyme activity of T5 at 120 h and respective activity for different microcosms. T1: scaffold-immobilized enzyme; T2: scaffold-immobilized enzyme cross-linked with 0.02% GTA; T3: scaffold-immobilized bacteria; T4: scaffold-immobilized bacteria cross-linked with 0.02% GTA and T5= free *A. borkumensis* cells. 68
Figure 4.7: Degradative capability (expressed as C10-C50 petroleum hydrocarbons residue) of different microcosms T1: scaffold-immobilized enzyme; T2: scaffold-immobilized enzyme cross-linked with 0.02% GTA; T3: scaffold-immobilized bacteria; T4: scaffold-immobilized bacteria cross-linked with 0.02% GTA and T5= free *A. borkumensis* cells. 69

ABBREVIATIONS

4-HBA – 4-hydroxy-benzoic acid
BET – Brunauer-Emmett-Teller
BTEX – Benzene, Toluene, Ethylbenzene, Xylene
C120 – Catechol 1,2-dioxygenase
C230 – Catechol 2,3-dioxygenase
CHAPS – 3-[(3-Cholamidopropyl)dimethylammonio]-1-propanesulfonate
DD – Degree of deacetylation
DMSO – Dimethyl sulfoxide
DSMZ – Deutsche Sammlung von Mikroorganismen und Zellkulturen (German Collection of Microorganisms and Cell Cultures)
DWH – Deepwater Horizon
GC-FID – Gas Chromatography Flame Ionization Detection
GC-MS – Gas Chromatography-Mass Spectrometry
GDO – Gentisate 1,2-dioxygenase
GTA – Glutaraldehyde
HCB – Hydrocarbonoclastic Bacteria
MB – Marine Broth
MCP – Methyl-accepting chemotaxis protein
MOFs – Metal-organic frameworks
MWCO – Molecular Weight Cut-Off
NaCl – Sodium chloride
NADH – Nicotinamide adenine dinucleotide (reduced form)
OHCB – Obligate hydrocarbonoclastic bacteria
OPW – Oilfield-produced water
PAHs – Polyaromatic hydrocarbons
PHCs – Petroleum hydrocarbons
RHD – Ring-hydroxylating dioxygenase
SEM – Scanning electron microcopy
TCA – Tricarboxylic acid cycle
USA – United States of America
UV – Ultraviolet
2,4-DTBP – 2,4-Di-tert-butylphenol

PUBLICATIONS WITHIN THIS THESIS

Jean Carlos Viccari Pereira, Carlos S. Osorio-Gonzalez, Saba Miri, Satinder Kaur Brar (2023). Petroleum hydrocarbons bioremediation by halotolerant enzymes – Progress & advances. Journal of Environmental Chemical Engineering, 12:111726. https://doi.org/10.1016/j.jece.2023.111726

PUBLICATIONS OUTSIDE OF THIS THESIS

Jean Carlos Viccari Pereira, Rahul Saini and Satinder Kaur Brar (2024). Biohydrogen Production by Photosynthetic Microorganisms. In: Soccol, C.R., Brar, S.K., Permaul, K., Pakshirajan, K., de Carvalho, J.C. (eds) Biohydrogen - Advances and Processes. Biofuel and Biorefinery Technologies, vol 13. Springer, Cham. https://doi.org/10.1007/978-3-031-49818-3_6

Diego Alejandro Hernandez-Ospina, **Jean Carlos Viccari Pereira**, Carlos Saul Osorio-González and Satinder Kaur Brar (2024). Microbial Indicators for Monitoring Pollution and Bioremediation. In: Kumar, A., Singh, J., De Azevedo, L.C.B. (eds) Microbiome-Based Decontamination of Environmental Pollutants. Elsevier. https://doi.org/10.1016/B978-0-443-21781-4.00012-8

Diego Alejandro Hernandez-Ospina, **Jean Carlos Viccari Pereira**, Reema Kumar and Satinder Kaur Brar (2023). Bisphenol A and Bis (2-ethylhexyl) Adipate releases from different facilities across Canada.
Retrieved from the Environment and Climate Change Canada website: https://www.canada.ca/content/dam/eccc/documents/pdf/npri-/NPRI%20Project%20Final%20Report%20-%20Diego%2c%20Reema%2c%20Jean.pdf

.

CONFERENCES

Pereira J., Osorio-González C.S., Brar S.K. (2023). Effect of salinity on enzymes produced by *Alcanivorax borkumensis* using diesel as a model substrate. International conference of the global Network on Persistent, Emerging and Organic Pollution in the Environment, August 9, 2023, Concordia University, Quebec, Canada. *Accepted*.

Pereira J., Osorio-González C.S., Leung S.N, Brar S.K. (2024). Enzyme production by *Alcanivorax Borkumensis* for diesel contaminated water. World Water Congress & Exhibition, August 12, 2024, Toronto, Ontario, Canada. *Accepted*.

CHAPTER ONE: BACKGROUND

1. INTRODUCTION

Petroleum hydrocarbons (PHCs) are an essential constituent of fossil fuel energy resources, and their consumption has witnessed a substantial surge in recent decades because of the worldwide growth in population and industrialization [1]. In addition, they are by far the most important raw materials for a wide range of products such as fuel, synthetic polymers, and petrochemicals [2]. Along with their increasing consumption, the contamination of marine environments with PHCs has emerged as a significant environmental concern. The primary cause of this contamination includes oil spills, transportation by the sea, waste burnouts, industrial effluent discharges, and sediment drilling activities [3], [4]. Saline and hypersaline environments are linked to oil exploration and active petroleum seeps. These environments are considered the primary and ultimate repositories for PHC pollution resulting from nearby human activities [5]. In broader terms, saline and brine environments are classified by the sodium chloride (NaCl) concentrations exceeding 1% and in seawater 3 to 3.5%, resulting in an additional challenge to implement bioremediation strategies [6],[7],[8]. Therefore, the development of technologies for the efficient remediation/decontamination of those sites is needed. Several attempts have been made to treat hypersaline wastewater contaminated with PHCs. For instance, physical and chemical methods such as incineration, *in situ* burning, base-catalyzed dechlorination, UV oxidation, coagulation, fixation, adsorption, filtration, and dispersants have been used [9]. Although these technologies are available, existing research recognizes several drawbacks in their practical applications including costs. For instance, mechanical methods such as skimming are strictly limited by weather conditions and require a quick response after the oil spill event [7]. Similarly, thermal methods such as *in-situ* burning oblige a toxicity assessment

because incomplete combustion may result in the production of carcinogenic compounds [10]. Additionally, the chemical compositions of commercial dispersants employed in physicochemical methods contain hazardous compounds, including salts such like organic sulfonic acid and propylene glycol that are considered highly toxic to the marine ecosystem [11],[12]. In contrast, an increasing number of studies acknowledge the significance of bioremediation as a viable approach for efficiently and affordably eliminating petroleum hydrocarbons from saline environments [13],[14].

Bioremediation using microorganisms is a natural, economical, and efficient way to convert PHCs into less toxic compounds relying on biological processes [13],[14]. Although bioremediation is very promising, one of the main obstacles and concerns in recent studies is the application under saline and hypersaline conditions, which can adversely affect the employed microorganisms [5],[15],[16]. The slow rate of petroleum hydrocarbons biodegradation can be attributed to the extreme environmental conditions [17] damaging mainly the cell membrane, with the concomitant loss of intracellular water and enzyme denaturation [10], [18].

Bioremediation of petroleum hydrocarbons could be potentially ameliorated by the use of enzymes instead of whole microorganisms. Enzymatic applications may be appropriate in sites where rapid bioremediation is required and to prevent an antagonistic effect on the native microbiome [19]. Recently, biotechnological improvements such as the use of halotolerant enzymes in conjunction with immobilization methods have opened new possibilities to overcome practical barriers and increase bioremediation effectiveness. Attributes of these enzymes such as higher resistance towards denaturation and catalysis ability in aqueous or solid environments are beneficial to extend their applications during the waste treatment from oil deposits [20]. The high solubility in environments with high

salt concentration due to the negatively charged surface proteins, thermal stability, and increased hydrophobicity of haloenzymes contributes to the hydrocarbon uptake [21] in high salinities and make them excellent agents for the bioremediation of saline-petroleum contaminated environments. In the last decade, several reports have characterized halotolerant enzymes including dioxygenases such as catechol 1,2-dioxygenase, 3,4-dihydroxyphenylacetate or protocatechuate 3,4-dioxygenase that contribute to the breakdown of aromatic compounds in saline environments [22],[23],[24]. However, the information about their feasibility and use in bioremediation in saline environments is very limited. Most of the existing literature has been focused on PHCs biodegradation using whole-cell. Thus, a clear understanding of how halotolerant enzymes contribute to PHCs biodegradation in saline environments is necessary.

This dissertation examines the effect of salinity on enzyme production and diesel fuel biodegradation by the halotolerant bacteria *Alcanivorax borkumensis* SK2. Chapter 2 (Literature Review) includes the most important aspects to be considered for the biodegradation of PHCs by halotolerant enzymes. A discussion on the characteristics of haloenzymes and the strategies that are used by these enzymes to resist saline conditions is presented. Additionally, the chapter addresses the challenges of using haloenzymes for bioremediation and explores potential methods to enhance their efficiency, particularly through the use of advanced materials for enzyme immobilization.

Based on the literature review, the research gaps, hypothesis, objectives, and originality of the study are identified.

In Chapter 4, the thesis provides an analysis of salinity effect on the growth and enzymatic activity of *Alcanivorax borkumensis* using diesel as an energy source. Lastly, Chapter 5 presents a novel approach to enhance enzyme stability and diesel degradation at higher

salinities using an immobilized system. In summary, this thesis enhances the knowledge and strategies for decontaminating petroleum hydrocarbons in environments with elevated salinities.

CHAPTER TWO: LITERATURE REVIEW

2. REVIEW OF LITERATURE

2.1. Sources and diversity of halophilic microorganisms used for PHCs degradation

Halophiles belong to a diverse group of extremophilic microorganisms (including *Archaea*, Bacteria, and Eukaryote domains) that can grow in saline and hypersaline environments, as depicted in Figure 1. Based on their sodium chloride (NaCl) requirements, they can be classified into three main groups: slightly, moderately and extreme halophiles tolerant with a sodium chloride-based concentration of 2-5% (w/v), 5-20 % (w/v) and 20-30% (w/v), respectively [21]. Because of the ubiquitous presence of halophiles in marine environments, they are constantly vulnerable to PHC pollution. PHCs encompass a wide spectrum of individual hydrocarbons and possess the potential for toxicity and carcinogenicity. They can be categorized into four principal structural groups: alkanes, cycloalkanes, alkenes, and aromatics. A significant number of PHCs have been reported as exhibiting persistence in marine environments. Noteworthy examples (Table 2) encompass aliphatic compounds like alkanes, tetracosane, and octadecane [24],[25],[26] as well as polycyclic aromatic hydrocarbons (PAHs) such as pyrene, phenanthrene, phenol and BTEX [27], [28], [29].

Table 2. Solubilities of PHCs present in crude oil and adverse health effects from exposure. Adapted from [21].

Category	**Example Compound**	**Solubility in water (mg L^{-1} at 20°C)**	**Dose (mg L^{-1})**	**Toxicological effect**
Alkanes	n-hexanes	9.5	10-100	Neurological disorders
Cycloalkanes	Naphthalene	30	0.0007	Respiratory epithelial adenomas and olfactory epithelial neuroblastomas
Alkenes	Ethene	131	950000	Depression of the central nervous system
Aromatics	Benzene	1750	10-100	Respiratory, hematological,

Category	Example Compound	Solubility in water (mg L^{-1} at 20°C)	Dose (mg L^{-1})	Toxicological effect
				dermal, and neurological disorders
			10,000 – 100,000	Death
			10 – 100	Immunological and lymphoid disorders
			1	Hematological, immunological, and lymphoid disorders

The majority of PHC degrading species belong to the *Halomonadaceae* and *Halobacteriaceae* families. Notable examples (Figure 1) from the *Halobacteriaceae* family include *Haloferax*, *Natromonas*, *Halobacterium*, *Haloarcula*, and *Natrialba* [30], [31]. Conversely, the *Halomonadaceae* family is renowned for its association with *Halomonas*. In the last decades, halophilic archaea have been isolated from salterns, coastal waters, and lakes with a salt tolerance of up to 30% (w/v) [32]. Notably, halophiles from the genera, such as *Halobacterium, Marinobacter, Alcanivorax, Haloferax, Haloarcula,* and *Halomonas* have demonstrated proficiency in the degradation of PHCs [33]. Several studies have highlighted the role of *Halomonas* and *Marinobacter* in the bioremediation of alkanes and crude oil in hypersaline waters, with *Halomonas* being considered a model organism for halophilism and commonly enriched in oil-rich seawater. Additionally, recent studies have focused on the aerobic degradation of PAHs by *Halomonas* species [34].

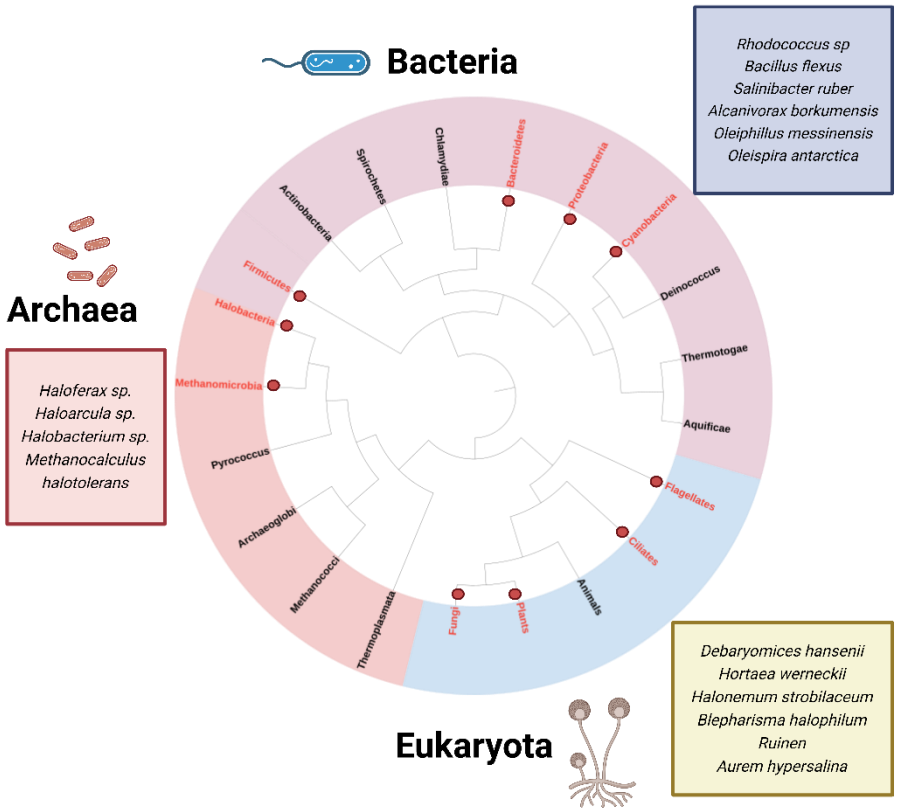


Figure 2. The distribution of halophiles exhibits a wide range of diversity across the three domains of life. Adapted from [35]. Groups highlighted in red contain a minimum of one halophilic representative shown in different colours.

The Haloferax genus accounts for several isolates known to degrade aromatic hydrocarbons. For instance, Bonfá et al. (2011) [36] isolated 10 strains related to *Haloferax alexandrinus*, *Haloferax prahovense* and *Haloferax sulfurifontis* from five environments classified as hypersalines. The isolated strains demonstrated the ability to degrade more than 50% of model compounds (naphthalene, anthracene, phenanthrene, pyrene and benzo[a]anthracene) under 20% (w/v) NaCl conditions. Likewise, it has been reported that *Haloferax mucosum* strain isolated from salterns collected from the Dead Sea degraded 100 mg L^{-1} of naphthalene after 384 h [37]. The authors found the optimum 3.5 M NaCl concentration for the degradation of naphthalene. Similarly, *Halobacterium salinarum* isolates collected from Turkey also showed the ability to use pyrene, phenanthrene, and

naphthalene (20-200 mg L^{-1}) as an energy source at 20% NaCl (seawater media) [38]. In the work conducted by Al-Mailem et al. (2015) [30], isolated species were obtained from the Persian Gulf. This strain exhibited the capability to degrade up to 70% of crude oil under 3.3 M of NaCl. More recently, phylogenetic analysis of sediment samples from Rozel Point at Great Salt Lake (USA) revealed that *Halobacterium* strains degraded more than 90% and 75% of the initial concentration of benzoate (2.5 mM) and 4-hydroxy-benzoic acid (4-HBA) (2 mM), in the presence of 4 M and 5 M of NaCl [39]. In addition, phylogenetic analyses of the gammaproteobacteria reveal a significant and varied assemblage of obligate hydrocarbonoclastic bacteria (OHCB) present in marine ecosystems that have been exposed to oil contamination. Halotolerant members from *Alcanivorax, Oleiphilus, Oleispira*, and *Thalassolitus* genus are capable of degrading linear or branched saturated hydrocarbons and a minor number of PAHs. For instance, *Alcanivorax* sp. is considered a microorganism moderately halophilic, with optimal growth at NaCl concentrations between 30 and 100 g/L. Moreover, this microorganism exhibits a wide-range of adaptive capacity to utilize oils across various temperatures and salinities as well as some studies investigated the capability of this genera to degrade aliphatic hydrocarbons in saline environments. The highest and most critical oil spill on record, was at the Gulf of Mexico by the Deepwater Horizon (DWH), in which a considerable number of *Alcanivorax* species was revealed in both surface slick and plume water samples [32]. Additional research aiming to identify genes of hydrocarbon degradation pathways after the DWH spill also found naphthalene degrading communities of *Alcanivorax*. This underscores a wider capability within this genus to degrade alkanes and PAHs [40]. These findings together indicate the potential of *Alcanivorax* to contribute to the bacterial microbiome capable of degrading PAHs. Previous research showed that *Alcanivorax*

borkumensis could produce enzymes such as alkane hydroxylase and lipases, capable of degrading petroleum compounds [41]. As for *Oleiphilus* genera, the messinensis family represented by *Oleiphilus messinensis* strain found in seawater samples contains alkane-1-monooxygenase gene and other proteins equivalent to alkane hydroxylase (AlkB1) of *Alcanivorax borkumensis* SK2 [42]. Similarly, the strain growth on n-hexadecane is optimum at NaCl concentration between 2.5 and 5.0% [42],[43]. Moreover, *Oleispira antarctica* from Antarctic superficial seawater samples also showed an increase in growth at a NaCl concentration of up to 5% (w/v) [44]. Comparably, *Thalassolitus* isolates grow using alkanes as an energy source, with an optimal NaCl concentration of 2.7% [45]. In addition, a new halophilic strain named *Thalassospira* sp. TSL5-1 isolated from the Yellow Sea in China showed to be an effective strain to degrade PAHs (pyrene) in 25 days, with optimal NaCl concentrations ranging from 3.5% to 5% [46]. These studies found a convergence between the optimum NaCl concentration (3-5% w/v NaCl) for the metabolism of saturated and PAH by OHCB via phthalate or salicylic acid routes. Gomes et al. (2018) [47] isolated several strains capable of degrading hydrocarbons. Under a concentration of 9% of NaCl, the genus *Idiomarina* showed significant degradation of phenanthrene, pyrene, and benzopyrene (64%, 58%, and 60%, respectively) after 20 days of monitoring. Similarly, *Bacillus, Brevibacterium, Modicisalibacter* and *Nitratreductor* showed affinity to degrade aromatic hydrocarbons (phenanthrene, pyrene, benzopyrene, naphthalene and phenol) with *Modicisalibacter* sp degrading 100% of phenol. According to this study, these species preferentially degrade aromatic compounds over saturated hydrocarbons [47].

Table 1.1 shows that the majority of PHCs-degrading species isolated from diverse

environments, exhibit a preference for moderate NaCl concentrations. These species demonstrate optimal growth in media containing between 5% to 20% NaCl by mass, highlighting their remarkable ability to degrade PHCs in naturally occurring saline environments. Conversely, the genus archaea stands out as hyper-halophiles and grows in substrates having NaCl at concentrations higher than 20%. Isolation and characterization studies specializing in halophiles and their enzymes from saline environments are relatively scarce. Existing literature has reported that hydrocarbon degradation in environments with high salinity is linked to the enzymes and intermediate products found in non-halophiles [10]. For instance, both halophilic and non-halophilic microorganisms have been found to exhibit the presence of intermediate products related to ring oxidation and ring cleavage mechanisms, exemplified by catechol during aromatic hydrocarbon degradation [22]. However, there is a lack of information on the mechanisms of bioremediation of PHCs in saline environments using haloenzymes.

Table 1.1. Examples of halophilic bacteria with hydrocarbon-degrading ability.

Microorganism	Enzyme	Salinity (%)	Compound	Removal	Reference
Halomonas titanicae *Marinobacter lutaoensis*	Alkane1-monooxygenase	10%	Crude oil	75%	[48]
Marinobacter sp.	Ring-hydroxylating dioxygenase	10%	Phenanthrene	75%	[49]
Halomonas shengliensis and *Halomonas smyrnensis*	Mono or dioxygenases	20%	Pyrene	50%	[27]
Halomonas desertis	Alkane hydroxylase and dioxygenase	10%	Crude oil and phenanthrene	92.2 and 89.0% of alkanes and PAHs, respectively.	[29]
Alcanivorax sp.	Alkane monooxygenase	9%	Octadecane and crude oil	100% of octadecane after 4 days and 100% crude oil after 15 days	[25]
	Alkane monooxygenase	5%	Tetracosane	90% tetracosane in 20 days	[50]
	Alkane monooxygenase	10%	Tetracosane and octacosane	60% tetracosane and 65% octacosane after 2 weeks	[26]
	Alkane monooxygenase	20%	Crude oil (n-alkanes)	95% after 20 days	[51]
Acinetobacter sp.	Alkane hydroxylase	12%	Crude oil	95.8% in 10 days	[52]
	NR	7%	Alkanes	51.7% after 14 days of incubation	[53]

Microorganism	Enzyme	Salinity (%)	Compound	Removal	Reference
	Cathecol 2,3-dioxygenase	7%	BTEX	100% degradation of benzene, toluene and ethylbenzene after 12 days	[28]
Natrialba sp.	Catechol 1,2-dioxygenase	25%	Phenol, naphthalene and pyrene	NR	[54]
	Catechol 1,2-dioxygenase	25%	Oil-contaminated saline water	NR	[31]
Haloferax sp.	Alkane monooxygenases and dioxygenases	22%	Crude oil	Crude oil 47%, octadecane 67%, phenanthrene 30% after 3 weeks	[55]

NR: Not reported

2.2. Degradation of PHCs by haloenzymes

The enzymes from halobacteria are a key example of the adaption of macromolecules to saline environments. Enzymes from halophiles not only differ from their non-halophilic counterparts in the sense of salt tolerance, but also most cases, they require the presence of salts (>0,2 M) to be stable. Previous research has established that their molecular halo-adaptation relies on two primary features: i) a substantial overabundance of acidic amino acids (especially aspartic acid, lysine and asparagine) and, ii) a diminished proportion of hydrophobic amino acids (including phenylalanine, isoleucine, and leucine). In the first case, the negative charge conferred by the acidic amino acids attracts water molecules, hydrating the proteins by forming hydrogen bonds [20]. In terms of the second characteristic, the protein molecules exhibit weak hydrophobic interactions due to their low content of hydrophobic residues. These two features enable halophilic enzymes to maintain the structural stability required at high salt concentrations [35].

Although several studies have investigated the degradation paths and the involved enzymes in the oxidation of PHCs in non-halophiles [56], [57] there is a paucity of literature concerning the intricate mechanisms underpinning the aerobic metabolism of petroleum-derived compounds within halophilic organisms. The initial stage in the aerobic degradation of alkanes by bacteria is catalyzed by oxygenases, specifically alkane hydroxylases (Figure 2.1). The hydroxylation of alkanes ranging from C5 to C16 is orchestrated by two distinct categories of enzymes: the non-heme iron alkane hydroxylases (AlkB) embedded within the integral membrane, and the alkane hydroxylases from the cytochrome P450 CYP153 family [58]. For alkanes with long carbon chains (>C_{18}), enzymes such as flavoprotein-dependent LadA and flavin-binding monooxygenase (AlmA) facilitate their efficient degradation [58].

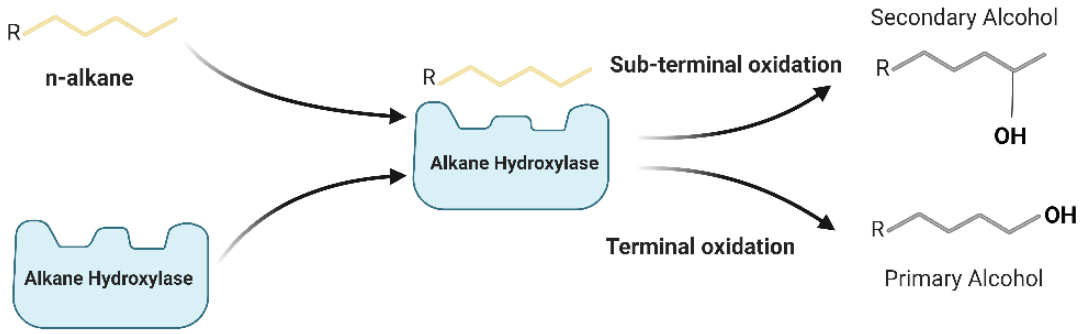


Figure 1.1. Mechanism of alkanes oxidation by alkane hydroxylase.

Likewise, aromatic hydrocarbon degradation under aerobic conditions consists of aromatic ring oxidation by monooxygenases or dioxygenases. Previous studies suggest that the first intermediates generated by monooxygenases (gentisate, catechol, and protocatechuate) further cleaved into two different orientations (*ortho* or *meta* dioxygenases). The meta-cleavage of catechol is facilitated by the enzymatic action of catechol 2,3-dioxygenase, whereas its ortho-cleavage is orchestrated by catechol 1,2-dioxygenase (Figure 2.2). Ultimately, this metabolic pathway involves the integration of succinyl-CoA and acetyl-CoA molecules into the Krebs cycle [24].

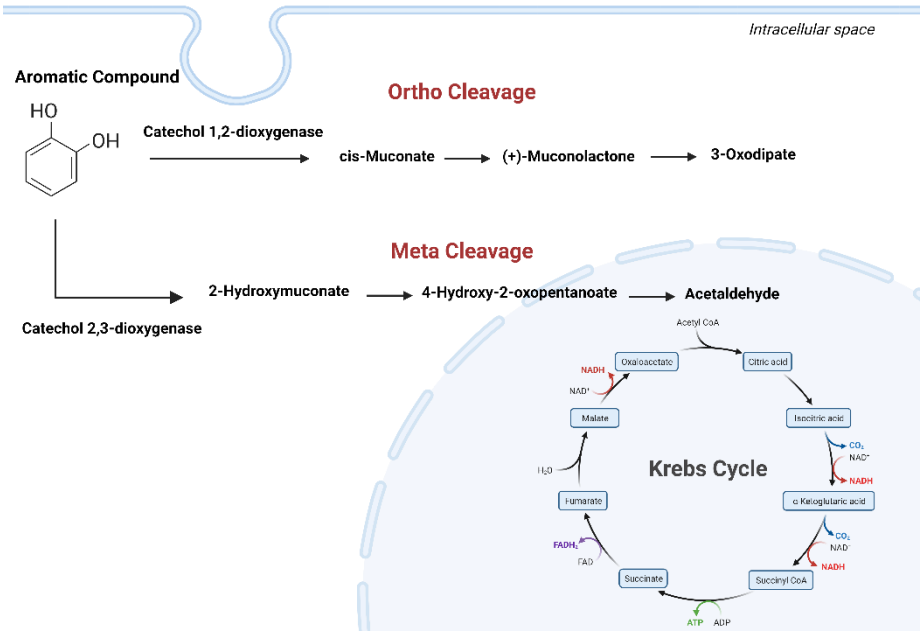


Figure 2.2. Transformation of aromatic compounds by catechol 1,2 and 2,3-dioxygenases.

Nevertheless, the literature on metabolic routes of hydrocarbon degradation in saline environments is limited. For instance, monooxygenase enzymes play a dual role in the biochemical progression: they are involved not only in the initial phase of alkane oxidation but also in the conclusive phase of ω-hydroxy fatty acid oxidation within crude oil substrates [48]. Likewise, the authors found that *Marinobacter lutaoensis* encodes two forms of monooxygenase: the nonheme iron-containing AlkB and AlmA (flavin-dependent); although *Halomonas titanicae* TAT1 only possesses the AlkB [48].

According to Wang et al. (2018) [49], the phenanthrene degradation metabolic route evidenced in a halophilic consortium demonstrated that *Marinobacter* spp. played a role in the upstream degradation using ring-hydroxylating dioxygenase, especially at high salt concentrations. Subsequently, *Halomonas* spp. degraded catechol using catechol 1,2-dioxygenase.

Afterward, Neifar et al. (2019) [29] characterized the genes for phenanthrene degradation

in *Halomonas desertis*. Briefly, degradation underwent a 3,4-dioxygenation reaction that produced cis-3,4-dihydroxy-3,4-dihydrophenanthrene. Subsequently, this compound undergoes enzymatic dehydrogenation to form 3,4-dihydroxy phenanthrene. Later, the diol group is cleaved through ortho or meta configurations into naphthalene-1,2-diol to enter into the tricarboxylic acid cycle (TCA).

Similarly, Budiyanto et al. (2018) [27] identified intermediates of pyrene-degrading in *Halomonas* spp. and showed evidence of aromatic group cleavage using mono or dioxygenases. Nevertheless, no report is available describing the involved enzymes at initial or subsequent degradation steps.

Hassan et al. (2018) [28] studied the catechol 2,3-dioxygenase genes from three *Pseudomonas* strains (HA10, HA12 and HA14) with the capacity to degrade BTEX at 7% (w/v) of NaCl. They found differences between the three strains regarding the ability to grow in mono and polyaromatic hydrocarbon, in which only HA10 can grow on both types of compounds. This observation implies that each strain may possess distinct genes responsible for the oxidation of different aromatic molecules, as evidenced by the unique genetic profiles and enzyme activity patterns observed in each strain. Further studies using molecular tools are required to elucidate the specific genes and mechanisms driving these differences among different strains. Besides, in the absence of NaCl it was observed that the three strains were unable to utilize BTEX as an energy source. This suggests that the isolated *Pseudomonas* strains have a strict dependency on NaCl, requiring a minimum concentration of 1.5% for BTEX degradation.

These findings are similar to those reported by SadrAzodi et al. (2019) [26], in which the alkB gene from *Alcanivorax* shows a remarkable phylogenetic difference in comparison with the *Pseudomonas* strain. According to the authors, the unique alkB gene and its

function of the alkane hydroxylase may have contributed to the selective biodegradation of long-chain alkanes by the strain. Similarly, it appears that individual genes within each strain are accountable for the oxidation of distinct alkane molecules.

Hassanshahian et al. (2016) [59] studied the alkane monooxygenase dynamics during crude oil biodegradation by *Alcanivorax borkumensis* SK2 in natural seawater. The results showed that the proportion of alk-B1 was positively correlated to the concentration of crude oil [59]. Likewise, as demonstrated by Liu et al. (2010) [25], the activation of the alkB gene expression occurred in response to octadecane exposure within a NaCl concentration range of 20-90 g/L. According to their findings, *Alcanivorax* sp. 2B5 exhibited the capability to degrade C13–C30 n-alkanes present in crude oil, whereas *P. fluorescens* KOB241 harboring the pCom8-alkB gene was unable to thrive on C12 and C13 n-alkanes. This discrepancy indicated the potential existence of alternative alkane hydroxylases in *Alcanivorax* sp. 2B5, contributing to the degradation of both shorter and longer chain alkanes [25].

To delve into the preliminary responses exhibited by *Alcanivorax* species in the presence of alkanes, Wang and Shao (2014) [60] generated a random genome mutation library for *Alcanivorax dieselolei* B5. Through this approach, they identified genes within bacterial mutants that displayed irregular growth patterns when subjected to various alkanes. Notably, the authors unveiled the essential role of the outer membrane protein OmpS in alkane degradation. This protein served as a signalling conduit and emerged as the primary sensor of extracellular alkanes, instigating the subsequent activation of alkane-sensing chemotaxis complex proteins CheA/CheW and methyl-accepting chemotaxis protein (MCP). Consequently, the CheW protein conveyed the alkane stimulus to the regulatory system, culminating in the induction of cytochrome or terminal oxidase expression (Cyo), responsible for initiating the transport of long-chain alkanes and the respective oxidation by

the alkane hydroxylase AlmA. Nevertheless, researchers have not yet studied the mechanisms of Cyo expression.

2.3. Effect of salinity on PHCs biodegradation

2.3.1. Slightly halophilic enzymes (2-5% NaCl)

The halotolerant properties of enzymes from slightly halophilic bacteria remain an area that requires further research to fully understand their potential . For instance, Wang et al. (2017) [61] proposed that the halotolerant property of a newly cloned ring-hydroxylating dioxygenase (RHD) from phenanthrene degrading *Marinobacter* species may result from horizontal gene transfer between mesophiles and halophiles and consequent evolutionary process towards salinity adaptation. The authors found a pool of genes responsible for the PAHs degradation (hpah), originating from nah-related clusters in mesophiles. The expression of the RHD in hpad revealed halotolerant properties of the hpah-related enzyme. For instance, an excess of amino acids (aspartic, glutamic, and cysteic acids) at the protein surface, provided evidence of a gene transfer event and evolution towards saline adaptation. Comparably, Akbari et al. (2021) [62] demonstrated the heightened expression of genes associated with the degradation of hydrocarbons within a microbial community when subjected to saline environmental conditions of up to 5% (w/v) NaCl, highlighting the expression of alkane hydroxylases genes in *Dietzia maris* with the salinity increase. In addition, it was observed that the increase in salt concentrations from 2.5% to 5% (w/v) without the addition of nutrients resulted in higher expression of cyp153 and alkB during diesel (68 µL) and hexadecane (2 µL) degradation.

2.3.2. Moderate and extreme halophilic enzymes (5-30% NaCl)

As of now, there is limited available information concerning the pathways and impact of extreme salinity concentration on the enzymatic biodegradation of hydrocarbons. Guo et al.

(2016) [63] showed that the NaCl content changes the degradation pathway of a halophilic consortium. They found that when the salt content increased by 10% (w/v), the activity of catechol 1,2- dioxygenase (C120) was higher than catechol 2,3 dioxygenase (C230). The authors suggested the oxidation of catechol by catechol 1,2-dioxygenase and catechol 2,3-dioxygenase under a salt concentration of 20% and 10% (w/v), respectively. With the increase in salinity, the authors also observed a lower PAHs dioxygenase (PDO) activity. During phenanthrene degradation, a higher accumulation of phenolic compounds at higher salinities was found, which further inhibited phenanthrene degradation. Nevertheless, when 0.02% yeast extract was introduced at a NaCl content of 20%, it resulted in an enhancement of both the biodegradation rate and the activities of PDO, C12O, and C23O. These findings align with previous research that has established the additional nutritional requirements of halophilic bacteria at high salt concentrations. It has been established that yeast extract serves as a stimulant for the growth of halophiles [35]. Similar results were reported by Fang et al. (2016) [64] when the authors studied a naphthalene dioxygenase enzyme from *Halomonas*, *Alcanivorax*, *Marinobacter*, *Idiomarina*, *Martelella* bacterial consortium during phenanthrene degradation at several NaCl concentrations. The authors found that at 25% (w/v) NaCl, the strains utilized yeast, which contributed to their ability to withstand long-term exposure to phenanthrene. While the functional genes of naphthalene dioxygenase demonstrated stability within ranges of 20% NaCl concentration, the degradation activity may experience inhibition due to the decreased bioavailability of phenanthrene and the heightened energy demand necessary to uphold the osmotic balance of the bacterial consortium.

The molecular mechanism of haloarchaeal genus has yet to be elucidated and the understanding of the biodegradation of long-chain alkanes is very limited. For instance,

Halorientalis hydrocarbonoclasticus IM1011 has a β-oxidation pathway for hexadecane degradation [65]. The enzyme activity of 3-hydroxyacyl-CoA dehydrogenase suggests the presence of a β-oxidation pathway in the haloarchaeal strain. Likewise, a study performed using *Haloferax mediterranei* in how the strain response to the NaCl increase showed that 3-hydroxyacyl-CoA dehydrogenase was upregulated by 1.36-fold with an increase in NaCl concentration up to 250 g/L [66]. Similarly, *Natrialba sp.* C21 utilized the ortho-cleavage pathway during the biodegradation of pyrene, naphthalene, and phenol via catechol 1,2-dioxygenase in the presence of 25% NaCl concentration [54].

Overall, the presented findings contribute to the understanding of the role of enzymes during petroleum hydrocarbons degradation within saline environments. Consequently, further investigations are necessary to explore the potential of different enzymes in saline environments. As previously discussed, several enzymes have been observed to be upregulated under increased salinity conditions, highlighting the need for in-depth studies on more oxidative enzymes, particularly for the degradation of long-chain alkenes.

2.4. Fundamental challenges and future research needs

2.4.1. Expression of functional genes and enzyme activity

The special features and traits of haloenzymes such as highly acidic residues on their surfaces to tolerate high salt concentrations make them excellent candidates for the bioremediation of PHCs in saline environments. For this reason, extensive research has been done on the overexpression of functional genes to enhance the production of haloenzymes for bioremediation applications. For instance, Huang et al. (2015) [67] overexpressed the gentisate 1,2-dioxygenase (GDO) gene, as a key intermediate during the microbial degradation of PAHs by *Martelella AD-3* expressed in *E. coli.* The maximum enzyme activity was observed at 12% (w/v) of NaCl content, where the authors observed that the

amino acid sequence of *Martelella* AD-3 GDO contains 16.7% more acidic residues (glutamic acid and aspartic acid) in comparison to the GDO of *Haloferax* sp. D1227. This suggested a positive association between the acidic residue content and the optimum enzyme activity. Nonetheless, the modifications that halophilic proteins have undergone to survive in high salt environments within or outside of halophilic cells make it challenging to overexpress these proteins in common heterologous hosts such as *E. coli* [68]. Nevertheless, haloarchaeal proteins aggregate when they are expressed in *E. coli,* due to the lower salt concentrations within the host cells, which can disrupt the correct folding of these proteins. Nonetheless, many opportunities still exist for the use of haloarchaea as a host to overexpress and produce haloenzymes [18]. For instance, Allers (2010) [69] reported the overexpression mechanism and protein purification of halophilic enzymes in *Haloferax volcanii*. Likewise, hydrolytic enzymes, specifically lipases and esterases derived from halophilic archaea can also be used. These enzymes exhibit optimal activity at high salt concentrations, making them ideal candidates for applications related to hydrocarbon degradation. Lipase, in particular, can serve as a valuable biochemical and biological indicator for assessing the efficiency of hydrocarbon degradation processes [70].

Difficulties may arise, however, in applying the recombinant hydrolytic enzymes from haloarchaea at mesophilic temperature, since most of the haloarchaeal enzymes show optimal activity only at temperatures higher than 40ºC [68]. However, recent studies by Tutuncu et al. (2019) [71] identified a novel esterase from *Halomonas gudaonensis*, named hAGEst (first halophile-recombinant enzyme) that was isolated from a hypersaline lake (7.5% w/v) and recombinantly produced with a maximum activity at 30ºC. As an outstanding feature for application in marine environments, it is interesting to note that at low temperatures (5°C to 10°C) only 50% of the enzyme activity was used. Maintaining

enzyme activity at low temperatures is an important feature of oil bioremediation in the ocean. During oil spills, oil droplets are spread from the seawater surface into the water column at different temperatures (0-10ºC). Hence, the application of enzymes in deep ocean bioremediation exposes them to abrupt temperature fluctuations, underscoring the significance of their capacity to retain activity at lower temperatures.

2.4.2. Enhanced bioremediation through biotechnological advances

Free enzymes are more susceptible to hydraulic shear stress and may require replenishment after contact with pollutants as they can lose their reactivity after a single use. Therefore, more stable enzymes are required for use in saline environments. To overcome the practical barriers associated with salinity, which can negatively affect halotolerant enzymes due to inhibitors, potential denaturation, and increased costs, studies have explored immobilizing various haloenzymes on different supports. These efforts have resulted in notable improvements, making them a suitable alternative for industrial applications [68]. However, the literature on halotolerant enzyme immobilization for bioremediation purposes is very limited. For instance, researchers employed the enzyme alcohol dehydrogenase derived from the halophilic archaeon *Haloferax volcanii* (HvADH2) and covalently immobilized it onto metal-derivatized epoxy Sepabeads® [72]. Due to the inherent comparatively diminished hydrophobic core of halophilic enzymes, the investigators strategically generated a notably hydrophilic vicinity surrounding the relatively weaker hydrophobic core using ethylamine. This meticulous approach served to mitigate unspecific interactions between the enzyme core and the support matrix. It engendered a propitious microenvironment wherein the halophilic enzyme could attain enhanced structural stability, conformational integrity, and heightened thermal activity [72]. This would be particularly interesting for the application of halophilic enzymes in transient environments such as

supra-tidal zones, which experience important changes between sessions (mainly in temperature and salinity) from moderate (3-4%) to extreme (16%) daily variations [5]. These outcomes show that cross-linking immobilization is a potential method to be used to increase the stability and activity of halophilic enzymes even in supra-tidal zones, which according to Abou et al. (2020) [7] are commonly exposed to oil spills. Likewise, previous research employed the ionotropic gelation method utilizing chitosan to nano-encapsulate alkane hydroxylase and lipase from *Alcanivorax borkumensis*, with hexadecane serving as the alkane substrate. The obtained result showed a remaining enzyme activity of 70% even after four days [73].

Recent development of support materials to immobilize enzymes have been increasingly using nanomaterials. Moreover, 3D printing technologies may open new avenues for the application of haloenzymes in bioremediation. One of the main advantages of this technique is the lower cost of a quick prototype fabrication [74]. Common and inexpensive materials suggested include metal-organic frameworks (MOFs), hydrogels, and polylactic acids [75]. The suitability of a material as a carrier is determined by its ability to exhibit favourable flow properties and enable the printer to generate a wide range of optimal shapes and structures. This attribute makes it highly applicable in scenarios involving high hydraulic shear stress, such as aquatic environments [74]. Despite the enhanced rheological properties of hydrogels and polylactic acids, their application in bioremediation is still scarce, possibly due to their poor mechanical properties which would cause the leakage of the enzyme. In contrast, Carucci et al. (2018) [76] devised a method for immobilizing hyperhalophilic alcohol dehydrogenase within a MOF material under *in situ* conditions. These conditions encompassed an aqueous solution with a neutral pH, conducted at room temperature. The process of encapsulating the enzyme within the MOF matrix yielded a resilient milieu that

afforded stability to the enzyme. This stability was notable as it enabled the enzyme to sustain its catalytic activity even when exposed to reduced salt concentrations, specifically those below 223. 7 g/L. It is suggested that the reduction in KCl needs may be caused by the electrostatic interactions between the enzyme, characterized by an excess of negative charge attributable to its elevated acidic amino acid composition, and the inherent ionic attributes of the MOF. The clustering of acid residues on the halophilic enzyme surface repels each other electrostatically. However, this effect is balanced by the K^+ ions that shield the enzyme surface and prevent them from unfolding. Therefore, the MOF may potentially work as an alternative stabilizing compound influencing K^+ ions, thereby establishing a conducive ion-pair milieu, favouring enzyme stability. Further research is required to analyze new types of materials as carriers, especially those with proven biocompatibility such as biopolymers.

As biocatalysts produced by ubiquitous microorganisms in saline environments that are closely associated with petroleum hydrocarbon contamination, halotolerant enzymes are valuable models for understanding the biodegradation of PHCs under salt stress. As discussed earlier, the mechanisms of PHCs degradation by halophiles are similar to their non-halophilic counterparts, however, only a few researchers studied the effects of salinity on the activity of PHCs-degrading enzymes. The precise mechanisms of haloenzymes in treating PHCs remain to be elucidated. Further research with putative genes that encode enzymes for PHC degradation at different salinities needs to be carried out to comprehend how they are coordinated and regulated. Further work should be conducted to simulate the dynamics of marine environments and mimic real-world oil spill scenarios, as most studies have only been conducted using synthetic wastewater. Continued efforts are needed to improve the salt tolerance of haloenzymes through the use of genetic engineering. However,

challenges such as the expression efficiency of functional genes in non-halophiles remain to be overcome. Besides, there are still obstacles that need to be addressed, such as improving the efficiency of functional gene expression in organisms that are not tolerant of high salt concentrations. Further studies in enzyme encapsulation techniques are required, such as the use of biodegradable and biocompatible carriers, that could offer new possibilities for using haloenzymes to remediate PHCs in harsh environments.

2.5. Research gaps

The distinct features of halotolerant enzymes and biotechnological improvement methods such as immobilization are some of the most important tools to enhance the bioremediation rate of petroleum hydrocarbons in saline waters. However, certain problems need to be addressed for an effective clean-up of petroleum hydrocarbons in saline waters:

1. The understanding of halotolerant enzymes for bioremediation purposes is still at its early stage. Most of the existing relevant studies in saline environments assessed only the effect of salinity on the growth of halophilic bacteria. *Studies evaluating the effect of salinity on the growth of bacteria, enzyme activity and petroleum hydrocarbon degradation are limited.*

2. Halotolerant enzymes have mainly found applications in the food industry for their ability to withstand high salinity levels, both in terms of their utilization and immobilization. *There is a limited number of applied biocatalysts for petroleum hydrocarbon biodegradation.* Thus, immobilization systems and studies of halotolerant enzymes to enhance stability under increased salinity conditions can help advance the research in the right direction.

2.6. Hypotheses

To meet the need for effective decontamination of petroleum hydrocarbons in saline environments, it is necessary to prove the following hypotheses:

Hypothesis I: *Alcanivorax borkumensis* produces salt-tolerant enzymes in saline

conditions, which can be effectively applied to diesel-contaminated water at brine conditions of salinity. .

Hypothesis II: Immobilization of target enzymes on a suitable carrier can enhance the enzyme stability and degradability of diesel in saline water.

2.7. Objectives

To demonstrate the hypotheses aforementioned, the following specific objectives have been pursued:

Objective I: Study of alkane hydroxylase, esterase and lipase production by *Alcanivorax borkumensis* in saline water environments.

Objective II: Evaluate the immobilization of whole cells and crude enzymes of *Alcanivorax borkumensis* using porous chitosan carriers and covalent binding to biodegrade petroleum hydrocarbons (C10-C50) in saline water.

2.8. Originality

"Enhanced biodegradation of diesel-contaminated saline water using immobilized whole-cell and salt-tolerant enzyme systems". The thesis presents a novel approach to enhance enzyme stability and diesel degradation at higher salinities using a porous chitosan scaffold. The novel approach combines oil absorption and biological degradation using an enzyme-immobilized system for the *in situ* degradation of PHCs in saline environments. The proposed approach reduces or eliminates costs related to the transfer, treatment, and disposal of oil spills.

CHAPTER THREE: SALINITY EFFECT ON THE ENZYMATIC ACTIVITY AND DIESEL FUEL DEGRADATION BY *Alcanivorax borkumensis* SK2

3.1. Salinity effect on enzymatic activities and diesel fuel degradation by *Alcanivorax borkumensis* SK2

Jean Viccari Pereira[1], Carlos S. Osorio-González[1], SN Leung[2], Satinder K Brar[1*]

[1]Department of Civil Engineering, Lassonde School of Engineering, York University, North York, Toronto, M3J 1P3, Ontario, Canada

[2]Department of Mechanical Engineering, Lassonde School of Engineering, York University, North York, Toronto, M3J 1P3, Ontario, Canada

*Corresponding author: satinder.brar@lassonde.yorku.ca

Abstract

Halotolerant bacteria are important allies in the bioremediation of contaminating fuels within hypersaline environments, where such pollutants pose significant environmental challenges. This work focuses on the study of diesel fuel toxicity to the oil-degrading bacteria *Alcanivorax borkumensis* SK2 under three salinity conditions (0.3 M,0.6 M, and 1.2 M, respectively) using diesel as the only energy source (10% v/v). The results showed that *A. borkumensis* can grow and degrade shorth chain alkenes at 1.2 MNaCl concentration. In addition, large-chain and branched alkanes present in diesel fuel (10% v:v) were degraded within 72 hours without lag time at saline conditions (0.6 M NaCl). Enzyme assays showed that additional research is required to enhance enzyme activity and stability in salt brine (1.2 M NaCl) conditions for the degradation of petroleum hydrocarbons. This study offers novel insights into the decontamination of petroleum hydrocarbons in saline environments by halotolerant bacteria.

Keywords Halotolerant bacteria; Petroleum hydrocarbons; Salinity; Alkane hydroxylase; Biosurfactants

Introduction

Saline (<1% NaCl) and brine (>3.5% NaCl) environments are linked to oil exploration and active petroleum seeps. These environments are the primary and ultimate repositories for PHC pollution resulting from nearby human activities related to oil exploration and transportation by oil tanks. Recent statistics indicate that 2.95 billion tonnes of crude oil and petroleum products are shipped annually in the ocean. Among all global fleets, 98.8% of them rely on conventional fuels such as diesel for transportation [77]. Diesel fuel is considered a critical environmental contaminant and has garnered attention due to its detrimental toxic effects on humans, as well as on the ecosystem [78]. Diesel comprises a blend of hydrocarbons such as aliphatic constituents within the C10–C19 (~64%), olefinic components (1–2%), and aromatic compounds (~35%) [79].

In this context, several attempts have been made to treat ocean oil spills contaminated with petroleum hydrocarbons (PHCs) using mechanical and physicochemical methods such as incineration, *in situ* burning, base-catalyzed dichlorination, UV oxidation, coagulation, fixation, adsorption, filtration, and dispersants [9], [10]. However, chemical methods require toxicity assessment due to the formation of carcinogenic byproducts and mechanical methods are strictly limited to weather conditions [10]. Furthermore, complete degradation relies on biological processes by indigenous hydrocarbonoclastic bacteria (HCB) in the contaminated areas [11], [14]. During the last decade, alternative biological processes to remove PHCs from different environments have been increased. For instance, oil-degrading bacteria with halotolerant characteristics such as *Alcanivorax borkumensis* have demonstrated several advantages to degrade various hydrocarbons in marine environments [80],[81]. *A. borkumensis* can thrive at NaCl concentrations from 30 to 100 g L^{-1} and utilize various hydrocarbons due to its alkane hydroxylase system, consisting in AlkB1 and AlkB2

[80]. AlkB1 oxidizes medium-chain alkanes from C5 to C12 and AlkB2 medium-to-large chain alkanes ranging from C8 to more than C30. Hydrolytic enzymes such as lipase and esterase are also produced and serve as valuable biochemical indicators for assessing the efficiency of hydrocarbon degradation processes as they disrupt major chemical bonds and facilitate the degradation [41]. In addition, a glycine-glucolipid biosurfactant produced by the strain facilitates the hydrocarbon uptake within an emulsified droplet [82].

Salinity plays an important role in *A. borkumensis* as it uses Na^+ pumps to facilitate and increase the nutrient uptake [82]. Thus, their metabolic features and osmoregulation mechanisms make them excellent candidates for bioremediation of saline environments. However, studies evaluating the effect of salinity on *A. borkumensis* SK2 growth, enzyme production, and diesel degradation are limited. The understanding of these factors broadens the application of hydrocarbonoclastic bacteria, including the use of crude enzymes for PHCs saline-contaminated sites. Using enzymes for bioremediation has several advantages over whole microbial cells, including the ability to degrade contaminants in a shorter treatment period in harsh environments, high specificity for the pollutant, and no environmental risk. The main aim of the present study is to investigate the salinity effect on diesel degradation and on the production and enzyme activity of alkane hydroxylase, lipase and esterase.

Materials and methods

Bacterial strain and inoculum preparation

Alcanivorax borkumensis strain SK2 (DSMZ 11573) was procured from the Leibniz Institute DSMZ (Germany). Marine broth (MB) consisted (g/L): peptone 5, yeast extract 1, ferric-citrate 0.10, $MgCl_2$ 5.90, Na_2SO_4 3.24, $CaCl_2$ 1.80, KCl 0.55, $NaHCO_3$ 0.16, KBr 0.08, $SrCl_2$ 0.034 mg, H_3BO_3 0.022 mg, Na-silicate 0.004 mg, NaF 0.0024 mg, $(NH_4)NO_3$

0.0016 mg, Na_2HPO_4 0.008 mg, 0.3 M NaCl, and pH of 7.6 was used for bacterial preservation and inoculum preparation. For inoculum preparation, the strain was pre-cultured for up to two generations in a shaker incubator at 150 rpm and 30±1°C for 48 h.

Salinity effect on the performance of *A. borkumensis* during diesel degradation

To study the effect of salinity in *A. borkumensis* SK2 performance during diesel degradation two sodium chloride concentrations were used 0.6 M (saline conditions), 1.2 M (brine conditions) and 0.3 M NaCl was used as positive control. The media was supplemented with 10% (v:v) of commercial diesel as the sole carbon source and inoculated with 3% (v:v) of the inoculum seed to an initial 0.1 OD_{600nm}. The growth was monitored at 30±1°C, 150 rpm for 72 hours. Diesel fuel concentration mimics the conditions of an oil spill (high C/N ratio). All experiments were conducted in duplicate.

Analytical methods

Microbial growth

Growth was monitored by measuring the optical density at 600_{nm}. Briefly, 1 mL samples were taken every 8 h and centrifuged at 4°C for 10 min at 5000 ×g. After centrifugation, the microbial biomass was washed with 0.05 M phosphate buffer (pH=7) two times under the previous centrifuge conditions to remove the excess diesel. Microbial biomass was used for alkane hydroxylase assays and the supernatant was reserved at 4°C for soluble protein analysis.

Total protein concentration

Total protein concentration was determined according to the standard Bradford method [83]. Briefly, a 1 mL sample was mixed with Coomassie blue dye and the shift of absorbance (595 nm) during protein determination was recorded.

Alkane hydroxylase assay

Alkane hydroxylase activity was assessed according to Mishra and Singh (2012) [84], and Jauhari et al. (2014) [85]. *A. borkumensis* cell pellet was sonicated by using two frequencies (22 kHz and 30 kHz) for 6 min at 4°C using 1 mL of Tris-HCl buffer with a pH of 7.4 (20 mmol). After sonication, the mixture was centrifuged at 13000 ×g for 20 min at 4ºC and the supernatant was used as a crude enzyme for enzyme activity determination. The crude enzyme (50 µL) assay was carried out in 935 µL of 20 mmol L^{-1} of Tris-HCl buffer (pH of 7.4) and 0.15% (v:v) of CHAPS lysis buffer ($C_{32}H_{58}N_2O_7S$). A solution of diesel fuel (1% v:v) and 10 µL DMSO (80% v:v) was used as a substrate. The addition of 5 µL of NADH (0.1 mmol L^{-1}) initiated the reaction, and the reduction of absorbance was measured at 340 nm. One unit of alkane hydroxylase activity was determined as the amount of enzyme necessary to oxidize 1 µmol of NADH per minute.

Lipase assay

The supernatant (crude enzyme solution) was used for lipase enzyme activity determination. 30 mg of p-nitrophenyl palmitate was diluted in 10 mL of isopropanol:acetonitrile solution (4/1 v:v) after mixing with a solution of 90 mL of 0.05 M Sorensen phosphate buffer (pH 8.0), containing 1% w/v of $CaCl_2$, 4% v/w of Triton X-100, 0.2% w/v of gum Arabic. Consequently, both solutions were mixed and incubated in a water bath at 60°C until the solution became transparent. Then, 960 µL of the pre-warmed substrate solution (37 °C) was mixed with 40 µL of the crude enzyme solution. After 15 min of incubation at 37 °C, the enzyme activity was evaluated at 410 nm against an enzyme-free control. One unit of lipase activity was defined as 1 µmol of the p-nitrophenol released per minute.

Esterase assay

Similarly to the lipase determination, the supernatant (crude enzyme solution) was used for esterase enzyme activity determination. A reaction mixture was prepared by mixing 980 µL of 4-nitrophenyl acetate (1.12 mM), 50 mM potassium phosphate buffer (pH 7) with 11.3 mM sodium deoxycholate and 0.43 M of tetrahydrofuran. After that, 20 µL of the sample was added to the reaction mixture and monitored against a blank solution for 15 min at room temperature. One unit of esterase activity was defined as the amount of esterase required to release 1 µmol of p-nitrophenol in one minute, under the specified conditions.

Degradation analysis

Gas Chromatography-Mass Spectrometry (GC-MS) was used to evaluate diesel fuel transformation by *A. borkumensis*. 500 µL sample taken at different intervals of *A. borkumensis* culture (16 h, 32 h, 48 h, 64 h, 72 h) grown on diesel was diluted with hexane to 1.1 mL. The prepared samples were analyzed by a Thermo Trace 1310 gas chromatograph coupled to a Thermo ISQ mass detector. The gas chromatograph was equipped with a 30 m length, 0.25 mm internal diameter, and 0.25 µm film thickness capillary column (Make: Restek). Sample injection was carried out at 330°C in splitless mode. The oven temperature ramped from 80°C to 330°C at a rate of 10°C per minute, with a final temperature hold for 10 minutes. Mass spectrometry detection covered a mass range of 100 to 400 m/z.

Results and discussion

Growth of *A. borkumensis* and protein production

Figure 3 shows the performance of *A. borkumensis* SK2 growth and protein concentration under high salinity content. A similar trend was observed in the growth despite the salinity concentration. Notably, at 72h, growth in the presence of 1.2 M NaCl surpassed that of the positive control in contrast to earlier findings where no growth of *A. borkumensis* was observed using 1% (v:v) *n*-dodecane at 1 M NaCl [86]. In addition, Deng et al. (2024) [87]

explored the growth of *A. borkumensis* in NaCl concentration up to 2.5 M NaCl using 2% (v:v) motor oil as a carbon source. A maximum growth of OD_{600} = 1.7 at 0.9 M NaCl concentration was found whereas the present study shows a slightly lower growth (OD_{600} = 1.5) but with higher NaCl concentration (1.2 M). This trend is mainly because of the carbon source (i.e., diesel), which is a preference for metabolizing a diverse mixture of hydrocarbons over a single carbon source has been observed by *Alcanivorax borkumensis* SK2, as suggested by earlier reports [80],[88],[89]. In this context, the robustness of *A. borkumensis* to growth in elevated salinities (1.2 M NaCl) is likely attributed to the composition of diesel fuel. In addition to short- and long-chain alkanes, diesel contains a mixture of cycloalkanes and isoprenoids."

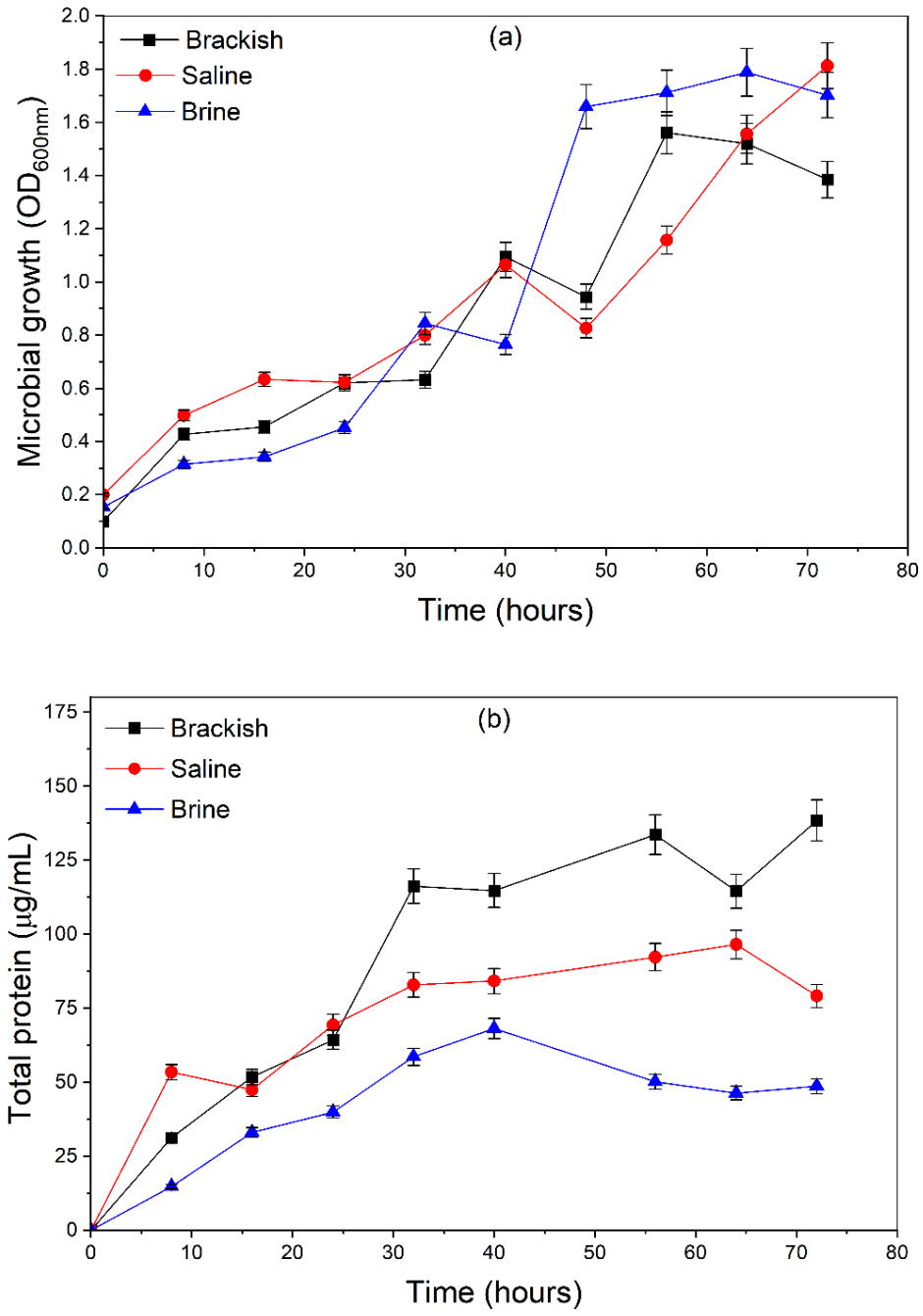


Figure 3. Performance of *A. borkumensis* under high salinity conditions. (a) Microbial growth; (b) total protein content. Brackish: 0.3 MNaCl; Saline: 0.6 M NaCl; Brine: 1.2 M NaCl.

Figure 3b shows the total protein content of *A. borkumensis* under high salinity concentrations. Overall, a decreasing trend in the protein content was observed when the salinity increased in the treatment. A maximum protein concentration at 1.2 M and 0.6 M of NaCl was 68. 2 µg/mL and 96.5 µg/mL, respectively, being 51% and 30.3% lower than the positive control. As previously suggested, the adaptation of halotolerant bacteria to increased salinities occurs in two phases (lag and exponential phases) [35],[90].

In the first phase (lag), it is well known that most cellular functions, such as amino acid transport and protein synthesis are initiated, and the bacteria are in an adaptation period to the cultivation conditions. During this adaptation period, cells are prone to starvation and delayed growth, accompanied by protein production. These proteins help the cells adjust to the high salinity environment by producing osmolytes, which balance the internal and external osmotic pressure. It has been reported that *A. borkumensis* produces ectoine in response to salt stress [91]. However, this protective mechanism requires substantial energy, which may account for the observed lag phase during the first 10 hours (data not shown). In the second phase (exponential), a rapid increase in protein production was observed up to 40 hours, after that, negligible changes in protein production were observed. In this case, the salinity concentration has a significant effect during the protein production rather than the microbial growth (Figure 3a and 3b). Notwithstanding, the total protein production under brine conditions (1.2 M NaCl) in this work (68. 2 µg/mL) surpassed the results reported by Nekouei and Nekouei (2017) [92] and Kadri et al. (2018) [93] with a maximum concentration of 30 µg/mL, and 20 µg/mL, using hexadecane (5% v:v) and motor oil (3% v:v) at 0.3 M NaCl respectively.

Notably, *A. borkumensis* showed outstanding microbial growth and total protein production given the elevated concentration of diesel (10% v:v) and sodium chloride (1.2

M) in the culture media. These results align with previous reports indicating that hyperosmotic conditions lead to an increased in cell metabolism and cell integrity in *A. borkumensis* [86]. However, the specific pathway and salinity effects as well as its adeptness in sustaining growth and protein production, particularly in the presence of elevated concentrations of diesel and sodium chloride are not completely elucidated.

Effect of salinity on the activity of enzymes

Lipase

Figure 4.1 shows the maximum enzyme activity for lipase, esterase and alkane hydroxylase.

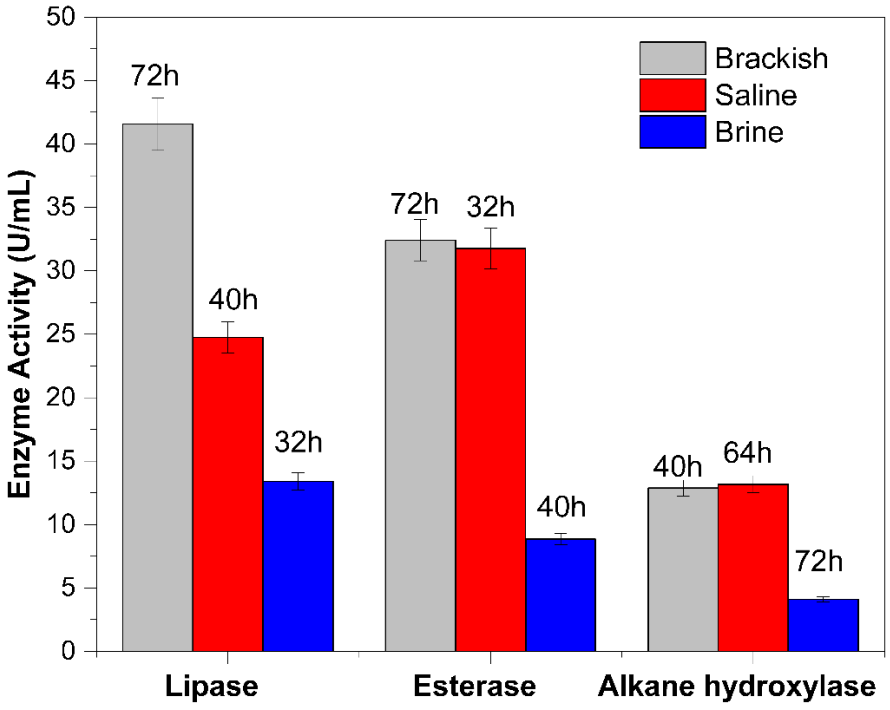


Figure 3.1. Maximum enzyme activity at different salinities concentrations and respective time to achieve it. Brackish: 0.3 M NaCl (positive control); Saline: 0.6 M NaCl; Brine: 1.2 M NaCl.

The enzyme activity for the produced lipase by *A. borkumensis* shows a proportional decrease with the increase in salinity concentration. Maximum lipase activity (41.6 U/mL)

was observed at 72 h in treatments using 0.3 M of NaCl, followed by 0.6 MNaCl with (24.7 U/mL) at 40 h and 13.4 U/mL for 1.2 Mof NaCl at 32 hours. The lipolytic activity of *A. borkumensis* aligns with protein production patterns, with reduced enzyme activity likely due to the increased energy demand during the osmolyte production at higher salinities. For instance, Cunha et al. (2010) [94] investigated the impact of environmental factors on extracellular enzymatic activity in coastal sediments. They found that higher salinity increases the energy demand during osmolyte production instead of using it for the production of extracellular enzymes, such as lipase.

Notwithstanding the decrease in the lipase activity of the present study with respect to the increase in salinity, the enzyme activity is superior if we consider the present results of brine conditions (1.2 M NaCl) as a factor compared to other halophilic strains. For instance, Suganthi et al. (2018) [95], reported lipase activity of 28 U/mL for *Halomonas hamiltonii* grew in a salt medium with a 10-fold decrease (0.05% w/v) of NaCl concentration using 1% (w/v) of petroleum oil sludge as a carbon source. Similarly, Zhang et al. (2023) [95] reported a lipase activity of only 0.061 U/mL by *Serratia marcescens* subsp. using two times lower salinity concentration (0.5 M NaCl) and 2% (v:v) cooking oil as a carbon source. In this sense, the lipolytic potential of *A. borkumensis* even at brackish conditions is a prominent feature to contribute with the bioremediation of oil spills in saline environments, as well as the lipase activity is a valuable tool for monitoring diesel degradation due to the high content of aliphatic compounds [96].

Esterase

The esterase produced by *A. borkumensis* retained a similar activity between brackish (0.3 M) and saline (0.6 M) conditions achieving 32.4 U/mL and 31.8 U/mL, respectively. However, a 40-hour difference to achieve the maximum enzyme activity was observed. At

brine conditions (1.2 M) maximum activity of 8.8 U/ml was observed at 40 hours.

It is already known that the esterase from *A. borkumensis* exhibits up to 100 times higher enzymatic activity than typical esterases and lipases, and has a broad substrate profile, notable enantioselectivity, and high chemical resistance [91]. Its halotolerance, due to previously reported negatively charged residues (glutamate and aspartate) [97],[98], likely contributes to the faster and sustained activity at elevated salinities. For instance, purified esterases from *A. borkumensis* (ABO_1197 and ABO_1251) retained their activity at 0.5 M NaCl and a 40% decrease (250 units) at 1.2 M NaCl was observed [98]. Another purified esterase from the same strain showed the same reduction in activity (250 units) when exposed to a salinity concentration of 1.2 M NaCl [99] confirming that *A. borkumensis* esterase lacks the adaptation to hypersaline conditions. Notably, compared to previous reports, the esterase in the present study demonstrated remarkable activity despite not being purified.

Alkane hydroxylase

The activity of alkane hydroxylase in positive control achieved its peak (12.9 U/mL) in the first stages of degradation (40h). A slight increase from 12.9 to 13.2 U/mL in alkane hydroxylase activity was observed with the increase in salinity from brackish (0.3 M) to saline (0.6 M) conditions. At brine conditions (1.2 M), activity significantly reduced to 4.1 U/mL (Figure 3.1).

Increased sodium chloride concentration has been previously reported to enhance alkane hydroxylase activity. For instance, the alkane hydroxylase gene expression of *Dietzia maris* in diesel-spiked systems showed a two-fold increase from 0.4 M to 0.8 M NaCl [62]. The authors reported that the expression of alkane hydroxylase coding cyp153 gene was

enhanced in diesel systems with a high C/N ratio and high salinity. Similarly, enzymes related to alkane degradation such as cytochrome P450 and the alkane-1-mono-oxygenase have been upregulated two times in *A. borkumensis* under high hydrostatic pressure (10 MPa) caused mainly by the increase of osmolarity in the culture media due to the high salinity content [86]. In this study, the sustained activity of alkane hydroxylase under saline conditions (0.6 M) likely results from the abundance of highly soluble and bioavailable substrates present in diesel [62]. The rise in salinity appears to primarily influence the time required to reach peak activity rather than the overall activity level itself.

The increase of NaCl concentration to 1.2 M decreased alkane hydroxylase activity by 68%. Typically, high salinities decrease diesel fuel solubility, particularly affecting the alkanes fraction of which the alkane hydroxylase system of *A. borkumensis* has more affinity [100]. In addition, the presence of 2,4-DTBP and other phenolic compounds has been reported during naphthalene and crude oil biodegradation studies [101], [102]. 2,4-DTBP is commonly used to prevent autoxidation and gumming of diesel fuels during storage [103]. 2,4-DTBP induces oxidative stresses through the enhanced generation of reactive oxygen species [104], thus affecting the activities of metalloenzymes such as alkane hydroxylase [105]. However, the findings presented here indicate that the activity is still significantly higher (4.1 U/mL) in brine conditions, at least twice or more than in previous studies under brackish conditions. Using 3% (v/v) motor oil as a carbon source under brackish conditions (0.3 M NaCl), Kadri et al. (2018) [93] reported an alkane hydroxylase activity of 2.62 U/mL. Similarly, a maximum activity of 1.3 U/mL was observed with 5% (v/v) hexadecane under brackish conditions.

Diesel transformation by *Alcanivorax borkumensis* at high salinities

The complex mixture of diesel fuel and the presence of its major hydrophobic components

like n-alkanes, cycloalkane, aromatics, resins and asphaltenes are well established [100]. The metabolite degradation analysis at different salinities is shown in Table 1.

Table 3. Analysis of metabolites formed due to diesel fuel biodegradation by *A. borkumensis* SK2 at different salinities.

<table>
<tr><th colspan="4">Brackish conditions (0.3 M NaCl)</th></tr>
<tr><th rowspan="2">Abiotic control</th><th colspan="3">Degradation time (hours)</th></tr>
<tr><th>16</th><th>48</th><th>72</th></tr>
<tr><td rowspan="3">Heptacosane</td><td>Heptacosane</td><td>Naphthalene, 1,2,3,4-tetrahydro-6-methyl</td><td rowspan="3">Naphthalene, 1,2,3,4-tetrahydro-5,7-dimethyl- Biphenylene,</td></tr>
<tr><td>Tetratetracontane</td><td>Naphthalene, 1,2,3,4-tetrahydro-5,7-dimethyl- 48h</td></tr>
<tr><td rowspan="2">2,4 -DTBP</td><td rowspan="2">9-Methyltricyclo[4.2.1.1(2,5)]deca-3,7-diene-9,10-diol</td></tr>
<tr><td>Tetratetracontane</td><td rowspan="3">1,2,3,6,7,8,8a,8b-octahydro-, trans- Hex-3-ene-1,5-diyne, 3,4-diisopropyl-</td></tr>
<tr><td rowspan="2">2,4-DTBP</td><td rowspan="2">2,5-di-tert-Butyl-1,4-benzoquinone</td><td>Cyclohexanol</td></tr>
<tr><td>D-Homo-24-nor-17-oxachola-20,22-diene-3,16-dione, 7-(acetyloxy)-1,2:14,15:21,23-triepoxy-4,4,8-trimethyl-, (5a,7a,13a,14ß,15ß,17aa)-</td></tr>
<tr><th colspan="4">Saline conditions (0.6 M NaCl)</th></tr>
<tr><th rowspan="2">Abiotic control</th><th colspan="3">Degradation time (hours)</th></tr>
<tr><th>16</th><th colspan="2">72</th></tr>
<tr><td>Heptacosane</td><td rowspan="3">D-Homo-24-nor-17-oxachola-20,22-diene-3,16-dione, 7-(acetyloxy)-1,2:14,15:21,23-triepoxy-4,4,8-trimethyl-, (5a,7a,13a,14ß,15ß,17aa)-</td><td colspan="2" rowspan="2">1,3-di-iso-propylnaphthalene</td></tr>
<tr><td>Tetratetracontane</td></tr>
<tr><td>2,4-DTBP</td><td colspan="2">2,4-DTBP</td></tr>
<tr><th colspan="4">Brine conditions (1.2 M NaCl)</th></tr>
<tr><th rowspan="2">Abiotic control</th><th colspan="3">Degradation time (hours)</th></tr>
<tr><th colspan="2">48</th><th>72</th></tr>
<tr><td rowspan="3">Heptacosane</td><td colspan="2" rowspan="3">Heptacosane</td><td>Phytane</td></tr>
<tr><td>Pentacosane</td></tr>
<tr><td>Heptacosane</td></tr>
</table>

Tetratetracontane		Tetratetracontane
		2,4 -DTBP
2,4-DTBP		Octadecane, 3-ethyl-5-(2-ethylbutyl)-

The initial stage in the aerobic degradation of alkanes by *A. borkumensis* is catalyzed by alkane hydroxylases and for long-chain alkenes of C_{32} and longer the *AlmA* gene (ABO_0282) encodes a putative monooxygenase belonging to the flavin-binding family which functions as a long-chain alkane hydroxylase [106]. For instance, AlmA monooxygenase in *Alcanivorax dieselolei* was shown to have activity against alkanes ranging in length from *n*-C_{10} up to *n*-C_{36} [107].

Long-chain hydrocarbons such as heptacosane and tetratetracontane were degraded by *A. borkumensis* after 3 days of cultivation. Diesel fuel (*n*-C_{10} *n*-C_{50}) represents a higher chain length suggesting that the alkane hydroxylase system of *A. borkumensis* has a higher substrate range and accordingly the expression of alkane hydroxylase is higher in the presence of larger alkanes present.

Many refractory compounds were identified at brackish and saline conditions, including PAHs derivatives such as naphthalene and biphenylene. Evidence of the use of alkyl side chains of PAH by *A. borkumensis* as energy sources was identified by the formation of alkylated naphthalene derivatives at brackish and saline conditions. As the capability of *A. borkumensis* for aromatics ring fission has not been documented so far, the assimilation of alkyl side chains could explain the changes presented in aromatic metabolites [108]. For instance, transformation products of the toxic compound 2,4-DTBP were detected only at brackish conditions, which was characterized by the presence of Biphenylene, 1,2,3,6,7,8,8a,8b-octahydro-trans. In addition, 2,5-di-tert-Butyl-1,4-benzoquinone identified at brackish conditions has been observed as a derivative of PAH degradation. The same compound was found during the degradation of Benzo (a) pyrene by microbial consortia including the halophilic strain *Serratia marcescens* [109].

Linear or branched alkanes are oxidized through three routes: terminal oxidation produces a primary alcohol or carboxylic acid at the end of the chain, subterminal oxidation yields a secondary alcohol or ketone near the end, and terminal oxidation results in the formation of diols at both terminal positions [100]. Considering that the different pathways can coexist within the same microorganism [110] and given the complex composition of diesel fuel and its identified metabolites, *A. borkumensis*

assimilated hydrocarbons using at least two oxidation pathways. For instance, the appearance of metabolites such as 9-Methyltricyclo[4.2.1.1(2,5)]deca-3,7-diene-9,10-diol, indicates a subterminal route of degradation where hydroxyl groups are introduced at positions close to each other within the cyclic structure. Another example is D-Homo-24-nor-17-oxachola-20,22-diene-3,16-dione, 7-(acetyloxy)-1,2:14,15:21,23-triepoxy-4,4,8-trimethyl-, (5a,7a,13a,14ß,15ß,17aa)- metabolite containing the ketone moiety that was identified at brackish and saline conditions, also indicating subterminal oxidation. The referred compound was previously identified during the biodegradation of petroleum refinery wastewater by microbial consortia and aniline by halophilic bacteria *Halomonas* sp. NRS-01 [111].

Previous research demonstrated the oxidation of cyclohexane by the alkane hydroxylase system of *A. borkumensis*. This system employs alkB1 or alkB2 to initiate the breakdown of cyclic alkanes. Sabirova et al. (2006) [89] observed that *A. borkumensis* can not utilize cyclohexane alone as an energy source but can efficiently co-metabolize it when grown on mixed carbon sources like crude oil. The present study also revealed an increase in alkane hydroxylase activity under brackish conditions, peaking between 32 and 40 hours. This finding aligns with the conversion of cyclohexane to cyclohexanol within 48 hours of cultivation (Table 3), confirming *A. borkumensis* ability to co-metabolize a complex hydrocarbon mixture such as diesel fuel.

Production of metabolites at brackish and saline conditions

In addition to diesel degradation products, "non-toxic metabolites" were identified under brackish and saline conditions, as detailed in Table 3.1. Among these metabolites, the ketocarotenoid astaxanthin, along with the corticosteroids betamethasone acetate and flurandrenolide, are of significant biotechnological interest. Astaxanthin is primarily produced by marine microorganisms under stress conditions such as excessive light or salinity and is known for its antioxidant properties and nutritional benefits [112]. Betamethasone acetate and flurandrenolide possess anti-inflammatory and anti-allergic properties [113].

Table 3.1. Analysis of metabolites produced in response to salinity.

<table>
<tr><th colspan="3">Brackish (0.3 M NaCl)</th></tr>
<tr><th colspan="3">Cultivation time (hours)</th></tr>
<tr><th>32</th><th>64</th><th>72</th></tr>
<tr><td rowspan="2">monoolein TMS</td><td>monoolein TMS</td><td rowspan="2">Astaxanthin</td></tr>
<tr><td>Methyl glycocholate, 3TMS derivative</td></tr>
<tr><th colspan="3">Saline (0.6 M NaCl)</th></tr>
<tr><th colspan="3">Cultivation Time (hours)</th></tr>
<tr><th>32</th><th>64</th><th>72</th></tr>
<tr><td>monoolein TMS</td><td rowspan="2">monoolein TMS</td><td rowspan="2">Flurandrenolide</td></tr>
<tr><td>Betamethasone acetate</td></tr>
</table>

To the best of the authors' current knowledge, only a few studies have investigated the role of bacterial secondary metabolites against induced salt stress which are limited to rhizobacteria. Ullah and Bano (2021) [114] evaluated the metabolite production by the coculture of *Pseudomonas putida* AMUPP-2 and *Lysinibacillus sphaericus* OUG29GKBB supplemented with 125 mM NaCl and concluded that salt stress induced the production of oxoesteroids, steroids esters and steroidal saponins with anti-inflammatory and antimicrobial activity.

According to Varnava et al. (2024) [113], methoxylated trimethylsilyl (TMS) derivatives like monoolein TMS and methyl glycocholate are recognized as part of microbial biosurfactants. These compounds facilitate the creation of surface-active glycine-glucolipids during growth in the presence of long-chain alkanes, aiding in the binding and solubilization of alkanes at the lipid-water interface. In the present study, biosurfactant formation under the examined conditions was not observed.

Research on secondary metabolites, particularly those of biotechnological relevance, remains limited for *A. borkumensis* and further investigation is needed to elucidate their roles during diesel degradation.

Conclusion

The present study showed that *A. borkumensis* can degrade long-chain alkanes and branched alkanes present in diesel fuel (10% v:v) within 72 hours without lag time at saline conditions (0.6 M NaCl)

and short-chain alkanes at brine conditions (1.2 M NaCl). Lipase (13.4 U/mL), esterase (8.8 u/mL) and alkane hydroxylase (4.1 U/mL) enzymes produced by *A. borkumensis* exhibited outstanding activity under brine conditions (1.2 M NaCl), though osmotic and oxidative stress significantly reduced their activity. Further work is required to improve the activity and stability of *A. borkumensis* enzymes, enabling them to resist high salinity and enhance the degradation of petroleum hydrocarbons at brine conditions.

CHAPTER FOUR: IMMOBILIZATION OF ENZYMES FOR THE BIODEGRADATION OF PETROLEUM HYDROCARBONS IN SALINE WATER ENVIRONMENT

4.1. Chitosan-based scaffold for improvement of *A. borkumensis* activity and biodegradation of diesel fuel at brine conditions

Jean Viccari Pereira[1], Carlos S. Osorio-González[1], SN Leung[2], Satinder K Brar[1*]

[1]Department of Civil Engineering, Lassonde School of Engineering, York University, North York, Toronto, M3J 1P3, Ontario, Canada

[2]Department of Mechanical Engineering, Lassonde School of Engineering, York University, North York, Toronto, M3J 1P3, Ontario, Canada

*Corresponding author: satinder.brar@lassonde.yorku.ca

Abstract

This study explores the synthesis of chitosan scaffolds via freeze-casting for immobilizing *A. borkumensis* cells and enzymes to degrade petroleum hydrocarbons in brine (1.2 M NaCl) conditions of salinity. Scaffolds were characterized by their degree of deacetylation and freeze-casting temperatures. Scaffolds with a high degree of deacetylation (95.6%) and produced at -20ºC and -80ºC were resistant and had favourable porous structures for enzyme and cell entrapment, while those made at -196ºC were brittle. The scaffold produced at -80ºC (Ch80) and cross-linked with glutaraldehyde (0.02% v/v) showed improved structural integrity and water resistance, reducing protein release and enhancing enzyme stability in brine conditions. Cross-linked scaffolds exhibited up to 25.5% less protein release and scaffolds containing immobilized bacteria showed only 1.80% protein release. Enzyme activities for alkane hydroxylase (0.35 U/mL), lipase (3.7 U/mL), and esterase (4.1 U/mL) cross-linked scaffolds were lower in the supernatant due to reduced biomaterial degradation. Ch80 produced scaffold demonstrated over 61% diesel degradation within 7 days, with glutaraldehyde cross-linking enhancing both structural stability and degradation efficiency. The chitosan scaffold holds significant promise for improving hydrocarbon biodegradation in saline environments.

Keywords Chitosan scaffolds; Freeze-casting; Enzyme immobilization; Hydrocarbon biodegradation

Introduction

Petroleum spills pose a significant threat to marine and coastal environments, affecting biodiversity and ecosystem health, and becoming a serious environmental concern in the petroleum industry. Several have been employed for oil spill remediation, including mechanical recovery (oil spill booms) and physicochemical methods using chemical dispersants. Despite the range of available methods, physical methods have limitations in terms of costs and energy for recovery and post-treatment of oil, while chemical treatment methods require toxicity assessment due to the formation of carcinogenic byproducts [9], [10]. Consequently, the necessity and demand for low-cost hybrid technology that combines the physical absorption of oil residues and potential biological degradation has recently increased.

One of the main bottlenecks in the current bioremediation methods for petroleum hydrocarbons is that they often fall short in high-salinity environments, such as brine conditions (> 1.2 M NaCl), where the effectiveness of biological treatments can be severely compromised. It is well known that high salinity content can inhibit the growth and activity of oil-degrading microorganisms, reducing the overall efficiency during the bioremediation processes. This phenomenon represents a significant challenge, as many oil spills occur in marine environments where salinity levels are naturally high. Additionally, effluents from the petroleum industry, such as oilfield-produced water (OPW) from underground oil and natural gas extraction are discharged into the marine environment and can reach about 300 g/L NaCl concentration [115], [116]. Therefore, there is a critical need for new approaches to overcome salinity-related challenges and enhance the biodegradation of oil pollutants.

Likewise, sorbents have been used to recover oil spills and include synthetic polymers such as polypropylene, polyethylene, and polyurethane materials, but they are difficult to degrade [117]. Consequently, natural and renewable materials, such as agricultural and biological wastes, are being pursued to develop biosorbents [118]. Chitin, the second most abundant polysaccharide in nature [119], is mainly found in the shells of marine crustaceans and fungal mycelia. The deacetylation and

depolymerization of chitin are used to synthesize chitosan, which shows a unique chemical structure and functional versatility, allowing it to form gels, films, and scaffolds tailored for specific applications [120]. The biopolymer has garnered attention for its potential in environmental remediation due to its biocompatibility, biodegradability, and non-toxic properties [121].

Chitosan porous scaffolds such as sponges and have been extensively as a carrier-support in different living systems to enhance their stability and activity [122], [123]. Additionally, the possibility to fabricate different derivatives such as gels and sponges with porous structures facilitates mass transfer and provides a conducive environment for biological processes. Various research efforts have demonstrated the effectiveness of chitosan-based materials as sorbents for oil spill clean-up [120]. However, few studies have explored the intersection of biopolymeric materials as carriers for the biological degradation of petroleum hydrocarbons [124]. Recently, the freeze-casting method has been widely used to fabricate chitosan scaffolds with tunable and oriented porous morphology and interconnected structures, which are particularly advantageous for enzyme entrapment and microbial culture [125]. However, few studies have used chitosan scaffolds fabricated by freeze-casting as carriers of enzymes and/or oil-degrading bacteria for oil bioremediation.

In this study, chitosan-based scaffolds were successfully fabricated using a facile freeze-casting process. The oil-degrading bacterium *A. borkumensis* and its crude enzyme extract were immobilized in the scaffold by entrapment and covalent binding. The resulting enzyme-scaffold and whole-cell scaffold systems were tested for diesel biodegradation under brine conditions of high salinity (1.2 M NaCl).

Material and methods

Immobilization support preparation

To prepare the immobilization support for diesel-contaminated saline water using whole-cell *A. borkumensis* and its cocktail enzyme, chitosan was used as a biodegradable and renewable polymer. The effect of three chitosan deacetylation degrees (85%, 95%, and 95.6%) and three freeze casting

temperatures (-20 ºC, -80 ºC, and -196 ºC) were investigated.

40 mg/mL chitosan solution was prepared by dissolving 4g of chitosan in 100 mL of 0.3 M acetic acid solution with agitation at 60°C for 24 hours until chitosan had completely been dissolved. The chitosan solution was then transferred to cylindrical tubes to perform the freeze-casting process. After that, the chitosan scaffold was obtained through lyophilization at -55°C for 48 hours.

A second set of support was prepared as previously described, with the addition of 0.02% (v:v) glutaraldehyde to the chitosan solution to cross-link the hydroxyl groups of chitosan, enhancing water resistance and improving cell and enzyme immobilization via covalent binding.

Bacterial strain and inoculum preparation

Alcanivorax borkumensis strain SK2 (DSMZ 11573) was procured from the Leibniz Institute DSMZ (Germany). Marine broth (peptone 5 g/L, yeast extract 1 g/L, ferric-citrate 0.10 g/L, $MgCl_2$ 5.90 g/L, Na_2SO_4 3.24 g/L, $CaCl_2$ 1.80 g/L, KCl 0.55 g/L, $NaHCO_3$ 0.16 g/L, KBr 0.08 g/L, $SrCl_2$ 0.034 mg/L, H_3BO_3 0.022 mg/L, Na-silicate 0.004 mg/L, NaF 0.0024 mg/L, $(NH_4)NO_3$ 0.0016 mg/L, Na_2HPO_4 0.008 mg/L, 0.3 M of NaCl), with a initial pH of 7.6 was used for bacterial preservation and inoculum preparation. For inoculum preparation, the strain was pre-cultured for up to two generations in a shaker incubator at 150 rpm and 30±1°C for 48 h.

Scaffold-bacteria system preparation

Cultures were prepared by inoculating 3% (v/v) of *A. borkumensis* into 1 liter of MB medium supplemented with 10% (v/v) of diesel as the sole energy source. The culture was grown in a shaker incubator at 30°C and 150 rpm for 48 hours. After incubation, cells were harvested by centrifugation at 4°C for 10 minutes at 5000 ×g, washed twice with MB, and re-suspended in a chitosan solution to an initial $OD_{600\ nm}$ of 1.

Scaffold-enzymes system preparation

The cocktail enzyme was produced using 10% (v:v) diesel as the sole energy source for *A.*

borkumensis, grown at 30°C and 150 rpm for 48 h. After that, cells were harvested by centrifugation at 4°C for 10 minutes at 5000 ×g and washed twice with a sterile MB medium. The supernatant containing soluble proteins (lipase and esterase) was kept at 4°C for further analysis. The disruption of microbial biomass was performed by sonication at 22 kHz and 30 kHz for 6 minutes at 4°C in 1 mL of 20 mM Tris-HCl buffer (pH 7.4). The sonicated mixture was then centrifuged at 13000 ×g for 20 minutes at 4°C. The intra and extracellular enzymes (alkane hydroxylase, lipase, and esterase) were mixed and immediately frozen and lyophilized at -55ºC for 48 hours. The lyophilized enzyme was stored at 4ºC for future use.

For enzyme immobilization, 2.5 mL solution of the crude enzyme (10 mg/mL) in 50 mM potassium phosphate buffer (pH 7), was mixed with an equal volume of chitosan solution and stirred at 200 rpm for 30 minutes.

Salinity effects on the scaffold-systems performance during diesel degradation

To study the performance of the whole-cells and enzyme scaffold-systems during diesel degradation in a high-salinity environment the scaffolds were incubated separately under brine salinity (1.2 MNaCl) and supplemented with 10% (v:v) of commercial diesel as the sole energy source to mimic the conditions of an oil spill (high C/N ratio). Scaffolds were incubated separately in a rotary shaker (Infors HT Multitron Standard) at 30 ºC and 180 rpm for 7 days. Abiotic controls (without bacteria or enzymes) and free-cell controls (without scaffold) were studied to assess diesel degradation purely due to physicochemical effect. Each treatment was prepared in triplicate for every condition.

Analytical methods

Scaffold characterization

The scaffold morphology was performed with cross and longitudinal-sections using a Scanning Electron Microscope (SEM) (Thermofisher Quanta 3D). The thermal stability was analyzed by a thermogravimetric analyzer (TGA55 Discovery) at a heating rate of $10^{\circ}C\ min^{-1}$ from 30°C to 800°C under a nitrogen atmosphere. To determine the surface area of the scaffolds, all samples were first

degassed for 6 hrs at 25°C. Consequently, the surface area was determined utilizing a Brunauer-Emmett-Teller (BET) by measuring the N_2 adsorption isotherm at 77 K using a NOVA 1200e BET instrument. After that, the samples were separately degassed for 6 hrs at 101°C under vacuum followed by a N_2 gas physisorption analysis.

Microbial growth

The microbial growth was monitored by measuring optical density at 600_{nm}. Briefly, 1 mL samples were taken every 24 h and centrifuged at 4°C for 10 min at 5000 ×g. After centrifugation, the microbial biomass was washed with 0.05 M phosphate buffer (pH=7) two times under the aforementioned centrifuge conditions to remove the diesel excess. Microbial biomass was used for alkane hydroxylase assays and the supernatant was reserved at 4°C for total protein, lipase, esterase and diesel determinations.

Total protein concentration

Total protein concentration was determined according to the standard Bradford method [83]. A 5 µL fermented broth was mixed with 250 µL Coomassie blue dye and the shift of absorbance (595 nm) during protein determination was recorded (Agilent Bio Tek Epoch Microplate Spectrophotometer). Total protein concentration was reported in the unit of mg/L.

Alkane hydroxylase assay

Alkane hydroxylase activity was assessed according to Mishra and Singh (2012) [84], and Jauhari et al. (2014) [85]. *A. borkumensis* cell pellet was sonicated using two frequencies (22 kHz and 30 kHz) for 6 min at 4°C using 1 mL of Tris-HCl buffer with a pH of 7.4 (20 mmol). After sonication, the mixture was centrifuged at 13000 ×g for 20 min at 4ºC and the supernatant was used to determine the enzyme activity. The crude enzyme (50 µL) was mixed in 935 µL of 20 mmol L^{-1} of Tris-HCl buffer (pH of 7.4) and 0.15% (v:v) of CHAPS lysis buffer ($C_{32}H_{58}N_2O_7S$). A solution of diesel fuel (1% v:v) in 10 µL of DMSO (80% v:v) was used as a substrate. The addition of 5 µL of NADH (0.1 mmol L^{-1})

initiated the reaction, and the reduction of absorbance was measured at 340 nm. One unit of alkane hydroxylase activity was determined as the amount of enzyme necessary to oxidize 1 µmol of NADH per minute.

Lipase assay

The crude enzyme solution (supernatant) was used for lipase enzyme activity determination. 30 mg of p-nitrophenyl palmitate was dissolved in 10 mL of isopropanol: acetonitrile solution (4/1 v:v). This was then mixed with a solution of 90 mL of 0.05 M Sorensen phosphate buffer (pH 8.0), containing 1% (w/v) of $CaCl_2$, 4% (v/w) of Triton X-100, 0.2% (w/v) of gum Arabic. After that, both solutions were mixed and incubated in a water bath at 60°C until the solution became transparent. Then, 960 µL of a pre-warmed substrate solution (at 37 °C) was mixed with the crude enzyme solution (40 µL). After 15 min of incubation at 37°C, the enzyme activity was evaluated at 410 nm against an enzyme-free control. One unit of lipase activity was defined as 1 µmol of the p-nitrophenol released per minute.

Esterase Assay

Similar to the lipase determination, the crude enzyme solution (supernatant) was used. A reaction mixture was prepared by mixing 980 µL of 4-nitrophenyl acetate (1.12 mM), in 50 mM potassium phosphate buffer (pH 7) with 11.3 mM sodium deoxycholate and 0.43 M of tetrahydrofuran. After that, 20 µL of the sample was added to the reaction mixture and monitored against a blank solution for 15 min at room temperature. One unit of esterase activity was defined as the amount of esterase required to release 1 µmol of p-nitrophenol in one minute, under the specified conditions.

Degradation analysis

A Gas Chromatography Flame Ionization Detection (GC-FID) was used to analyze diesel degradation. Briefly, 500 µL sample taken was diluted with hexane to 1.1 mL and analyzed by an Agilent 7890B gas chromatograph equipped with a DB-1 column (30 m x 250 µm x 0.25 µm) and a flame ionization detector. The injection was performed in pulsed splitless mode at 310°C. The oven temperature

program started at 40°C for 1 minute, ramped to 55°C at 7°C/min, then to 325°C at 40°C/min for 4 minutes, and finally to 340°C at 40°C/min for 6 minutes. The FID operated at 330°C with hydrogen, air, and makeup flow rates of 30 mL/min, 400 mL/min, and 20 mL/min, respectively.

Results and discussion

Chitosan scaffold characterization

The morphology of the chitosan scaffolds demonstrated distinct structural characteristics depending on the degree of deacetylation (DD) and freeze-casting temperature. Scaffolds with 95.6% deacetylated chitosan prepared at -20 ºC and -80 ºC resulted in more compact, flexible, and consistent cylindrical shapes (annotated in red). In contrast, scaffolds prepared at -196 ºC were more brittle (Figure 4).

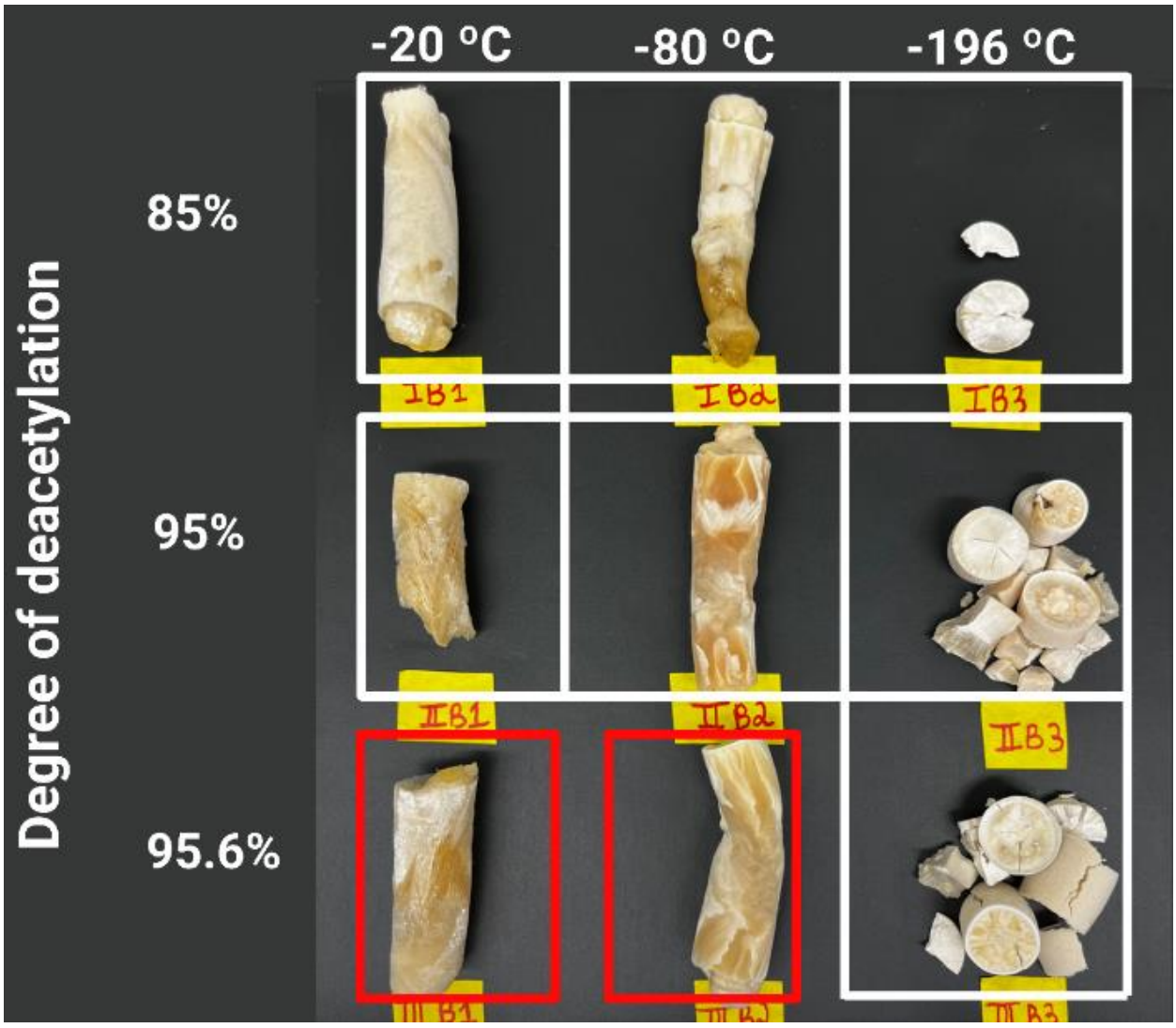


Figure 5. Top view of chitosan scaffolds produced at different degree of deacetylations and freezing temperatures.

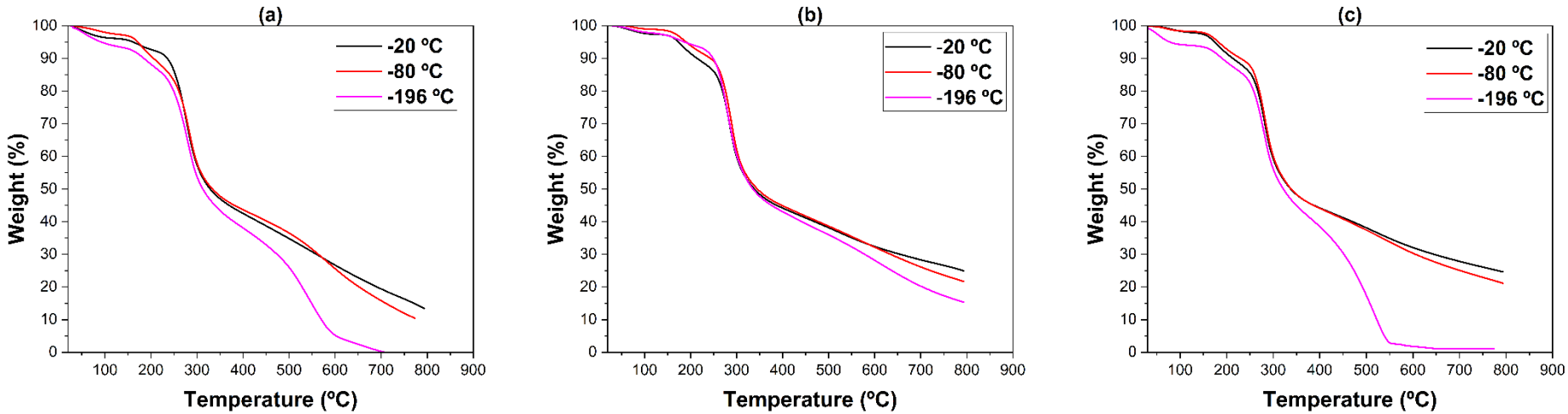


Figure4.1. Thermogravimetry curves 30-800 ºC. (a) 85%, (b) 95% and (c) 95.6% degree of deacetylation.

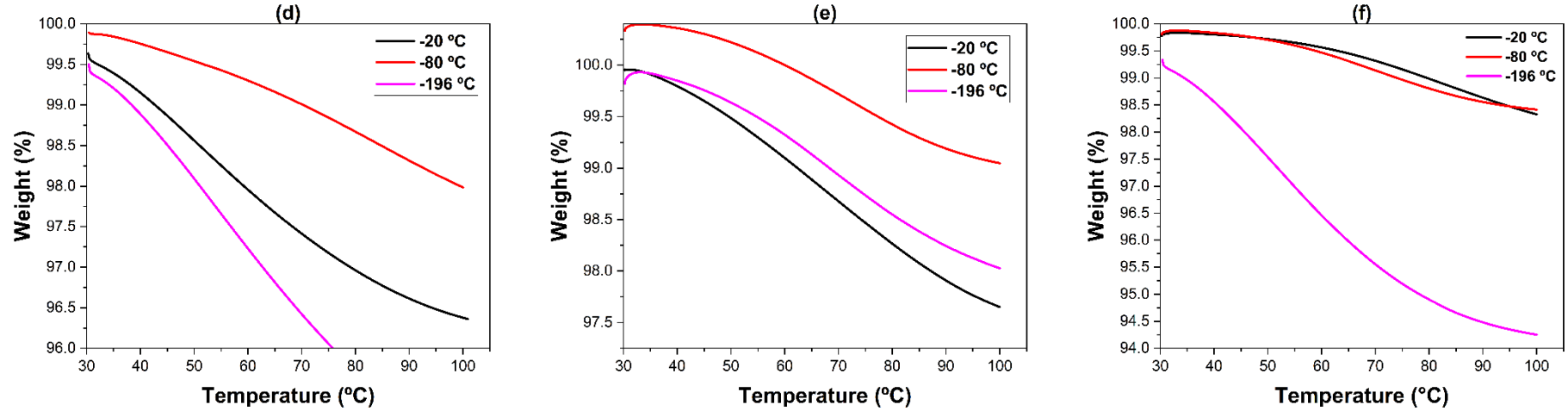
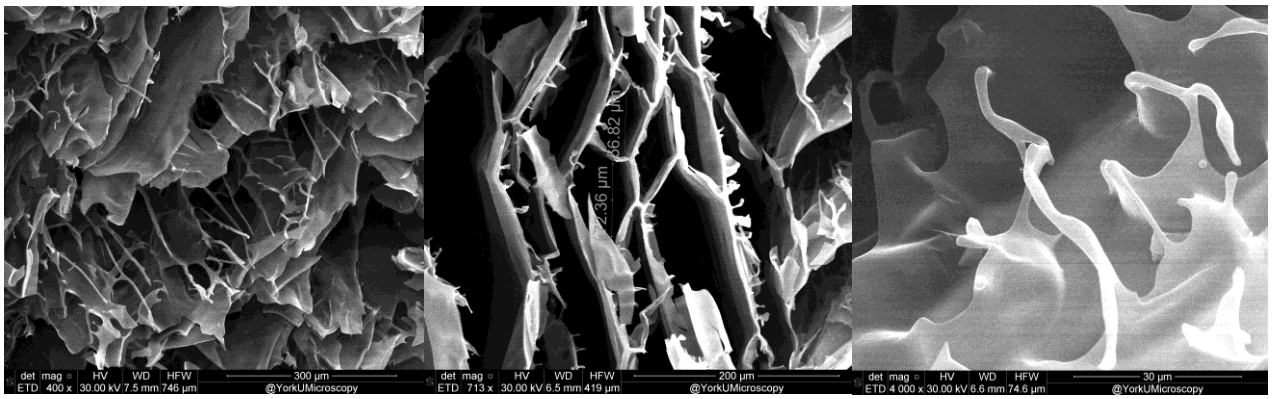


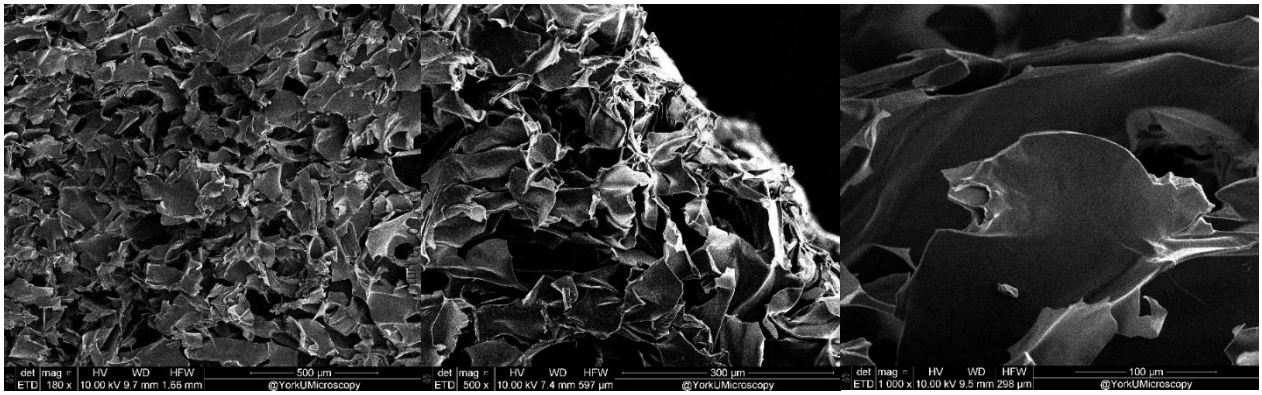
Figure 4.2. Thermogravimetry curves 30-100 ºC. (d) 85% DD, (e) 95% DD and (f) 95.6% DD.

Thermogravimetric analysis assessed the impact of different deacetylation levels and freeze-casting temperatures on scaffold thermal stability (Fig. 4.1). The peak decomposition temperature of scaffolds increased from 281ºC to 287ºC as the degree of deacetylation rose from 85% to 95.6%, corresponding to the degradation of the biopolymer polysaccharide structure and suggested that higher DD enhanced thermal stability [126]. The onset decomposition temperature (T_0) also increased with higher DD, from ~ 131ºC (85% DD) to ~165 ºC (95% DD) and ~166 ºC (95.6% DD), due to the degradation of 2-amino-2-deoxy-d-glucopyranose (GlcN) amino units, the main group in chitosan backbone [127]. Thermal stability between 30-100 ºC was analyzed to compare different freeze-casting temperatures (Fig. 4.2). Scaffolds fabricated at −80 °C with 85% (Fig. 4.2d) and 95% (Fig. 4.2e) DD exhibited the lowest weight loss, showing similar behaviour to those produced at −20 °C with 95.6% DD (Fig. 4.2f). Previous studies have noted that increasing DD improves mechanical strength, making materials less brittle and more flexible due to increased hydroxyl groups enhancing hydrogen bonding and material deformability under stress [128], [129].

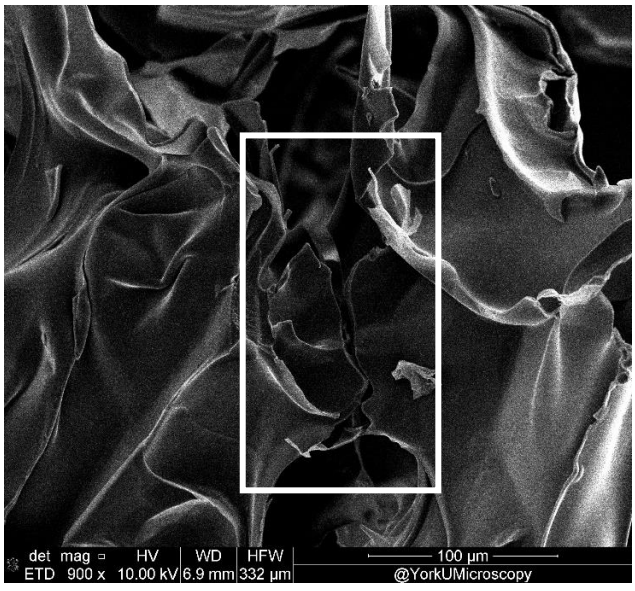
It is well known that the morphology of biomaterials is highly influenced by the feedstock nature and the manufacturing process. To identify the most suitable scaffold for enzyme and cell entrapment, the porous morphology of cross and longitudinal sections of scaffolds produced at -20 ºC (Ch20), -80 ºC (Ch80) and -196ºC (Ch196) were examined using SEM images (Fig. 4.3). Ch80 yielded a chitosan scaffold with a highly porous, interconnected structure (Fig. 4.3a). The elongated honeycomb morphology observed in cross-sectional images results from unidirectional ice crystal growth, enhancing permeability and mass transfer (Figure 4.3b). In contrast, Ch20 displayed a more irregular porous structure with fewer elongated pores and a layered arrangement (Fig. 4.3f), due to the lower nucleation rate of ice crystals at the higher temperature. Higher freeze-casting temperatures also produced lower connectivity (Fig. 4.3e). Madihally and Matthew (1999) [130] showed that the freezing temperature influences the pore size and connectivity of chitosan scaffolds.



(a) **(b)** **(c)**



(d) **(e)** **(f)**



(g)

Figure 4.3. SEM images of cross-section and longitudinal section of (a, b and c) Ch80 scaffold, (e, f, and g) Ch20 scaffold and (g) Ch196 scaffold (with details of fractured material).

Similarly, the SEM image of Ch196 (Fig. 4.3g) confirmed the brittleness and low connectivity of scaffolds.

At lower magnification, Ch80 scaffold showed a rough pore wall texture, indicating a high surface area beneficial for cell attachment (Fig. 4.3a). High magnification revealed a fibrous texture, which may support cell adhesion as previously reported [131] (Fig. 4.3c). According to previous literature, the honeycomb morphology of Ch80 shows suitable characteristics for enzyme immobilization. For instance, Jiang et al. (2024) [132] found that the honeycomb structure of chitosan spheres offered a large specific surface area and abundant amino group interactions, allowing immobilized cellulase to perform well under harsh conditions. Similarly, Huang et al. (2024) [133] reported that metal-organic frameworks with an ordered honeycomb structure provided immobilized lipase with a large external surface, efficient mass transfer channels, and numerous active sites for the enzymes.

BET analysis determined the surface area and pore sizes of the scaffolds, as shown in Figure 4.4, indicating that the scaffolds have mesoporous characteristics ($2.0\ nm \leq d \leq 50\ nm$).

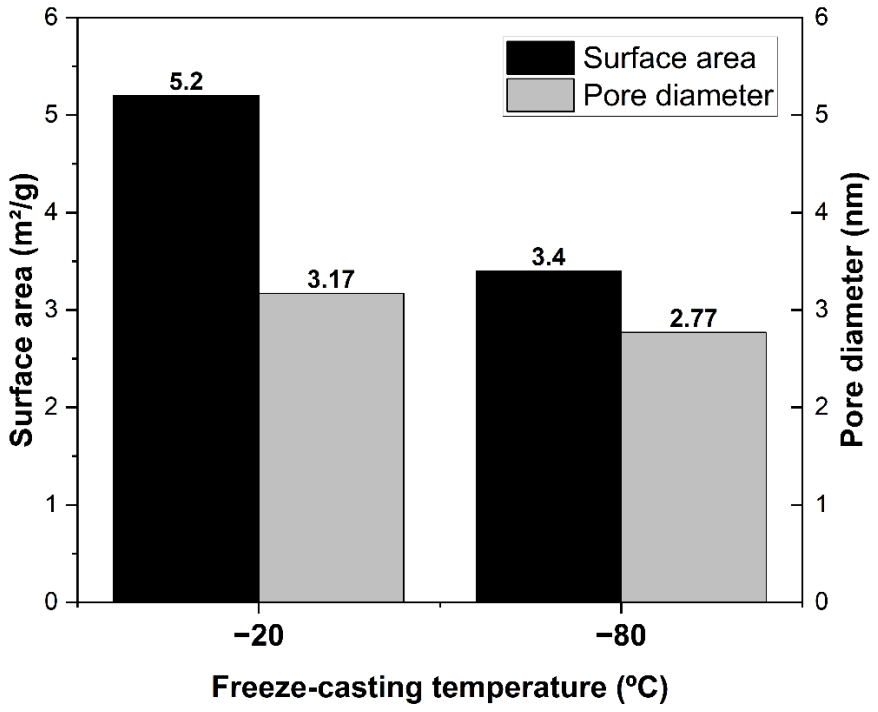


Figure 4.4. Brunauer-Emmett-Teller (BET) surface area and pore diameter for Ch20 and Ch80.

Although Ch20 exhibited a higher surface area, the porosity and elongated honeycomb morphology of Ch80 were expected to facilitate enzyme entrapment, cell attachment, mass transfer, and proper contact between the enzyme and substrate. The crude enzyme extract from *A. borkumensis* shows a protein molecular weight range of 20-90 kDa [93]. For better retention of proteins in the scaffold, a Molecular Weight Cut-Off (MWCO) should be ⅓ to ½ the target molecular weight or size for maximum retention of most macromolecules. Considering a MWCO of 10 kDa, the recommended pore size is 2.5 nm [134]. Therefore, the Ch80 scaffold was chosen to synthesize the scaffold-bacteria and scaffold-enzyme systems in this study.

5.3.2 Ch80 scaffold immobilization performance under brine conditions

5.3.2.1 Total protein concentration

The structural integrity and immobilization capacity (whole-cells/enzyme) of the chitosan-scaffold as well as the addition of glutaraldehyde as a reinforcement was monitored over 7 days under brine

conditions. Figure 4.5 illustrates the integrity of the chitosan scaffold indirectly by the release of the immobilized enzyme in terms of total protein. Overall, treatments in which glutaraldehyde was added as a reinforcement (T2 and T4), the cross-linked chitosan scaffolds showed better immobilization by decreasing the protein release up to 25.5% (39.1 µg/mL), in comparison with chitosan scaffold-immobilized enzyme (T1) and chitosan scaffold with immobilized bacteria (T4) showing 1.80% (0.29 µg/mL) release, with respect to T3.

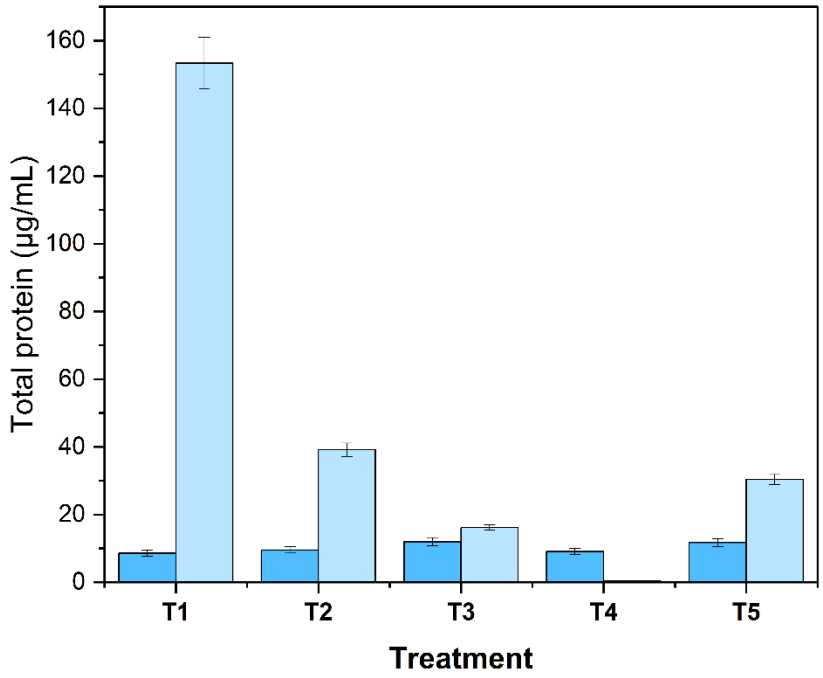


Figure 4.5. Total protein released at t = 48h and T = 168h. T1: scaffold-immobilized enzyme; T2: scaffold-immobilized enzyme cross-linked with 0.02% GTA; T3: scaffold-immobilized bacteria; T4: scaffold-immobilized bacteria cross-linked with 0.02% GTA and T5= free *A. borkumensis* cells.

One chemical fact that supports the previous results is that the cross-linking of chitosan hydroxyl functional groups with GTA increases the chitosan hydrophobicity and as a consequence increases the water resistance [135]. Moreover, brine salinity probably had a greater impact on the scaffold produced without GTA, likely causing material damage, as GTA is known to reduce the permeability of monovalent ions like Na^+ [136].

The performance of the cross-linked chitosan scaffold suggests potential applications with other renewable, inert, and hydrophobic materials. For instance, Miri et al. (2021) [137] showed a total

protein release of 10% from micro and nanobiochar-chitosan matrices crosslinked with 0.02% v/v glutaraldehyde after 48h.

5.3.2.2 Oxidative enzymes

Figure 4.6 shows the maximum enzyme activity in the fabricated chitosan scaffolds under brine conditions. In general, the results showed that the use of glutaraldehyde as a cross-linker reinforcement during the chitosan scaffold synthesis improves the immobilization capacity of the produced biomaterial. For instance, the enzyme activity of oxidative enzymes such as alkane hydroxylase (0.35 U/mL), lipase (3.7 U/mL), and esterase (4.1 U/mL) in chitosan scaffolds including glutaraldehyde shows a lower activity present in the supernatant due to reduced biomaterial degradation. Additionally, the immobilized alkane hydroxylase is likely utilized faster as the material hydrophobicity increases with GTA [136], [138], enhancing contact between the enzyme and the diesel (substrate). Moreover, lipases tend to have a higher number of exposed lysine residues (amino groups) on their surface [139], which increases glutaraldehyde cross-linking compared to esterases.

For instance, in the particular case of alkane hydroxylase and lipase, Kadri et al. (2018) [73] reported a release of 36.7% and 41% of the enzyme from chitosan-nanoparticles after 7 days using 0.02% (v:v) of GTA as a cross-linker. In the case of esterase, Hegde and Veeranki (2014) [140] reported a 29% release of an immobilized esterase from chitosan beads containing 3% v:v of glutaraldehyde as a cross-linker. It is known that several factors such as immobilization methods, carrier materials, and enzyme loading amount influence the immobilization process [141]. However, one of the main challenges for the immobilization support and immobilization process is the working conditions and environments in which the immobilization system will be used. In this study, three main factors have a critical role in the performance of the immobilization system. The culture media composition, presence of hydrocarbons, and brine conditions (high salinity) create a challenging environment, as the changes in ionic strength from the salt content greatly influence enzyme release. Likewise, it has been reported that lower or moderate concentrations of NaCl can increase swelling and disintegration

of chitosan biomaterials, enhancing the enzyme release [73]. In this context, glutaraldehyde enhances immobilization support by reducing ion permeability and forming covalent bonds that strengthen structural integrity, while also stabilizing the process by mitigating pH decreases [142].

On another hand, it is worth mentioning that compared with free bacteria, alkane hydroxylase, lipase, and esterase enzymes released from treatments T3 (0.48 U/mL, 4.1 U/mL and 5.8 U/mL) and T4 (0.46 U/mL, 2.6 U/mL and 3.0 U/mL) showed similar concentrations. The low release observed in T3 and T4 compared to free bacteria potentially enhances stability, allowing the enzyme to maintain activity over extended periods under harsh salinity conditions (brine conditions).

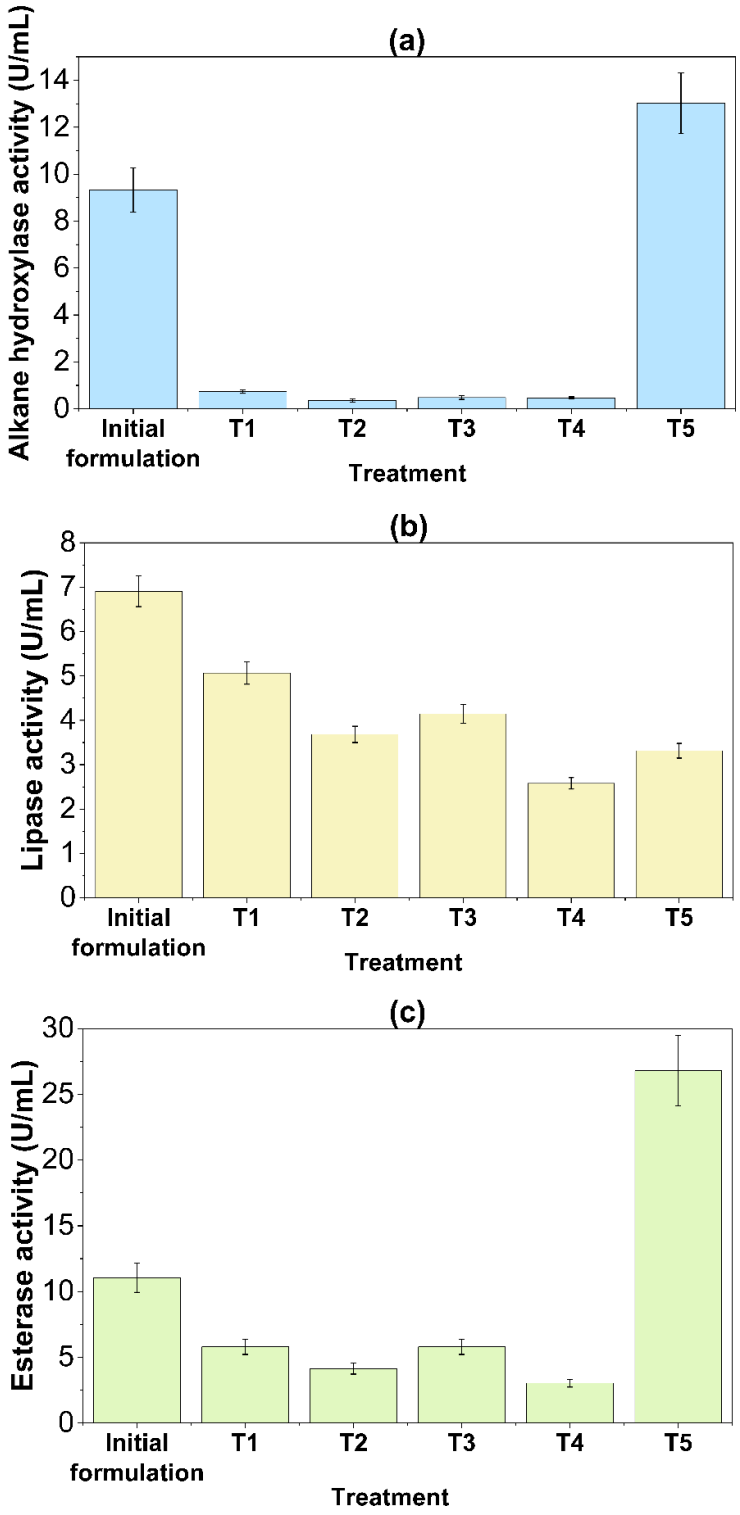


Figure 4.6. Maximum enzyme activity of T5 at 120 h and respective activity for different microcosms. T1: scaffold-immobilized enzyme; T2: scaffold-immobilized enzyme cross-linked with 0.02% GTA; T3: scaffold-immobilized bacteria; T4: scaffold-immobilized bacteria cross-linked with 0.02% GTA and T5= free *A. borkumensis* cells.

Overall, it is already known that the *A. borkumensis* enzymes exhibit a broad substrate profile, notable enantioselectivity, and high chemical resistance [91]. Furthermore, its halotolerance is higher compared with the same enzymes from other microorganisms, due to the presence of negatively charged residues such as glutamate and aspartate that contribute to the faster and increased activity observed for free cells even at elevated salinities [97], [98].

5.3.3 Ch80 scaffold as a tool for diesel degradation under brine conditions

Figure 4.7 shows the total petroleum hydrocarbon degradation after incubation scaffolds for 7 days.

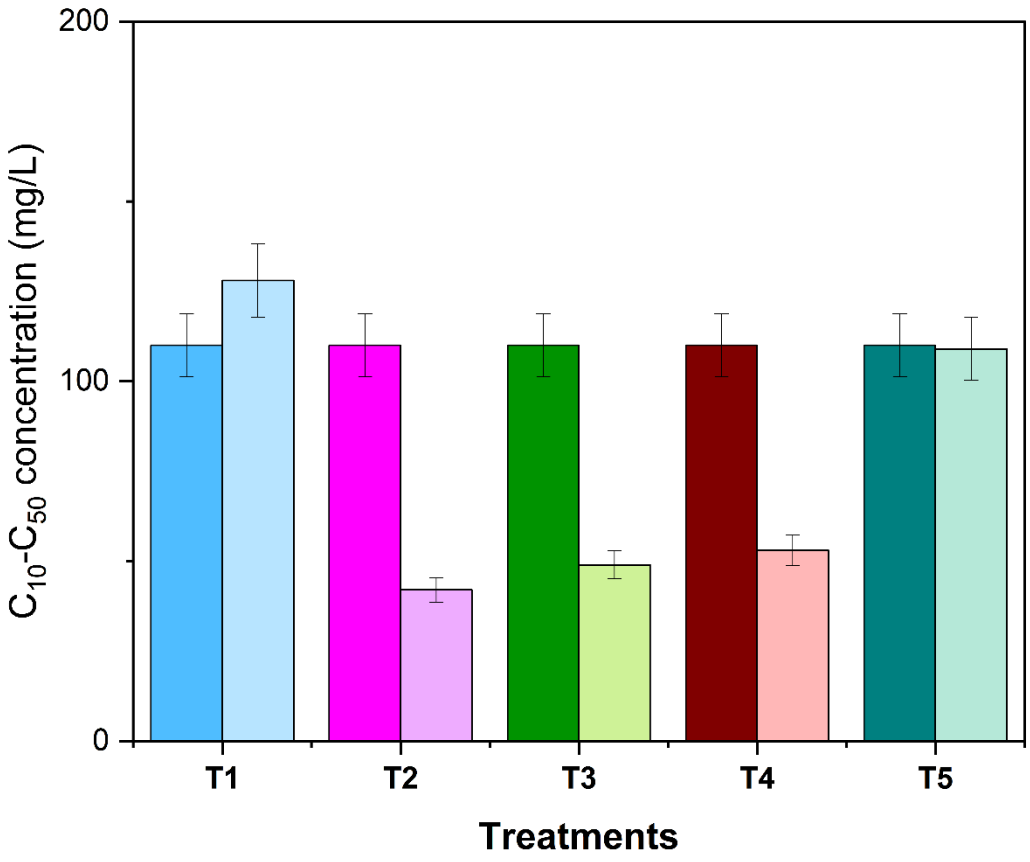


Figure 4.7. Degradative capability (expressed as C10-C50 petroleum hydrocarbons residue) of different microcosms T1: scaffold-immobilized enzyme; T2: scaffold-immobilized enzyme cross-linked with 0.02% GTA; T3: scaffold-immobilized bacteria; T4: scaffold-immobilized bacteria cross-linked with 0.02% GTA and T5= free *A. borkumensis* cells.

After 7 days, significant differences in total petroleum hydrocarbon degradation were observed

between the treatments. More than 61%, 55% and 51% diesel were degraded after 7 days on microcosms T2, T3 and T4, respectively. Fluctuations in the remaining diesel concentration were observed in microcosm T1, attributed to observed scaffold dissolution after the 7-day treatment and possibly enzyme washout in the media.

Adding glutaraldehyde as a cross-linker significantly improved the structural stability under a high salinity environment and led to enhanced degradation efficiency of T2 compared to microcosm T1. Conversely, microcosm T3 without the addition of GTA showed better degradative performance than T4. Although preventing cell damage during immobilization is challenging, the addition of GTA may reduce cell viability, as covalent binding is typically recommended for enzyme immobilization rather than whole-cell immobilization [143].

Glutaraldehyde likely enhanced scaffold stability, preventing enzyme washout and maintaining better catalytic activity over the incubation period. Improved scaffold's structural stability may protect immobilized enzymes from adverse effects of salinity and improve substrate-enzyme affinity, enhancing degradation rates. Several studies have shown that immobilized enzymes on various carriers exhibit reduced denaturation risk and resistance to environmental stress and shear forces [74]. For instance, Miri et al. (2021) [137] reported a 35% increase in BTEX degradation efficiency using Toluene/o-Xylene Monooxygenase and Catechol 1,2-dioxygenase enzymes from *Pseudomonas* strain S2TR-14 co-immobilized in a micro biochar-chitosan matrix compared to free enzymes. The authors attributed this to the reactive functional groups of chitosan and the bi-functional cross-linking potential of glutaraldehyde, which enhanced the binding capacity for multienzymes and material resistance, increasing biodegradation effectiveness [137].

Direct comparisons of microcosm T2 with different carrier-enzyme systems are challenging due to variations in experimental conditions and the limited number of studies on immobilized enzymes for diesel degradation. Nonetheless, microcosms T2, T3, and T4 demonstrated superior degrading performance compared to previous reports using immobilized cells for diesel degradation. For

instance, a diesel-degrading consortium of bacteria, fungi and yeasts immobilized into polyvinyl alcohol (PVA) degraded 53.5% diesel after 32 days [144]. Similarly, cinnamon shell microspheres were used as carriers for *Pseudomonas* YT-11 immobilization, achieving a diesel degradation rate of 69.57% in 5 days [145]. However, biodegradation experiments were conducted with an initial diesel concentration ten times lower (1% v/v) than the present study.

The chitosan scaffold provided a supportive and protective matrix that enhances the stability and activity of immobilized enzymes and bacteria. The porous structure of the scaffold likely facilitates better substrate access and retention, while the glutaraldehyde cross-linking further stabilizes the material and biocatalysts, preventing denaturation and washout. Under brine conditions of salinity, these factors are crucial for maintaining biodegradation activity, which is otherwise significantly reduced for free bacteria.

Conclusion

The present study showed a simple freeze-casting method for creating chitosan scaffolds that effectively immobilize *A. borkumensis* cells and enzymes, enhancing the removal of petroleum hydrocarbons in saline conditions. Cross-linking with glutaraldehyde (0.02% v/v) improved the immobilization of proteins up to 25.5% (39.1 μg/mL), which enhanced the structural integrity of scaffolds and consequently diesel degradation. The enzymes immobilized on the cross-linked scaffold demonstrated significant degradation of petroleum hydrocarbons, achieving over 61% degradation within 7 days. Overall, the produced scaffold demonstrated promising potential as a supportive matrix for enhancing the biodegradation of hydrocarbons under challenging salinity conditions.

5. CONCLUSIONS

5.1. *A. borkumensis* was able to utilize 10% v:v of diesel as the sole energy source simulating scenarios typical of oil spills with high carbon/nitrogen ratios.

5.2. Long-chain alkanes like heptacosane and tetratetracontane, and branched alkanes such as phytane present in diesel fuel, were degraded by *A. borkumensis* SK2 under saline conditions (0.6 M NaCl). Furthermore, short-chain alkanes, including octadecane, were also degraded under brine conditions (1.2 M NaCl).

5.3. The oxidative activity of the produced enzymes decreased under brine conditions (1.2 M NaCl), indicating osmotic and oxidative stress in *A. borkumensis* SK2 at high salinity concentrations.

5.4. The chitosan-scaffold fabricated at -80ºC (Ch80) exhibited a porous, honeycomb elongated morphology, providing an effective matrix for maintaining enzyme and cell activity.

5.5. Enzyme stability and hydrocarbon degradation efficiency under brine conditions (1.2 M NaCl) were enhanced by immobilizing *A. borkumensis* oxidative enzymes on freeze-cast chitosan scaffolds reinforced with glutaraldehyde (0.02% v/v).

6. RECOMMENDATIONS

6.1. Optimization of immobilization: While the chitosan scaffold demonstrated promising results, further optimization of the immobilization process should be explored. This includes testing different cross-linking agents and concentrations to maximize enzyme activity and longevity. Recyclability studies are also recommended to evaluate the leaching of enzymes after the reuse of scaffolds.

6.2. Reusability and stability studies: A robust immobilization support system should also be reusable. It is recommended to conduct studies on the chitosan scaffold to assess its potential for repeated use in petroleum hydrocarbon degradation. Additionally, long-term stability tests (over 30 days) should be performed under brine conditions to evaluate the half-life and performance of the immobilized system (material and enzymes).

6.3. Optimization of diesel recovery for quantification analysis: Throughout this study, extracting

diesel from the fermented broth of *A. borkumensis* presented challenges as it is already known that the bacteria produce biosurfactants for hydrocarbon emulsification. The presence of biosurfactants appears to affect diesel extraction. Therefore, optimizing diesel extraction from the fermented broth of *A. borkumensis* is necessary to improve the accuracy of quantification using chromatographic analysis.

6.4. Exploration of synergistic effects: Investigating the synergistic effects of combining *A. borkumensis* with other hydrocarbon-degrading microorganisms could enhance the overall degradation efficiency. Co-culturing different species or strains may improve the breakdown of a broader range of hydrocarbons in complex oil mixtures at high salinities.

6.5. Scale-up and field testing: The effectiveness of the immobilized enzymes and bacteria should be tested in larger-scale bioremediation projects and real-world marine environments. Field studies would provide valuable data on the practical application of this technology and its potential impact on environmental remediation efforts.

6.5. Environmental and economic feasibility studies: Comprehensive studies on the environmental impact, cost-effectiveness, and sustainability of using immobilized *A. borkumensis* and its oxidative enzymes for large-scale oil spill remediation in saline environments should be conducted. These studies would help to determine the practical viability of this bioremediation approach in various settings.

BIBLIOGRAPHY

[1] Varjani S, Pandey A, Upasani VN. Oilfield waste treatment using novel hydrocarbon utilizing bacterial consortium — A microcosm approach. *Science of The Total Environment*. 2020;745:141043. doi:10.1016/J.SCITOTENV.2020.141043

[2] Varjani SJ, Upasani VN. A new look on factors affecting microbial degradation of petroleum hydrocarbon pollutants. *Int Biodeterior Biodegradation*. 2017;120:71-83. doi:10.1016/J.IBIOD.2017.02.006

[3] Atlas RM, Stoeckel DM, Faith SA, Minard-Smith A, Thorn JR, Benotti MJ. Oil Biodegradation and Oil-Degrading Microbial Populations in Marsh Sediments Impacted by Oil from the Deepwater Horizon Well Blowout. Published online 2015. doi:10.1021/acs.est.5b00413

[4] Hazen TC, Prince RC, Mahmoudi N. Marine Oil Biodegradation. Published online 2015. doi:10.1021/acs.est.5b03333

[5] Paul VG, Mormile MR. A case for the protection of saline and hypersaline environments: a microbiological perspective. *FEMS Microbiol Ecol*. 2017;93:91. doi:10.1093/femsec/fix091

[6] Fathepure BZ. Recent studies in microbial degradation of petroleum hydrocarbons in hypersaline environments. *Front Microbiol*. 2014;5. doi:10.3389/fmicb.2014.00173

[7] Abou Khalil C, Prince VL, Prince RC, et al. Occurrence and biodegradation of hydrocarbons at high salinities. *Science of The Total Environment*. 2021;762:143165. doi:10.1016/j.scitotenv.2020.143165

[8] Rezaei Somee M, Dastgheib SMM, Shavandi M, et al. Distinct microbial community along the chronic oil pollution continuum of the Persian Gulf converge with oil spill accidents. *Sci Rep*. 2021;11(1):11316. doi:10.1038/s41598-021-90735-0

[9] Mapelli F, Scoma A, Michoud G, et al. Biotechnologies for Marine Oil Spill Cleanup: Indissoluble Ties with Microorganisms. *Trends Biotechnol*. 2017;35(9):860-870. doi:10.1016/j.tibtech.2017.04.003

[10] Jimoh AA, Ikhimiukor OO, Adeleke R. Prospects in the bioremediation of petroleum hydrocarbon contaminants from hypersaline environments: A review. *Environmental Science and Pollution Research*. 2022;29(24):35615-35642. doi:10.1007/s11356-022-19299-4

[11] Kleindienst S, Paul JH, Joye SB. Using dispersants after oil spills: impacts on the composition and activity of microbial communities. *Nat Rev Microbiol*. 2015;13(6):388-396. doi:10.1038/nrmicro3452

[12] Kleindienst S, Seidel M, Ziervogel K, et al. Chemical dispersants can suppress the activity of natural oil-degrading microorganisms. *Proceedings of the National Academy of Sciences*. 2015;112(48):14900-14905. doi:10.1073/pnas.1507380112

[13] Mahjoubi M, Cappello S, Souissi Y, Jaouani A, Cherif A. Microbial Bioremediation of Petroleum Hydrocarbon– Contaminated Marine Environments. In: *Recent Insights in Petroleum Science and Engineering*. InTech; 2018. doi:10.5772/intechopen.72207

[14] Roy A, Dutta A, Pal S, et al. Biostimulation and bioaugmentation of native microbial community accelerated bioremediation of oil refinery sludge. *Bioresour Technol*. 2018;253:22-32. doi:10.1016/J.BIORTECH.2018.01.004

[15] Bezza FA CE. Petroleum Hydrocarbon Spills in the Environment and Abundance of Microbial Community Capable of Biosurfactant Production. *J Pet Environ Biotechnol*. 2015;06(05). doi:10.4172/2157-7463.1000237

[16] Ebadi A, Khoshkholgh Sima NA, Olamaee M, Hashemi M, Ghorbani Nasrabadi R. Effective bioremediation of a petroleum-polluted saline soil by a surfactant-producing Pseudomonas aeruginosa consortium. *J Adv Res*. 2017;8(6):627-633. doi:10.1016/j.jare.2017.06.008

[17] Davoodi SM, Miri S, Taheran M, Brar SK, Galvez-Cloutier R, Martel R. Bioremediation of Unconventional Oil Contaminated Ecosystems under Natural and Assisted Conditions: A Review. *Environ Sci Technol*. 2020;54(4):2054-2067. doi:10.1021/acs.est.9b00906

[18] Li J, Gao Y, Dong H, Sheng GP. Haloarchaea, excellent candidates for removing pollutants from hypersaline wastewater. *Trends Biotechnol*. 2022;40(2):226-239. doi:10.1016/j.tibtech.2021.06.006

[19] Miri S, Naghdi M, Rouissi T, Kaur Brar S, Martel R. Recent biotechnological advances in petroleum hydrocarbons degradation under cold climate conditions: A review. *Crit Rev Environ Sci Technol*. 2019;49(7):553-586. doi:10.1080/10643389.2018.1552070

[20] Mokashe N, Chaudhari B, Patil U. Operative utility of salt-stable proteases of halophilic and halotolerant bacteria in the biotechnology sector. *Int J Biol Macromol*. 2018;117:493-522. doi:10.1016/j.ijbiomac.2018.05.217

[21] Kuppusamy S, Maddela NR, Megharaj M, Venkateswarlu K. An Overview of Total Petroleum Hydrocarbons. In: *Total Petroleum Hydrocarbons*. Springer International Publishing; 2020:1-27. doi:10.1007/978-3-030-24035-6_1

[22] Guo G, Fang T, Wang C, Huang Y, Cui Q, Wang H. Isolation and characterization of two novel halotolerant Catechol 2, 3-dioxygenases from a halophilic bacterial consortium OPEN. *Nature Publishing Group*. 2015;5:17603. doi:10.1038/srep17603

[23] Guo W, Zhou W, Zhou H, Chen X. Characterization of enzymatic properties of two novel enzymes, 3,4-dihydroxyphenylacetate dioxygenase and 4-hydroxyphenylacetate 3-hydroxylase, from Sulfobacillus acidophilus TPY. *BMC Microbiol*. 2019;19(1). doi:10.1186/s12866-019-1415-9

[24] Li H, Meng F, Duan W, Lin Y, Zheng Y. Biodegradation of phenol in saline or hypersaline environments by bacteria: A review. *Ecotoxicol Environ Saf*. 2019;184:109658. doi:10.1016/J.ECOENV.2019.109658

[25] Liu YC, Li LZ, Wu Y, et al. Isolation of an alkane-degrading Alcanivorax sp. strain 2B5 and cloning of the alkB gene. *Bioresour Technol*. 2010;101(1):310-316. doi:10.1016/j.biortech.2009.08.028

[26] SadrAzodi SM, Shavandi M, Amoozegar MA, Mehrnia MR. Biodegradation of long chain alkanes in halophilic conditions by Alcanivorax sp. strain Est-02 isolated from saline soil. *3 Biotech*.

2019;9(4):141. doi:10.1007/s13205-019-1670-3

[27] Budiyanto F, Thukair A, Al-Momani M, Musa MM, Nzila A. Characterization of Halophilic Bacteria Capable of Efficiently Biodegrading the High-Molecular-Weight Polycyclic Aromatic Hydrocarbon Pyrene. *Environ Eng Sci*. 2018;35(6):616-626. doi:10.1089/ees.2017.0244

[28] Hassan HA, Aly AA. Isolation and characterization of three novel catechol 2,3-dioxygenase from three novel haloalkaliphilic BTEX-degrading Pseudomonas strains. *Int J Biol Macromol*. 2018;106:1107-1114. doi:10.1016/j.ijbiomac.2017.08.113

[29] Neifar M, Chouchane H, Najjari A, et al. Genome analysis provides insights into crude oil degradation and biosurfactant production by extremely halotolerant Halomonas desertis G11 isolated from Chott El-Djerid salt-lake in Tunisian desert. *Genomics*. 2019;111(6):1802-1814. doi:10.1016/j.ygeno.2018.12.003

[30] Al-Mailem DM, Eliyas • M, Khanafer • M, Radwan • S S. Biofilms constructed for the removal of hydrocarbon pollutants from hypersaline liquids. Published online 2015. doi:10.1007/s00792-014-0698-x

[31] Khemili-Talbi S, Kebbouche-Gana S, Akmoussi-Toumi S, et al. Biodegradation of Petroleum hydrocarbons and Biosurfactant production by an extremely halophilic Archaea Halovivax sp. A21 ARTICLE INFO ABSTRACT/RESUME. *Algerian Journal of Environmental Science and Technology December edition*. 2017;3. www.aljest.org

[32] Gutierrez T, Singleton DR, Berry D, Yang T, Aitken MD, Teske A. Hydrocarbon-degrading bacteria enriched by the Deepwater Horizon oil spill identified by cultivation and DNA-SIP. *ISME J*. 2091;7:2091-2104. doi:10.1038/ismej.2013.98

[33] Varjani SJ. Microbial degradation of petroleum hydrocarbons. *Bioresour Technol*. 2017;223:277-286. doi:10.1016/J.BIORTECH.2016.10.037

[34] Govarthanan M, Khalifa AYZ, Kamala-Kannan S, et al. Significance of allochthonous brackish water Halomonas sp. on biodegradation of low and high molecular weight polycyclic aromatic hydrocarbons. *Chemosphere*. 2020;243:125389. doi:10.1016/j.chemosphere.2019.125389

[35] Edbeib MF, Wahab RA, Huyop F. Halophiles: biology, adaptation, and their role in decontamination of hypersaline environments. *World J Microbiol Biotechnol*. 2016;32(8):135. doi:10.1007/s11274-016-2081-9

[36] Bonfá MRL, Grossman MJ, Mellado E, Durrant LR. Biodegradation of aromatic hydrocarbons by Haloarchaea and their use for the reduction of the chemical oxygen demand of hypersaline petroleum produced water. *Chemosphere*. 2011;84(11):1671-1676. doi:10.1016/j.chemosphere.2011.05.005

[37] Temerk H. Isolation and characterization of Haloferax mucsum from Red sea saltern as an halobacterial Archea capable of growing on Naphtaline as an aromatic compounds. *THE EGYPTIAN JOURNAL OF EXPERIMENTAL BIOLOGY (Botany)*. 2019;(0):1. doi:10.5455/egyjebb.20181126081938

[38] Erdoğmuş SF, Mutlu B, Korcan SE, Güven K, Konuk M. Aromatic Hydrocarbon Degradation by Halophilic Archaea Isolated from Çamaltı Saltern, Turkey. *Water Air Soil Pollut*. 2013;224(3):1449. doi:10.1007/s11270-013-1449-9

[39] Dalvi S, Youssef NH, Fathepure BZ. Microbial community structure analysis of a benzoate-degrading halophilic archaeal enrichment. *Extremophiles*. 2016;20:311-321. doi:10.1007/s00792-016-0823-0

[40] Dombrowski N, Donaho JA, Gutierrez T, Seitz KW, Teske AP, Baker BJ. Reconstructing metabolic pathways of hydrocarbon-degrading bacteria from the Deepwater Horizon oil spill. *Nat Microbiol*. 2016;1(7):16057. doi:10.1038/nmicrobiol.2016.57

[41] Kadri T, Miri S, Robert T, et al. Pilot-scale production and in-situ application of petroleum-degrading enzyme cocktail from *Alcanivorax borkumensis*. *Chemosphere*. 2022;295:133840. doi:10.1016/j.chemosphere.2022.133840

[42] Toshchakov S V., Korzhenkov AA, Chernikova TN, et al. The genome analysis of Oleiphilus messinensis ME102 (DSM 13489 T) reveals backgrounds of its obligate alkane-devouring marine lifestyle. *Mar Genomics*. 2017;36:41-47. doi:10.1016/j.margen.2017.07.005

[43] Golyshin PN, Chernikova TN, Abraham WR, Lünsdorf H, Timmis KN, Yakimov MM. Oleiphilaceae fam. nov., to include Oleiphilus messinensis gen. nov., sp. nov., a novel marine bacterium that obligately utilizes hydrocarbons. *Int J Syst Evol Microbiol*. 2002;52(3):901-911. doi:10.1099/00207713-52-3-901

[44] Yakimov MM, Giuliano L, Gentile G, et al. Oleispira antarctica gen. nov., sp. nov., a novel hydrocarbonoclastic marine bacterium isolated from Antarctic coastal sea water. *Int J Syst Evol Microbiol*. 2003;53(3):779-785. doi:10.1099/ijs.0.02366-0

[45] Yakimov MM, Giuliano L, Denaro R, et al. Thalassolituus oleivorans gen. nov., sp. nov., a novel marine bacterium that obligately utilizes hydrocarbons. *Int J Syst Evol Microbiol*. 2004;54(1):141-148. doi:10.1099/ijs.0.02424-0

[46] Zhou H, Wang H, Huang Y, Fang T. Characterization of pyrene degradation by halophilic Thalassospira sp. strain TSL5-1 isolated from the coastal soil of Yellow Sea, China. *Int Biodeterior Biodegradation*. 2016;107:62-69. doi:10.1016/j.ibiod.2015.10.022

[47] Gomes MB, Gonzales-Limache EE, Sousa STP, et al. Exploring the potential of halophilic bacteria from oil terminal environments for biosurfactant production and hydrocarbon degradation under high-salinity conditions. *Int Biodeterior Biodegradation*. 2018;126:231-242. doi:10.1016/J.IBIOD.2016.08.014

[48] Tourova TP, Sokolova DS, Semenova EM, Ershov AP, Grouzdev DS, Nazina TN. Genomic and Physiological Characterization of Halophilic Bacteria of the Genera Halomonas and Marinobacter from Petroleum Reservoirs. *Microbiology (N Y)*. 2022;91(3):235-248. doi:10.1134/S0026261722300038

[49] Wang C, Huang Y, Zhang Z, Wang H. Salinity effect on the metabolic pathway and microbial function

in phenanthrene degradation by a halophilic consortium. *AMB Express*. 2018;8(1):67. doi:10.1186/s13568-018-0594-3

[50] Dastgheib SMM, Amoozegar MA, Khajeh K, Ventosa A. A halotolerant Alcanivorax sp. strain with potential application in saline soil remediation. *Appl Microbiol Biotechnol*. 2011;90(1):305-312. doi:10.1007/s00253-010-3049-6

[51] Hassanshahian M, Yakimov MM, Denaro R, Genovese M, Cappello S. Using Real-time PCR to assess changes in the crude oil degrading microbial community in contaminated seawater mesocosms. *Int Biodeterior Biodegradation*. 2014;93:241-248. doi:10.1016/j.ibiod.2014.06.006

[52] Chen W, Kong Y, Li J, Sun Y, Min J, Hu X. Enhanced biodegradation of crude oil by constructed bacterial consortium comprising salt-tolerant petroleum degraders and biosurfactant producers. *Int Biodeterior Biodegradation*. 2020;154:105047. doi:10.1016/J.IBIOD.2020.105047

[53] Dahal RH, Chaudhary DK, Kim J. Acinetobacter halotolerans sp. nov., a novel halotolerant, alkalitolerant, and hydrocarbon degrading bacterium, isolated from soil. *Arch Microbiol*. 2017;199(5):701-710. doi:10.1007/s00203-017-1349-2

[54] Khemili-Talbi S, Kebbouche-Gana S, Akmoussi-Toumi S, Angar Y, Gana ML. Isolation of an extremely halophilic arhaeon Natrialba sp. C21 able to degrade aromatic compounds and to produce stable biosurfactant at high salinity. *Extremophiles*. 2015;19(6):1109-1120. doi:10.1007/s00792-015-0783-9

[55] Al-Mailem DM, Sorkhoh NA, Al-Awadhi H, Eliyas M, Radwan SS. Biodegradation of crude oil and pure hydrocarbons by extreme halophilic archaea from hypersaline coasts of the Arabian Gulf. *Extremophiles*. 2010;14(3):321-328. doi:10.1007/s00792-010-0312-9

[56] Cao B, Nagarajan K, Loh KC. Biodegradation of aromatic compounds: current status and opportunities for biomolecular approaches. *Appl Microbiol Biotechnol*. 2009;85(2):207-228. doi:10.1007/s00253-009-2192-4

[57] Peixoto RS, Vermelho AB, Rosado AS. Petroleum-degrading enzymes: Bioremediation and new prospects. *Enzyme Res*. 2011;2011(1). doi:10.4061/2011/475193

[58] Nie Y, Chi CQ, Fang H, et al. Diverse alkane hydroxylase genes in microorganisms and environments. *Sci Rep*. 2014;4(1):4968. doi:10.1038/srep04968

[59] Hassanshahian M, Bayat Z, Cappello S, Smedile F, Yakimov M. Comparison the effects of bioaugmentation versus biostimulation on marine microbial community by PCR–DGGE: A mesocosm scale. *Journal of Environmental Sciences*. 2016;43:136-146. doi:10.1016/j.jes.2015.09.013

[60] Wang W, Shao Z. The long-chain alkane metabolism network of Alcanivorax dieselolei. *Nat Commun*. 2014;5(1):5755. doi:10.1038/ncomms6755

[61] Wang C, Guo G, Huang Y, Hao H, Wang H. Salt Adaptation and Evolutionary Implication of a Nah-related PAHs Dioxygenase cloned from a Halophilic Phenanthrene Degrading Consortium. *Sci Rep*.

2017;7(1):12525. doi:10.1038/s41598-017-12979-z

[62] Akbari A, David C, Rahim AA, Ghoshal S. Salt selected for hydrocarbon-degrading bacteria and enhanced hydrocarbon biodegradation in slurry bioreactors. *Water Res*. 2021;202:117424. doi:10.1016/j.watres.2021.117424

[63] Guo G, He F, Tian F, Huang Y, Wang H. Effect of salt contents on enzymatic activities and halophilic microbial community structure during phenanthrene degradation. *Int Biodeterior Biodegradation*. 2016;110:8-15. doi:10.1016/j.ibiod.2016.02.007

[64] Fang T, Pan R, Jiang J, He F, Wang H. Effect of salinity on community structure and naphthalene dioxygenase gene diversity of a halophilic bacterial consortium. *Front Environ Sci Eng*. 2016;10(6):16. doi:10.1007/s11783-016-0888-0

[65] Kumar S, Zhou J, Li M, Xiang H, Zhao D. Insights into the metabolism pathway and functional genes of long-chain aliphatic alkane degradation in haloarchaea. *Extremophiles*. 2020;24(4):475-483. doi:10.1007/s00792-020-01167-z

[66] Pacholak A, Gao ZL, Gong XY, Kaczorek E, Cui YW. The metabolic pathways of polyhydroxyalkanoates and exopolysaccharides synthesized by Haloferax mediterranei in response to elevated salinity. *J Proteomics*. 2021;232:104065. doi:10.1016/j.jprot.2020.104065

[67] Huang L, Hu H, Tang H, et al. Identification and Characterization of a Novel Gentisate 1,2-Dioxygenase Gene from a Halophilic Martelella Strain. *Sci Rep*. 2015;5(1):14307. doi:10.1038/srep14307

[68] Amoozegar MA, Siroosi M, Atashgahi S, Smidt H, Ventosa A. Systematics of haloarchaea and biotechnological potential of their hydrolytic enzymes. *Microbiology (United Kingdom)*. 2017;163(5):623-645. doi:10.1099/mic.0.000463

[69] Allers T. Overexpression and purification of halophilic proteins in *Haloferax volcanii*. *Bioeng Bugs*. 2010;1(4):290-292. doi:10.4161/bbug.1.4.11794

[70] Riffaldi R, Levi-Minzi R, Cardelli R, Palumbo S, Saviozzi A. Soil Biological Activities in Monitoring the Bioremediation of Diesel Oil-Contaminated Soil. *Water Air Soil Pollut*. 2006;170(1-4):3-15. doi:10.1007/s11270-006-6328-1

[71] Tutuncu HE, Balci N, Tuter M, Karaguler NG. Recombinant production and characterization of a novel esterase from a hypersaline lake, Acıgöl, by metagenomic approach. *Extremophiles*. 2019;23(5):507-520. doi:10.1007/s00792-019-01103-w

[72] Alsafadi D, Paradisi F. Covalent Immobilization of Alcohol Dehydrogenase (ADH2) from Haloferax volcanii: How to Maximize Activity and Optimize Performance of Halophilic Enzymes. *Mol Biotechnol*. 2014;56(3):240-247. doi:10.1007/s12033-013-9701-5

[73] Kadri T, Cuprys A, Rouissi T, Brar SK, Daghrir R, Lauzon JM. Nanoencapsulation and release study of enzymes from *Alcanivorax borkumensis* in chitosan-tripolyphosphate formulation. *Biochem Eng J*. 2018;137:1-10. doi:10.1016/j.bej.2018.05.013

[74] Somu P, Narayanasamy S, Gomez LA, Rajendran S, Lee YR, Balakrishnan D. Immobilization of enzymes for bioremediation: A future remedial and mitigating strategy. *Environ Res*. 2022;212:113411. doi:10.1016/J.ENVRES.2022.113411

[75] Shao Y, Liao Z, Gao B, He B. Emerging 3D Printing Strategies for Enzyme Immobilization: Materials, Methods, and Applications. *ACS Omega*. 2022;7(14):11530-11543. doi:10.1021/acsomega.2c00357

[76] Carucci C, Bruen L, Gascón V, Paradisi F, Magner E. Significant Enhancement of Structural Stability of the Hyperhalophilic ADH from *Haloferax volcanii* via Entrapment on Metal Organic Framework Support. *Langmuir*. 2018;34(28):8274-8280. doi:10.1021/acs.langmuir.8b01037

[77] *Review of Maritime Transport 2023*.; 2023. https://shop.un.org/

[78] Zdarta A, Smułek W, Pacholak A, Dudzińska-Bajorek B, Kaczorek E. Surfactant addition in diesel oil degradation – how can it help the microbes? *J Environ Health Sci Eng*. 2020;18(2):677-686. doi:10.1007/s40201-020-00494-9

[79] Lominchar MA, Santos A, de Miguel E, Romero A. Remediation of aged diesel contaminated soil by alkaline activated persulfate. *Science of The Total Environment*. 2018;622-623:41-48. doi:10.1016/j.scitotenv.2017.11.263

[80] Gregson BH, Metodieva G, Metodiev M V., McKew BA. Differential protein expression during growth on linear versus branched alkanes in the obligate marine hydrocarbon-degrading bacterium *Alcanivorax borkumensis* SK2 ^{T}. *Environ Microbiol*. 2019;21(7):2347-2359. doi:10.1111/1462-2920.14620

[81] Prasad M, Obana N, Lin SZ, et al. *Alcanivorax borkumensis* biofilms enhance oil degradation by interfacial tubulation. *Science (1979)*. 2023;381(6659):748-753. doi:10.1126/science.adf3345

[82] Cui J, Hölzl G, Karmainski T, et al. The Glycine-Glucolipid of *Alcanivorax borkumensis* Is Resident to the Bacterial Cell Wall. *Appl Environ Microbiol*. 2022;88(16). doi:10.1128/aem.01126-22

[83] Bradford MM. A rapid and sensitive method for the quantitation of microgram quantities of protein utilizing the principle of protein-dye binding. *Anal Biochem*. 1976;72(1-2):248-254. doi:10.1016/0003-2697(76)90527-3

[84] Mishra S, Singh SN. Microbial degradation of n-hexadecane in mineral salt medium as mediated by degradative enzymes. *Bioresour Technol*. 2012;111:148-154. doi:10.1016/j.biortech.2012.02.049

[85] Jauhari N, Mishra S, Kumari B, Singh SN. Bacteria-mediated aerobic degradation of hexacosane in vitro conditions. *Bioresour Technol*. 2014;170:62-68. doi:10.1016/j.biortech.2014.07.091

[86] Scoma A, Boon N. Osmotic Stress Confers Enhanced Cell Integrity to Hydrostatic Pressure but Impairs Growth in *Alcanivorax borkumensis* SK2. *Front Microbiol*. 2016;7. doi:10.3389/fmicb.2016.00729

[87] Deng S, Wang B, Zhang H, et al. Degradation and enhanced oil recovery potential of *Alcanivorax borkumensis* through production of bio-enzyme and bio-surfactant. *Bioresour Technol*. 2024;400:130690. doi:10.1016/j.biortech.2024.130690

[88] Yakimov MM, Golyshin PN, Lang S, et al. *Alcanivorax borkumensis* gen. nov., sp. nov., a new, hydrocarbon-degrading and surfactant-producing marine bacterium. *Int J Syst Bacteriol*. 1998;48(2):339-348. doi:10.1099/00207713-48-2-339

[89] Sabirova JS, Ferrer M, Regenhardt D, Timmis KN, Golyshin PN. Proteomic Insights into Metabolic Adaptations in *Alcanivorax borkumensis* Induced by Alkane Utilization. *J Bacteriol*. 2006;188(11):3763-3773. doi:10.1128/JB.00072-06

[90] Russell NJ. Adaptive modifications in membranes of halotolerant and halophilic microorganisms. *J Bioenerg Biomembr*. 1989;21(1):93-113. doi:10.1007/BF00762214

[91] Schneiker S, dos Santos VAM, Bartels D, et al. Genome sequence of the ubiquitous hydrocarbon-degrading marine bacterium *Alcanivorax borkumensis*. *Nat Biotechnol*. 2006;24(8):997-1004. doi:10.1038/nbt1232

[92] Nekouei F, Nekouei S. Enhanced enzymatic and *ex situ* biodegradation of petroleum hydrocarbons in solutions using *Alcanivorax borkumensis* enzymes in the presence of nitrogen and phosphorus co-doped reduced graphene oxide as a bacterial growth enhancer. *J Mater Chem A Mater*. 2017;5(46):24462-24471. doi:10.1039/C7TA05225A

[93] Kadri T, Rouissi T, Magdouli S, et al. Production and characterization of novel hydrocarbon degrading enzymes from *Alcanivorax borkumensis*. *Int J Biol Macromol*. 2018;112:230-240. doi:10.1016/j.ijbiomac.2018.01.177

[94] Cortés-Lorenzo C, Rodríguez-Díaz M, López-Lopez C, Sánchez-Peinado M, Rodelas B, González-López J. Effect of salinity on enzymatic activities in a submerged fixed bed biofilm reactor for municipal sewage treatment. *Bioresour Technol*. 2012;121:312-319. doi:10.1016/j.biortech.2012.06.083

[95] Suganthi SH, Murshid S, Sriram S, Ramani K. Enhanced biodegradation of hydrocarbons in petroleum tank bottom oil sludge and characterization of biocatalysts and biosurfactants. *J Environ Manage*. 2018;220:87-95. doi:10.1016/J.JENVMAN.2018.04.120

[96] Margesin R, Labbé D, Schinner F, Greer CW, Whyte LG. Characterization of Hydrocarbon-Degrading Microbial Populations in Contaminated and Pristine Alpine Soils. *Appl Environ Microbiol*. 2003;69(6):3085-3092. doi:10.1128/AEM.69.6.3085-3092.2003

[97] Hajighasemi M, Nocek BP, Tchigvintsev A, et al. Biochemical and Structural Insights into Enzymatic Depolymerization of Polylactic Acid and Other Polyesters by Microbial Carboxylesterases. *Biomacromolecules*. 2016;17(6):2027-2039. doi:10.1021/acs.biomac.6b00223

[98] Tchigvintsev A, Tran H, Popovic A, et al. The environment shapes microbial enzymes: five cold-active and salt-resistant carboxylesterases from marine metagenomes. *Appl Microbiol Biotechnol*. 2015;99(5):2165-2178. doi:10.1007/s00253-014-6038-3

[99] Swathi K V., Muneeswari R, Ramani K, Sekaran G. Biodegradation of petroleum refining industry oil sludge by microbial-assisted biocarrier matrix: process optimization using response surface methodology. *Biodegradation*. 2020;31(4-6):385-405. doi:10.1007/s10532-020-09916-9

[100] Khalid FE, Lim ZS, Sabri S, Gomez-Fuentes C, Zulkharnain A, Ahmad SA. Bioremediation of Diesel Contaminated Marine Water by Bacteria: A Review and Bibliometric Analysis. *J Mar Sci Eng*. 2021;9(2):155. doi:10.3390/jmse9020155

[101] Ferradji FZ, Mnif S, Badis A, et al. Naphthalene and crude oil degradation by biosurfactant producing Streptomyces spp. isolated from Mitidja plain soil (North of Algeria). *Int Biodeterior Biodegradation*. 2014;86:300-308. doi:10.1016/j.ibiod.2013.10.003

[102] Muthukamalam S, Sivagangavathi S, Dhrishya D, Sudha Rani S. Characterization of dioxygenases and biosurfactants produced by crude oil degrading soil bacteria. *Brazilian Journal of Microbiology*. 2017;48(4):637-647. doi:10.1016/j.bjm.2017.02.007

[103] Czarnocka J, Matuszewska A, Odziemkowska M. Autoxidation of Fuels During Storage. In: *Storage Stability of Fuels*. InTech; 2015. doi:10.5772/59807

[104] Zhao F, Wang P, Lucardi R, Su Z, Li S. Natural Sources and Bioactivities of 2,4-Di-Tert-Butylphenol and Its Analogs. *Toxins (Basel)*. 2020;12(1):35. doi:10.3390/toxins12010035

[105] Imlay JA. The molecular mechanisms and physiological consequences of oxidative stress: lessons from a model bacterium. *Nat Rev Microbiol*. 2013;11(7):443-454. doi:10.1038/nrmicro3032

[106] Liu C, Wang W, Wu Y, Zhou Z, Lai Q, Shao Z. Multiple alkane hydroxylase systems in a marine alkane degrader, *Alcanivorax dieselolei* B-5. *Environ Microbiol*. 2011;13(5):1168-1178. doi:10.1111/j.1462-2920.2010.02416.x

[107] Wang W, Shao Z. Enzymes and genes involved in aerobic alkane degradation. *Front Microbiol*. 2013;4. doi:10.3389/fmicb.2013.00116

[108] Yakimov MM, Timmis KN, Golyshin PN. Obligate oil-degrading marine bacteria. *Curr Opin Biotechnol*. 2007;18(3):257-266. doi:10.1016/j.copbio.2007.04.006

[109] Guntupalli S, Thunuguntla VBSC, Santha Reddy K, Issac Newton M, Rao C V., Bondili JS. Enhanced Degradation of Carcinogenic PAHs Benzo (a) Pyrene and Benzo (k) Fluoranthene by a Microbial Consortia. *Indian J Sci Technol*. 2016;9(35). doi:10.17485/ijst/2016/v9i35/93590

[110] Rojo F. Degradation of alkanes by bacteria. *Environ Microbiol*. 2009;11(10):2477-2490. doi:10.1111/j.1462-2920.2009.01948.x

[111] Khatoon K, Malik A. Cyto-genotoxic potential of petroleum refinery wastewater mixed with domestic sewage used for irrigation of food crops in the vicinity of an oil refinery. *Heliyon*. 2021;7(10):e08116. doi:10.1016/j.heliyon.2021.e08116

[112] de Carvalho JC, Goyzueta-Mamani LD, Molina-Aulestia DT, et al. Microbial Astaxanthin

Production from Agro-Industrial Wastes—Raw Materials, Processes, and Quality. *Fermentation*. 2022;8(10):484. doi:10.3390/fermentation8100484

[113] Varnava CK, Grenni P, Mariani L, et al. Characterization, production optimization and ecotoxicity of a lipopeptide biosurfactant by Pseudomonas citronellolis using oily wastewater. *Biochem Eng J*. 2024;205:109257. doi:10.1016/j.bej.2024.109257

[114] Ullah A, Bano A. Modulation of Secondary Metabolites: A Halotolerance Strategy of Plant Growth Promoting Rhizobacteria Against Sodium Chloride Stress. *Curr Microbiol*. 2021;78(12):4050-4059. doi:10.1007/s00284-021-02647-x

[115] Jiménez S, Micó MM, Arnaldos M, Medina F, Contreras S. State of the art of produced water treatment. *Chemosphere*. 2018;192:186-208. doi:10.1016/j.chemosphere.2017.10.139

[116] Amakiri KT, Canon AR, Molinari M, Angelis-Dimakis A. Review of oilfield produced water treatment technologies. *Chemosphere*. 2022;298:134064. doi:10.1016/j.chemosphere.2022.134064

[117] Sabir S. Approach of Cost-Effective Adsorbents for Oil Removal from Oily Water. *Crit Rev Environ Sci Technol*. 2015;45(17):1916-1945. doi:10.1080/10643389.2014.1001143

[118] Wolok E, Barafi J, Joshi N, Girimonte R, Chakraborty S. Study of bio-materials for removal of the oil spill. *Arabian Journal of Geosciences*. 2020;13(23):1244. doi:10.1007/s12517-020-06244-3

[119] Dutta PK, Ravikumar MN V., Dutta J. CHITIN AND CHITOSAN FOR VERSATILE APPLICATIONS. *Journal of Macromolecular Science, Part C: Polymer Reviews*. 2002;42(3):307-354. doi:10.1081/MC-120006451

[120] Ababneh H, Hameed BH. Chitosan-derived hydrothermally carbonized materials and its applications: A review of recent literature. *Int J Biol Macromol*. 2021;186:314-327. doi:10.1016/j.ijbiomac.2021.06.161

[121] Pellá MCG, Lima-Tenório MK, Tenório-Neto ET, Guilherme MR, Muniz EC, Rubira AF. Chitosan-based hydrogels: From preparation to biomedical applications. *Carbohydr Polym*. 2018;196:233-245. doi:10.1016/j.carbpol.2018.05.033

[122] Pereira A, Cartucho D, Duarte A, et al. Immobilisation of Cardosin A in Chitosan Sponges as a Novel Implant for Drug Delivery. *Curr Drug Discov Technol*. 2005;2(4):231-238. doi:10.2174/157016305775202973

[123] Tripathi A, Melo JS. Preparation of a sponge-like biocomposite agarose–chitosan scaffold with primary hepatocytes for establishing an in vitro 3D liver tissue model. *RSC Adv*. 2015;5(39):30701-30710. doi:10.1039/C5RA04153H

[124] Scaffaro R, Lopresti F, Catania V, et al. Polycaprolactone-based scaffold for oil-selective sorption and improvement of bacteria activity for bioremediation of polluted water. *Eur Polym J*. 2017;91:260-273. doi:10.1016/j.eurpolymj.2017.04.015

[125] Shahbazi MA, Ghalkhani M, Maleki H. Directional Freeze-Casting: A Bioinspired Method to

Assemble Multifunctional Aligned Porous Structures for Advanced Applications. *Adv Eng Mater*. 2020;22(7). doi:10.1002/adem.202000033

[126] Alassod A, Khalaji MS, Islam SR, et al. Polypropylene-chitosan sponges prepared via thermal induce phase separation used as sorbents for oil spills cleanup. *Polymer Bulletin*. 2023;80(5):4949-4964. doi:10.1007/s00289-022-04297-w

[127] Nam YS, Park WH, Ihm D, Hudson SM. Effect of the degree of deacetylation on the thermal decomposition of chitin and chitosan nanofibers. *Carbohydr Polym*. 2010;80(1):291-295. doi:10.1016/j.carbpol.2009.11.030

[128] Chatelet C. Influence of the degree of acetylation on some biological properties of chitosan films. *Biomaterials*. 2001;22(3):261-268. doi:10.1016/S0142-9612(00)00183-6

[129] Seda Tığlı R, Karakeçili A, Gümüşderelioğlu M. In vitro characterization of chitosan scaffolds: influence of composition and deacetylation degree. *J Mater Sci Mater Med*. 2007;18(9):1665-1674. doi:10.1007/s10856-007-3066-x

[130] Madihally S V., Matthew HWT. Porous chitosan scaffolds for tissue engineering. *Biomaterials*. 1999;20(12):1133-1142. doi:10.1016/S0142-9612(99)00011-3

[131] Liu B, Ying X, Zhang Y, et al. Polyurethane nanofiber membranes immobilized with Bacillus altitudinis LS-1 for bioremediation of diesel-contaminated wastewater. *Process Safety and Environmental Protection*. 2023;180:883-892. doi:10.1016/j.psep.2023.10.060

[132] Jiang Q, Li Y, Wang M, et al. In-situ honeycomb spheres for enhanced enzyme immobilization and stability. *Chemical Engineering Journal*. 2024;495:153583. doi:10.1016/j.cej.2024.153583

[133] Huang M, Luo Z, Zhang Q, et al. Encapsulation of lipase in zeolitic imidazolate framework-8 induced by polyethyleneimine to form a honeycomb structure with enhanced activity. *Int J Biol Macromol*. 2024;254:127787. doi:10.1016/j.ijbiomac.2023.127787

[134] Saxena A, Tripathi BP, Kumar M, Shahi VK. Membrane-based techniques for the separation and purification of proteins: An overview. *Adv Colloid Interface Sci*. 2009;145(1-2):1-22. doi:10.1016/j.cis.2008.07.004

[135] He Y, Cai J, Xu Y, Luo B, Liu M. Chitin nanocrystals scaffold by directional freezing for high-efficiency water purification. *Sep Purif Technol*. 2023;310:123177. doi:10.1016/j.seppur.2023.123177

[136] Beppu MM, Vieira RS, Aimoli CG, Santana CC. Crosslinking of chitosan membranes using glutaraldehyde: Effect on ion permeability and water absorption. *J Memb Sci*. 2007;301(1-2):126-130. doi:10.1016/j.memsci.2007.06.015

[137] Miri S, Perez JAE, Brar SK, Rouissi T, Martel R. Sustainable production and co-immobilization of cold-active enzymes from Pseudomonas sp. for BTEX biodegradation. *Environmental Pollution*. 2021;285:117678. doi:10.1016/J.ENVPOL.2021.117678

[138] Chen ZC, Chang TL, Liou DS, Fan JY, Wang CP. Fabrication of a bio-inspired hydrophobic thin film by glutaraldehyde crosslinking electrospun composite self-cleaning nanofibers. *Mater Lett*. 2021;298:129975. doi:10.1016/j.matlet.2021.129975

[139] Mendes AA, Giordano RC, Giordano R de LC, de Castro HF. Immobilization and stabilization of microbial lipases by multipoint covalent attachment on aldehyde-resin affinity: Application of the biocatalysts in biodiesel synthesis. *J Mol Catal B Enzym*. 2011;68(1):109-115. doi:10.1016/j.molcatb.2010.10.002

[140] Hegde K, Veeranki V. Studies on Immobilization of Cutinases from Thermobifida fusca on Glutaraldehyde Activated Chitosan Beads. *Br Biotechnol J*. 2014;4(10):1049-1063. doi:10.9734/BBJ/2014/12558

[141] Zhang DH, Yuwen LX, Peng LJ. Parameters Affecting the Performance of Immobilized Enzyme. *J Chem*. 2013;2013(1). doi:10.1155/2013/946248

[142] Gilani SL, Najafpour GD, Moghadamnia A, Kamaruddin AH. Stability of immobilized porcine pancreas lipase on mesoporous chitosan beads: A comparative study. *J Mol Catal B Enzym*. 2016;133:144-153. doi:10.1016/j.molcatb.2016.08.005

[143] Bayat Z, Hassanshahian M, Cappello S. Immobilization of Microbes for Bioremediation of Crude Oil Polluted Environments: A Mini Review. *Open Microbiol J*. 2015;9:48-54. doi:10.2174/1874285801509010048

[144] Cunningham CJ, Ivshina IB, Lozinsky VI, Kuyukina MS, Philp JC. Bioremediation of diesel-contaminated soil by microorganisms immobilised in polyvinyl alcohol. *Int Biodeterior Biodegradation*. 2004;54(2-3):167-174. doi:10.1016/j.ibiod.2004.03.005

[145] Fu XG, Shi K, Xue JL, et al. Systematic adsorption process of petroleum hydrocarbon by immobilised petroleum-degradation bacteria system in degradation pathways. *Pet Sci*. 2021;18(5):1543-1550. doi:10.1016/j.petsci.2021.09.009

APPENDICES

APPENDIX A. Supplementary information of section 3

Compounds identified by GC-MS

Commercial diesel (1000 ppm)

Ret.Time	1st Hit	CAS Number	Library Compound
min	SI		
TIC	TIC	TIC	TIC
6.98	766	264-09-5	Benzocycloheptatriene
7.24	738	2471-83-2	1H-Indene, 1-ethylidene-
7.92	801	581-42-0	Naphthalene, 2,6-dimethyl-
8.1	773	581-42-0	Naphthalene, 2,6-dimethyl-
8.15	875	581-42-0	Naphthalene, 2,6-dimethyl-
8.33	699	56554-57-5	5,8,11-Heptadecatriynoic acid, methyl ester
8.7	702	2131-41-1	Naphthalene, 1,4,5-trimethyl-
8.94	824	2245-38-7	Naphthalene, 1,6,7-trimethyl-
8.97	810	0	3-(2-Methyl-propenyl)-1H-indene
9.17	825	0	3-(2-Methyl-propenyl)-1H-indene
9.2	733	0	3-(2-Methyl-propenyl)-1H-indene
9.34	777	0	3-(2-Methyl-propenyl)-1H-indene
9.4	727	0	3-(2-Methyl-propenyl)-1H-indene
9.45	705	1191-85-1	5,8,11,14-Eicosatetraynoic acid
9.8	665	0	4-Hexenoic acid, 4-methyl-6-(fluorodimethylsilyl)-6-trimethylsilyl-
9.9	707	1191-85-1	5,8,11,14-Eicosatetraynoic acid
10.05	704	1191-85-1	5,8,11,14-Eicosatetraynoic acid
10.09	700	0	4a,10a-Methanophenanthren-9ß-ol, 11-syn-bromo-1,2,3,4,4a,9,10,10a-octahydro-
10.39	628	0	Bicyclo[3.1.0]hexan-2-one, 6,6-dicyano-5-(1-cycloocten-1-yl)-
10.81	716	82657-04-3	Bifenthrin
11.74	720	0	9,10-Ethanoanthracene, 9,10-dihydro-11,12-diacetyl-

12.41	775	832-69-9	Phenanthrene, 1-methyl-
12.49	778	832-69-9	Phenanthrene, 1-methyl-
12.7	687	949-41-7	1H-Cyclopropa[l]phenanthrene,1a,9b-dihydro-
12.74	628	949-41-7	1H-Cyclopropa[l]phenanthrene,1a,9b-dihydro-
13.14	716	1576-69-8	Phenanthrene, 2,7-dimethyl-
13.38	648	0	Spiro[2.3]hexane-5-carboxylic acid, 1,1-diphenyl-, methyl ester
13.47	677	1576-69-8	Phenanthrene, 2,7-dimethyl-
5.77	667	57156-91-9	2,5-Octadecadiynoic acid, methyl ester
6.32	700	0	Methyl 4,6-tetradecadiynoate
6.65	695	57156-91-9	2,5-Octadecadiynoic acid, methyl ester
6.71	662	21852-80-2	Falcarinol
6.76	698	0	Methyl 4,6-tetradecadiynoate
7.18	721	0	(4-Methoxymethoxy-hex-5-ynylidene)-cyclohexane
7.48	653	0	10-Methyl-8-tetradecen-1-ol acetate
7.55	688	56847-03-1	6,9-Octadecadiynoic acid, methyl ester
7.93	676	21852-80-2	Falcarinol
8.27	697	2571-81-5	Azuleno[4,5-b]furan-2,9-dione, decahydro-6a-hydroxy-6,9a-dimethyl-3-methylene-, [3aS-(3aa,6ß,6aa,9aß,9ba)]-
8.54	665	0	6-(1-Hydroxymethylvinyl)-4,8a-dimethyl-3,5,6,7,8,8a-hexahydro-1H-naphthalen-2-one
8.91	729	2571-81-5	Azuleno[4,5-b]furan-2,9-dione, decahydro-6a-hydroxy-6,9a-dimethyl-3-methylene-, [3aS-(3aa,6ß,6aa,9aß,9ba)]-
9.01	667	0	Isocalamendiol
9.73	700	2571-81-5	Azuleno[4,5-b]furan-2,9-dione, decahydro-6a-hydroxy-6,9a-dimethyl-3-methylene-, [3aS-(3aa,6ß,6aa,9aß,9ba)]-
10.4	716	76-43-7	Fluoxymesterone
10.83	728	77573-08-1	1b,4a-Epoxy-2H-cyclopenta[3,4]cyclopropa[8,9]cycloundec[1,2-b]oxiren-5(6H)-one, 7-(acetyloxy)decahydro-2,9,10-trihydroxy-3,6,8,8,10a-pentamethyl-
11.05	727	76-43-7	Fluoxymesterone
11.67	743	51906-13-9	2-Butenoic acid, 2-methyl-, 2-(acetyloxy)-1,1a,2,3,4,6,7,10,11,11a-decahydro-7,10-dihydroxy-1,1,3,6,9-pentamethyl-4a,7a-epoxy-5H-cyclopenta[a]cyclopropa[f]cycloundecen-11-yl ester, [1aR-[1aR*,2R*,3S*,4aR*,6S*,7S*,7aS*,8E,10R*,11R*(E),11aS*]]-

Abiotic control

Ret. Time (min)	CAS Number	Library Compound
6.83	19095-23-9	Heptasiloxane, 1,1,3,3,5,5,7,7,9,9,11,11,13,13-tetradecamethyl-
7.78	719-22-2	2,5-Cyclohexadiene-1,4-dione, 2,6-bis(1,1-dimethylethyl)-
7.96	541-01-5	Heptasiloxane, hexadecamethyl-
8.01	593-49-7	Heptacosane
8.22	96-76-4	Phenol, 2,4-bis(1,1-dimethylethyl)-
8.94	541-01-5	Heptasiloxane, hexadecamethyl-
9.51	593-49-7	Heptacosane
9.84	541-01-5	Heptasiloxane, hexadecamethyl-
10.66	541-01-5	Heptasiloxane, hexadecamethyl-
10.72	4130-42-1	Phenol, 2,6-bis(1,1-dimethylethyl)-4-ethyl-
11.43	541-01-5	Heptasiloxane, hexadecamethyl-
11.79	82304-66-3	7,9-Di-tert-butyl-1-oxaspiro(4,5)deca-6,9-diene-2,8-dione
12.16	541-01-5	Heptasiloxane, hexadecamethyl-
12.85	541-01-5	Heptasiloxane, hexadecamethyl-
13.25	7098-22-8	Tetratetracontane
13.52	541-01-5	Heptasiloxane, hexadecamethyl-
14.25	541-01-5	Heptasiloxane, hexadecamethyl-
15.14	541-01-5	Heptasiloxane, hexadecamethyl-
16.15	55521-22-7	9,12,15-Octadecatrienoic acid, 2,3-bis[(trimethylsilyl)oxy]propyl ester, (Z,Z,Z)-
22.66	0	Formic acid, 2-bromomethyl-4,4-dimethyl-3-(3-oxobut-1-enyl)cyclohex-2-enyl ester
24.35	55556-80-4	ß-D-Glucopyranosiduronic acid, 3-(5-ethylhexahydro-2,4,6-trioxo-5-pyrimidinyl)-1,1-dimethylpropyl 2,3,4-tris-O-(trimethylsilyl)-, methyl ester

Brackish salinity (0.3 M NaCl) - 16 hours

Ret.Time	1st Hit	CAS Number	Library Compound
min	SI		
TIC	TIC	TIC	TIC
6.33	698	593-49-7	Heptacosane
6.77	677	56196-88-4	a-D-Glucopyranoside, methyl 2-(acetylamino)-2-deoxy-3-O-(trimethylsilyl)-, cyclic butylboronate
7.78	651	2460-77-7	2,5-di-tert-Butyl-1,4-benzoquinone
8.02	766	593-49-7	Heptacosane
8.23	787	96-76-4	Phenol, 2,4-bis(1,1-dimethylethyl)-
9.51	767	593-49-7	Heptacosane
9.86	675	593-49-7	Heptacosane
10.87	729	593-49-7	Heptacosane
11.79	899	82304-66-3	7,9-Di-tert-butyl-1-oxaspiro(4,5)deca-6,9-diene-2,8-dione
13.26	623	7098-22-8	Tetratetracontane
22.66	581	0	Formic acid, 2-bromomethyl-4,4-dimethyl-3-(3-oxobut-1-enyl)cyclohex-2-enyl ester
24.36	579	55658-66-7	D-Homo-24-nor-17-oxachola-20,22-diene-3,16-dione, 7-(acetyloxy)-1,2:14,15:21,23-triepoxy-4,4,8-trimethyl-, (5a,7a,13a,14ß,15ß,17aa)-

Brackish salinity (0.3 M NaCl) - 32 hours

Ret.Time	1st Hit	CAS Number	Library Compound
min	SI		
TIC	TIC	TIC	TIC
5.53	699	19095-24-0	Octasiloxane, 1,1,3,3,5,5,7,7,9,9,11,11,13,13,15,15-hexadecamethyl-
6.82	717	19095-23-9	Heptasiloxane, 1,1,3,3,5,5,7,7,9,9,11,11,13,13-tetradecamethyl-
7.78	760	719-22-2	2,5-Cyclohexadiene-1,4-dione, 2,6-bis(1,1-dimethylethyl)-
7.96	769	541-01-5	Heptasiloxane, hexadecamethyl-
8.21	773	96-76-4	Phenol, 2,4-bis(1,1-dimethylethyl)-
8.94	772	541-01-5	Heptasiloxane, hexadecamethyl-
9.84	739	541-01-5	Heptasiloxane, hexadecamethyl-
10.66	762	541-01-5	Heptasiloxane, hexadecamethyl-
10.71	640	4130-42-1	Phenol, 2,6-bis(1,1-dimethylethyl)-4-ethyl-

11.43	780	541-01-5	Heptasiloxane, hexadecamethyl-
11.78	817	82304-66-3	7,9-Di-tert-butyl-1-oxaspiro(4,5)deca-6,9-diene-2,8-dione
12.15	740	541-01-5	Heptasiloxane, hexadecamethyl-
12.85	754	541-01-5	Heptasiloxane, hexadecamethyl-
13.52	719	541-01-5	Heptasiloxane, hexadecamethyl-
14.25	700	541-01-5	Heptasiloxane, hexadecamethyl-
15.14	685	541-01-5	Heptasiloxane, hexadecamethyl-
16.15	636	54284-45-6	1-Monolinoleoylglycerol trimethylsilyl ether
16.85	670	118978-72-6	3a,5a-Cyclo-ergosta-7,9(11),22t-triene-6ß-ol
17.29	623	54284-45-6	1-Monolinoleoylglycerol trimethylsilyl ether
22.65	596	472-61-7	Astaxanthin

Brackish salinity (0.3 M NaCl) - 48 hours

Ret.Time	1st Hit	CAS Number	Library Compound
min	SI		
TIC	TIC	TIC	TIC
5.78	628	0	Bicyclo[3.1.1]hept-3-ene-spiro-2,4'-(1',3'-dioxane), 7,7-dimethyl-
6.33	662	70220-91-6	10-Methoxytricyclo[4.2.1.1(2,5)]deca-3,7-dien-9-ol
6.72	691	1680-51-9	Naphthalene, 1,2,3,4-tetrahydro-6-methyl-
6.77	630	78323-73-6	9-Methyltricyclo[4.2.1.1(2,5)]deca-3,7-diene-9,10-diol
7.49	674	55521-23-8	9,12,15-Octadecatrienoic acid, 2-[(trimethylsilyl)oxy]-1-[[(trimethylsilyl)oxy]methyl]ethyl ester, (Z,Z,Z)-
7.56	692	21693-54-9	Naphthalene, 1,2,3,4-tetrahydro-5,7-dimethyl-
11.79	869	82304-66-3	7,9-Di-tert-butyl-1-oxaspiro(4,5)deca-6,9-diene-2,8-dione
12.86	713	55521-22-7	9,12,15-Octadecatrienoic acid, 2,3-bis[(trimethylsilyl)oxy]propyl ester, (Z,Z,Z)-
13.53	689	55521-22-7	9,12,15-Octadecatrienoic acid, 2,3-bis[(trimethylsilyl)oxy]propyl ester, (Z,Z,Z)-
16.85	698	0	2,2,4-Trimethyl-3-(3,8,12,16-tetramethyl-heptadeca-3,7,11,15-tetraenyl)-cyclohexanol
22.66	573	55556-80-4	ß-D-Glucopyranosiduronic acid, 3-(5-ethylhexahydro-2,4,6-trioxo-5-pyrimidinyl)-1,1-dimethylpropyl 2,3,4-tris-O-(trimethylsilyl)-, methyl ester
24.36	593	55658-66-7	D-Homo-24-nor-17-oxachola-20,22-diene-3,16-dione, 7-(acetyloxy)-1,2:14,15:21,23-triepoxy-4,4,8-trimethyl-, (5a,7a,13a,14ß,15ß,17aa)-

Brackish salinity (0.3 M NaCl) - 64 hours

Ret.Time	1st Hit	CAS Number	Library Compound
min	SI		
TIC	TIC	TIC	TIC
6.83	751	556-68-3	Cyclooctasiloxane, hexadecamethyl-
7.96	821	541-01-5	Heptasiloxane, hexadecamethyl-
8.93	809	541-01-5	Heptasiloxane, hexadecamethyl-
9.83	794	541-01-5	Heptasiloxane, hexadecamethyl-
10.64	811	541-01-5	Heptasiloxane, hexadecamethyl-
11.41	818	541-01-5	Heptasiloxane, hexadecamethyl-
12.13	812	541-01-5	Heptasiloxane, hexadecamethyl-
12.81	814	541-01-5	Heptasiloxane, hexadecamethyl-
13.48	812	541-01-5	Heptasiloxane, hexadecamethyl-
14.2	815	541-01-5	Heptasiloxane, hexadecamethyl-
15.07	805	541-01-5	Heptasiloxane, hexadecamethyl-
16.07	804	541-01-5	Heptasiloxane, hexadecamethyl-
17.22	811	541-01-5	Heptasiloxane, hexadecamethyl-
18.44	805	541-01-5	Heptasiloxane, hexadecamethyl-
19.75	793	541-01-5	Heptasiloxane, hexadecamethyl-
21.13	774	541-01-5	Heptasiloxane, hexadecamethyl-
22.01	718	541-01-5	Heptasiloxane, hexadecamethyl-
22.66	625	54284-45-6	1-Monolinoleoylglycerol trimethylsilyl ether
23.37	587	57326-16-6	Glycine, N-[(3a,5ß,7a,12a)-24-oxo-3,7,12-tris[(trimethylsilyl)oxy]cholan-24-yl]-, methyl ester
24.36	601	55556-80-4	ß-D-Glucopyranosiduronic acid, 3-(5-ethylhexahydro-2,4,6-trioxo-5-pyrimidinyl)-1,1-dimethylpropyl 2,3,4-tris-O-(trimethylsilyl)-, methyl ester

Brackish salinity (0.3 M NaCl) - 72 hours

Ret.Time	1st Hit	CAS Number	Library Compound
min	SI		
TIC	TIC	TIC	TIC
6.33	695	70220-91-6	10-Methoxytricyclo[4.2.1.1(2,5)]deca-3,7-dien-9-ol
6.68	678	0	Hex-3-ene-1,5-diyne, 3,4-diisopropyl-
6.72	670	28229-15-4	Biphenylene, 1,2,3,6,7,8,8a,8b-octahydro-, trans-
6.76	689	21852-80-2	Falcarinol

7.2	680	21852-80-2	Falcarinol
7.56	719	21693-54-9	Naphthalene, 1,2,3,4-tetrahydro-5,7-dimethyl-
7.94	699	21852-80-2	Falcarinol
10.41	692	507-61-9	Azafrin
10.84	714	1191-85-1	5,8,11,14-Eicosatetraynoic acid
11.79	800	82304-66-3	7,9-Di-tert-butyl-1-oxaspiro(4,5)deca-6,9-diene-2,8-dione
12.16	740	55521-22-7	9,12,15-Octadecatrienoic acid, 2,3-bis[(trimethylsilyl)oxy]propyl ester, (Z,Z,Z)-
12.86	736	55521-22-7	9,12,15-Octadecatrienoic acid, 2,3-bis[(trimethylsilyl)oxy]propyl ester, (Z,Z,Z)-
13.53	731	55521-22-7	9,12,15-Octadecatrienoic acid, 2,3-bis[(trimethylsilyl)oxy]propyl ester, (Z,Z,Z)-
14.26	711	55521-22-7	9,12,15-Octadecatrienoic acid, 2,3-bis[(trimethylsilyl)oxy]propyl ester, (Z,Z,Z)-
15.14	699	55521-22-7	9,12,15-Octadecatrienoic acid, 2,3-bis[(trimethylsilyl)oxy]propyl ester, (Z,Z,Z)-
22.66	578	472-61-7	Astaxanthin
24.35	576	55556-80-4	ß-D-Glucopyranosiduronic acid, 3-(5-ethylhexahydro-2,4,6-trioxo-5-pyrimidinyl)-1,1-dimethylpropyl 2,3,4-tris-O-(trimethylsilyl)-, methyl ester

Saline (0.6 M NaCl) – 16 hours

Ret.Time	1st Hit	CAS Number	Library Compound
min	SI		
TIC	TIC	TIC	TIC
6.83	725	19095-23-9	Heptasiloxane, 1,1,3,3,5,5,7,7,9,9,11,11,13,13-tetradecamethyl-
7.78	696	719-22-2	2,5-Cyclohexadiene-1,4-dione, 2,6-bis(1,1-dimethylethyl)-
7.96	775	541-01-5	Heptasiloxane, hexadecamethyl-
8.23	798	96-76-4	Phenol, 2,4-bis(1,1-dimethylethyl)-
8.95	798	541-01-5	Heptasiloxane, hexadecamethyl-
9.84	777	541-01-5	Heptasiloxane, hexadecamethyl-
10.67	791	541-01-5	Heptasiloxane, hexadecamethyl-
11.43	801	541-01-5	Heptasiloxane, hexadecamethyl-
11.79	777	82304-66-3	7,9-Di-tert-butyl-1-oxaspiro(4,5)deca-6,9-diene-2,8-dione
12.16	761	541-01-5	Heptasiloxane, hexadecamethyl-
12.86	768	541-01-5	Heptasiloxane, hexadecamethyl-
13.53	744	541-01-5	Heptasiloxane, hexadecamethyl-

14.26	721	541-01-5	Heptasiloxane, hexadecamethyl-
15.14	702	541-01-5	Heptasiloxane, hexadecamethyl-
16.16	665	541-01-5	Heptasiloxane, hexadecamethyl-
17.3	625	19095-23-9	Heptasiloxane, 1,1,3,3,5,5,7,7,9,9,11,11,13,13-tetradecamethyl-
22.66	565	987-24-6	Betamethasone acetate
24.36	603	55658-66-7	D-Homo-24-nor-17-oxachola-20,22-diene-3,16-dione, 7-(acetyloxy)-1,2:14,15:21,23-triepoxy-4,4,8-trimethyl-, (5a,7a,13a,14ß,15ß,17aa)-

Saline (0.6 M NaCl) – 32 hours

Ret.Time	1st Hit	CAS Number	Library Compound
min	SI		
TIC	TIC	TIC	TIC
5.53	706	995-82-4	Hexasiloxane, 1,1,3,3,5,5,7,7,9,9,11,11-dodecamethyl-
6.83	708	19095-23-9	Heptasiloxane, 1,1,3,3,5,5,7,7,9,9,11,11,13,13-tetradecamethyl-
7.78	747	719-22-2	2,5-Cyclohexadiene-1,4-dione, 2,6-bis(1,1-dimethylethyl)-
7.96	781	541-01-5	Heptasiloxane, hexadecamethyl-
8.22	799	96-76-4	Phenol, 2,4-bis(1,1-dimethylethyl)-
8.94	790	541-01-5	Heptasiloxane, hexadecamethyl-
9.84	769	541-01-5	Heptasiloxane, hexadecamethyl-
10.66	776	541-01-5	Heptasiloxane, hexadecamethyl-
11.43	793	541-01-5	Heptasiloxane, hexadecamethyl-
11.79	817	82304-66-3	7,9-Di-tert-butyl-1-oxaspiro(4,5)deca-6,9-diene-2,8-dione
12.16	748	541-01-5	Heptasiloxane, hexadecamethyl-
12.86	757	541-01-5	Heptasiloxane, hexadecamethyl-
13.53	726	541-01-5	Heptasiloxane, hexadecamethyl-
14.26	705	541-01-5	Heptasiloxane, hexadecamethyl-
15.14	684	541-01-5	Heptasiloxane, hexadecamethyl-
16.16	639	541-01-5	Heptasiloxane, hexadecamethyl-
17.29	611	54284-45-6	1-Monolinoleoylglycerol trimethylsilyl ether
22.66	567	987-24-6	Betamethasone acetate
24.36	595	55556-80-4	ß-D-Glucopyranosiduronic acid, 3-(5-ethylhexahydro-2,4,6-trioxo-5-pyrimidinyl)-1,1-dimethylpropyl 2,3,4-tris-O-(trimethylsilyl)-, methyl ester

Saline (0.6 M NaCl) – 48 hours

Ret.Time	1st Hit	CAS Number	Library Compound
min	SI		
TIC	TIC	TIC	TIC
5.53	690	995-82-4	Hexasiloxane, 1,1,3,3,5,5,7,7,9,9,11,11-dodecamethyl-
6.82	702	19095-23-9	Heptasiloxane, 1,1,3,3,5,5,7,7,9,9,11,11,13,13-tetradecamethyl-
7.78	707	719-22-2	2,5-Cyclohexadiene-1,4-dione, 2,6-bis(1,1-dimethylethyl)-
7.96	757	541-01-5	Heptasiloxane, hexadecamethyl-
8.22	689	96-76-4	Phenol, 2,4-bis(1,1-dimethylethyl)-
9.84	673	55521-22-7	9,12,15-Octadecatrienoic acid, 2,3-bis[(trimethylsilyl)oxy]propyl ester, (Z,Z,Z)-
10.66	727	55521-22-7	9,12,15-Octadecatrienoic acid, 2,3-bis[(trimethylsilyl)oxy]propyl ester, (Z,Z,Z)-
11.43	741	55521-22-7	9,12,15-Octadecatrienoic acid, 2,3-bis[(trimethylsilyl)oxy]propyl ester, (Z,Z,Z)-
11.78	790	82304-66-3	7,9-Di-tert-butyl-1-oxaspiro(4,5)deca-6,9-diene-2,8-dione
12.16	730	55521-22-7	9,12,15-Octadecatrienoic acid, 2,3-bis[(trimethylsilyl)oxy]propyl ester, (Z,Z,Z)-
12.85	717	55521-22-7	9,12,15-Octadecatrienoic acid, 2,3-bis[(trimethylsilyl)oxy]propyl ester, (Z,Z,Z)-
13.52	705	55521-22-7	9,12,15-Octadecatrienoic acid, 2,3-bis[(trimethylsilyl)oxy]propyl ester, (Z,Z,Z)-
14.25	689	55521-22-7	9,12,15-Octadecatrienoic acid, 2,3-bis[(trimethylsilyl)oxy]propyl ester, (Z,Z,Z)-
22.66	614	118978-72-6	3a,5a-Cyclo-ergosta-7,9(11),22t-triene-6ß-ol
24.35	606	55556-80-4	ß-D-Glucopyranosiduronic acid, 3-(5-ethylhexahydro-2,4,6-trioxo-5-pyrimidinyl)-1,1-dimethylpropyl 2,3,4-tris-O-(trimethylsilyl)-, methyl ester

Saline (0.6 M NaCl) – 64 hours

Ret. Time	1st hit	CAS Number	Library Compound
min	SI		
TIC	TIC	TIC	TIC
6.82	693	19095-23-9	Heptasiloxane, 1,1,3,3,5,5,7,7,9,9,11,11,13,13-tetradecamethyl-
7.77	641	719-22-2	2,5-Cyclohexadiene-1,4-dione, 2,6-bis(1,1-dimethylethyl)-
7.96	717	19095-23-9	Heptasiloxane, 1,1,3,3,5,5,7,7,9,9,11,11,13,13-tetradecamethyl-
8.93	738	19095-24-0	Octasiloxane, 1,1,3,3,5,5,7,7,9,9,11,11,13,13,15,15-hexadecamethyl-
9.84	738	541-01-5	Heptasiloxane, hexadecamethyl-
10.66	749	541-01-5	Heptasiloxane, hexadecamethyl-
11.43	763	541-01-5	Heptasiloxane, hexadecamethyl-
11.78	687	82304-66-3	7,9-Di-tert-butyl-1-oxaspiro(4,5)deca-6,9-diene-2,8-dione
12.15	734	541-01-5	Heptasiloxane, hexadecamethyl-
12.85	728	541-01-5	Heptasiloxane, hexadecamethyl-
13.51	708	541-01-5	Heptasiloxane, hexadecamethyl-
14.25	682	541-01-5	Heptasiloxane, hexadecamethyl-
15.14	667	541-01-5	Heptasiloxane, hexadecamethyl-
16.15	637	54284-45-6	1-Monolinoleoylglycerol trimethylsilyl ether
16.85	678	118978-72-6	3a,5a-Cyclo-ergosta-7,9(11),22t-triene-6ß-ol
17.28	621	54284-45-6	1-Monolinoleoylglycerol trimethylsilyl ether
22.65	636	118978-72-6	3a,5a-Cyclo-ergosta-7,9(11),22t-triene-6ß-ol
24.34	606	55658-66-7	D-Homo-24-nor-17-oxachola-20,22-diene-3,16-dione, 7-(acetyloxy)-1,2:14,15:21,23-triepoxy-4,4,8-trimethyl-, (5a,7a,13a,14ß,15ß,17aa)-

Saline (0.6 M NaCl) – 72 hours

Ret. Time (min)	1st Hit (SI)	CAS Number	Library Compound
5.53	684	995-82-4	Hexasiloxane, 1,1,3,3,5,5,7,7,9,9,11,11-dodecamethyl-
6.83	702	19095-23-9	Heptasiloxane, 1,1,3,3,5,5,7,7,9,9,11,11,13,13-tetradecamethyl-
7.78	741	719-22-2	2,5-Cyclohexadiene-1,4-dione, 2,6-bis(1,1-dimethylethyl)-
7.96	765	541-01-5	Heptasiloxane, hexadecamethyl-
8.23	731	96-76-4	Phenol, 2,4-bis(1,1-dimethylethyl)-
8.95	741	541-01-5	Heptasiloxane, hexadecamethyl-
9.85	636	541-01-5	Heptasiloxane, hexadecamethyl-
10.13	736	0	1,3-di-iso-propylnaphthalene
10.17	763	0	1,3-di-iso-propylnaphthalene
10.27	726	0	1,3-di-iso-propylnaphthalene
10.67	670	55521-22-7	9,12,15-Octadecatrienoic acid, 2,3-bis[(trimethylsilyl)oxy]propyl ester, (Z,Z,Z)-
11.44	696	55521-22-7	9,12,15-Octadecatrienoic acid, 2,3-bis[(trimethylsilyl)oxy]propyl ester, (Z,Z,Z)-
11.79	847	82304-66-3	7,9-Di-tert-butyl-1-oxaspiro(4,5)deca-6,9-diene-2,8-dione
12.86	674	55521-22-7	9,12,15-Octadecatrienoic acid, 2,3-bis[(trimethylsilyl)oxy]propyl ester, (Z,Z,Z)-
13.53	671	55521-22-7	9,12,15-Octadecatrienoic acid, 2,3-bis[(trimethylsilyl)oxy]propyl ester, (Z,Z,Z)-
22.66	626	1524-88-5	Flurandrenolide
24.36	584	55556-80-4	ß-D-Glucopyranosiduronic acid, 3-(5-ethylhexahydro-2,4,6-trioxo-5-pyrimidinyl)-1,1-dimethylpropyl 2,3,4-tris-O-(trimethylsilyl)-, methyl ester

Brine (1.2 M NaCl) – 16 hours

Ret.Time	1st Hit	CAS Number	Library Compound
min	SI		
TIC	TIC	TIC	TIC
5.53	682	995-82-4	Hexasiloxane, 1,1,3,3,5,5,7,7,9,9,11,11-dodecamethyl-
6.83	698	19095-23-9	Heptasiloxane, 1,1,3,3,5,5,7,7,9,9,11,11,13,13-tetradecamethyl-
7.78	745	719-22-2	2,5-Cyclohexadiene-1,4-dione, 2,6-bis(1,1-dimethylethyl)-
7.96	754	541-01-5	Heptasiloxane, hexadecamethyl-
8.23	834	96-76-4	Phenol, 2,4-bis(1,1-dimethylethyl)-
8.95	755	541-01-5	Heptasiloxane, hexadecamethyl-
9.85	667	541-01-5	Heptasiloxane, hexadecamethyl-
10.67	689	541-01-5	Heptasiloxane, hexadecamethyl-

11.44	714	541-01-5	Heptasiloxane, hexadecamethyl-
11.79	841	82304-66-3	7,9-Di-tert-butyl-1-oxaspiro(4,5)deca-6,9-diene-2,8-dione
12.17	654	541-01-5	Heptasiloxane, hexadecamethyl-
12.86	659	541-01-5	Heptasiloxane, hexadecamethyl-
13.53	605	55521-22-7	9,12,15-Octadecatrienoic acid, 2,3-bis[(trimethylsilyl)oxy]propyl ester, (Z,Z,Z)-
22.66	581	0	2-Hydroxyphenethyl alcohol, bis(tert-butyldimethylsilyl) ether
24.36	597	55556-80-4	ß-D-Glucopyranosiduronic acid, 3-(5-ethylhexahydro-2,4,6-trioxo-5-pyrimidinyl)-1,1-dimethylpropyl 2,3,4-tris-O-(trimethylsilyl)-, methyl ester

Brine (1.2 M NaCl) – 32 hours

Ret.Time	1st Hit	CAS Number	Library Compound
5.53	685	995-82-4	Hexasiloxane, 1,1,3,3,5,5,7,7,9,9,11,11-dodecamethyl-
6.83	700	19095-23-9	Heptasiloxane, 1,1,3,3,5,5,7,7,9,9,11,11,13,13-tetradecamethyl-
7.78	713	719-22-2	2,5-Cyclohexadiene-1,4-dione, 2,6-bis(1,1-dimethylethyl)-
7.96	748	541-01-5	Heptasiloxane, hexadecamethyl-
8.22	781	96-76-4	Phenol, 2,4-bis(1,1-dimethylethyl)-
8.95	738	19095-24-0	Octasiloxane, 1,1,3,3,5,5,7,7,9,9,11,11,13,13,15,15-hexadecamethyl-
9.84	691	541-01-5	Heptasiloxane, hexadecamethyl-
10.66	677	541-01-5	Heptasiloxane, hexadecamethyl-
11.43	697	541-01-5	Heptasiloxane, hexadecamethyl-
11.79	807	82304-66-3	7,9-Di-tert-butyl-1-oxaspiro(4,5)deca-6,9-diene-2,8-dione
12.16	626	541-01-5	Heptasiloxane, hexadecamethyl-
12.86	624	55521-22-7	9,12,15-Octadecatrienoic acid, 2,3-bis[(trimethylsilyl)oxy]propyl ester, (Z,Z,Z)-
13.53	616	55521-22-7	9,12,15-Octadecatrienoic acid, 2,3-bis[(trimethylsilyl)oxy]propyl ester, (Z,Z,Z)-
22.66	589	55556-80-4	ß-D-Glucopyranosiduronic acid, 3-(5-ethylhexahydro-2,4,6-trioxo-5-pyrimidinyl)-1,1-dimethylpropyl 2,3,4-tris-O-(trimethylsilyl)-, methyl ester
24.35	607	55556-80-4	ß-D-Glucopyranosiduronic acid, 3-(5-ethylhexahydro-2,4,6-trioxo-5-pyrimidinyl)-1,1-dimethylpropyl 2,3,4-tris-O-(trimethylsilyl)-, methyl ester

Brine (1.2 M NaCl) – 48 hours

Ret.Time	1st Hit	CAS Number	Library Compound
min	SI		
TIC	TIC	TIC	TIC
5.53	680	995-82-4	Hexasiloxane, 1,1,3,3,5,5,7,7,9,9,11,11-dodecamethyl-
6.83	705	19095-23-9	Heptasiloxane, 1,1,3,3,5,5,7,7,9,9,11,11,13,13-tetradecamethyl-
7.78	836	719-22-2	2,5-Cyclohexadiene-1,4-dione, 2,6-bis(1,1-dimethylethyl)-
7.96	762	541-01-5	Heptasiloxane, hexadecamethyl-
8.23	886	96-76-4	Phenol, 2,4-bis(1,1-dimethylethyl)-
8.95	755	541-01-5	Heptasiloxane, hexadecamethyl-
9.51	817	593-49-7	Heptacosane
9.85	649	541-01-5	Heptasiloxane, hexadecamethyl-
10.67	692	541-01-5	Heptasiloxane, hexadecamethyl-
10.72	695	1620-98-0	3,5-di-tert-Butyl-4-hydroxybenzaldehyde
11.44	735	541-01-5	Heptasiloxane, hexadecamethyl-
11.79	877	82304-66-3	7,9-Di-tert-butyl-1-oxaspiro(4,5)deca-6,9-diene-2,8-dione
12.17	653	541-01-5	Heptasiloxane, hexadecamethyl-
12.86	687	541-01-5	Heptasiloxane, hexadecamethyl-
13.53	620	541-01-5	Heptasiloxane, hexadecamethyl-
14.27	623	541-01-5	Heptasiloxane, hexadecamethyl-
22.66	585	0	Formic acid, 2-bromomethyl-4,4-dimethyl-3-(3-oxobut-1-enyl)cyclohex-2-enyl ester
24.36	568	55556-80-4	ß-D-Glucopyranosiduronic acid, 3-(5-ethylhexahydro-2,4,6-trioxo-5-pyrimidinyl)-1,1-dimethylpropyl 2,3,4-tris-O-(trimethylsilyl)-, methyl ester

Brine (1.2 M NaCl – 64 hours

Ret.Time	1st Hit	CAS Number	Library Compound
5.53	679	19095-24-0	Octasiloxane, 1,1,3,3,5,5,7,7,9,9,11,11,13,13,15,15-hexadecamethyl-
6.82	711	3782-85-2	Benzoic acid, 2,6-bis[(trimethylsilyl)oxy]-, trimethylsilyl ester
7.78	838	719-22-2	2,5-Cyclohexadiene-1,4-dione, 2,6-bis(1,1-dimethylethyl)-
7.96	768	541-01-5	Heptasiloxane, hexadecamethyl-
8.21	878	96-76-4	Phenol, 2,4-bis(1,1-dimethylethyl)-
8.94	758	541-01-5	Heptasiloxane, hexadecamethyl-
9.5	768	638-36-8	Hexadecane, 2,6,10,14-tetramethyl-
9.84	697	541-01-5	Heptasiloxane, hexadecamethyl-
10.66	725	541-01-5	Heptasiloxane, hexadecamethyl-
10.71	713	1620-98-0	3,5-di-tert-Butyl-4-hydroxybenzaldehyde
11.43	763	541-01-5	Heptasiloxane, hexadecamethyl-
11.78	876	82304-66-3	7,9-Di-tert-butyl-1-oxaspiro(4,5)deca-6,9-diene-2,8-dione
12.15	712	541-01-5	Heptasiloxane, hexadecamethyl-
12.85	726	541-01-5	Heptasiloxane, hexadecamethyl-
13.52	680	541-01-5	Heptasiloxane, hexadecamethyl-
14.25	672	541-01-5	Heptasiloxane, hexadecamethyl-
15.14	660	541-01-5	Heptasiloxane, hexadecamethyl-
22.65	591	0	Formic acid, 2-bromomethyl-4,4-dimethyl-3-(3-oxobut-1-enyl)cyclohex-2-enyl ester
24.35	565	55125-23-0	Benzoic acid, 3,5-dicyclohexyl-4-hydroxy-, methyl ester

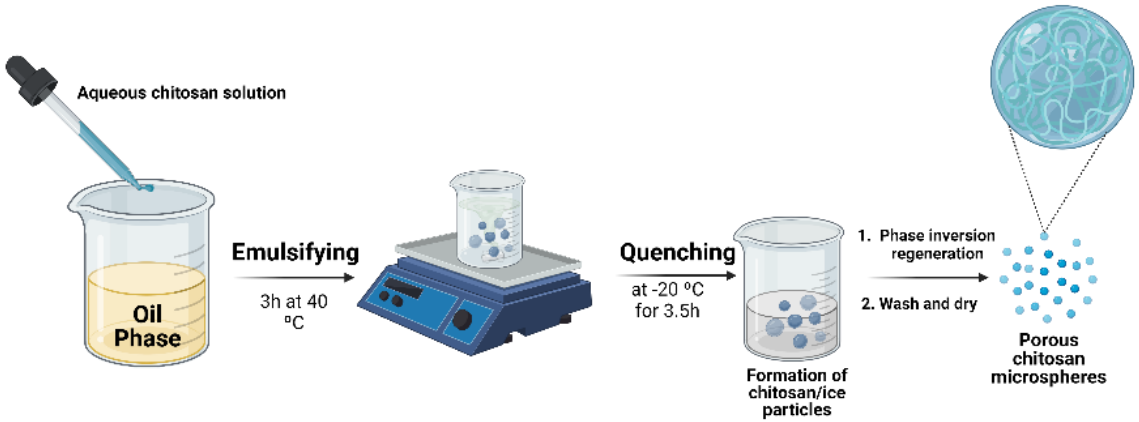
Brine (1.2 M NaCl) – 72 hours

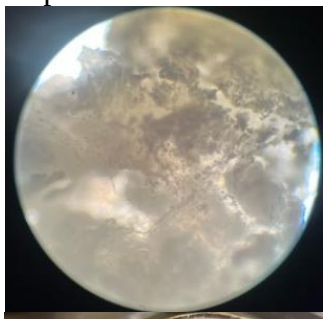
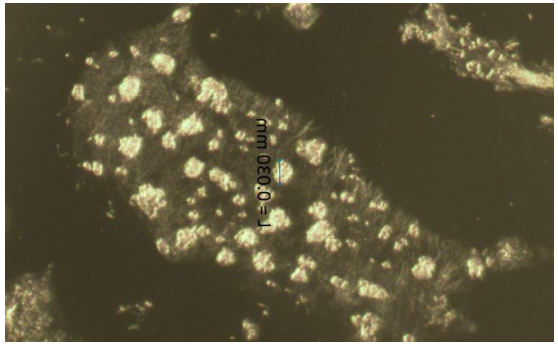
Ret.Time	1st Hit	CAS Number	Library Compound
5.53	685	19095-24-0	Octasiloxane, 1,1,3,3,5,5,7,7,9,9,11,11,13,13,15,15-hexadecamethyl-
6.82	698	19095-23-9	Heptasiloxane, 1,1,3,3,5,5,7,7,9,9,11,11,13,13-tetradecamethyl-
7.78	835	719-22-2	2,5-Cyclohexadiene-1,4-dione, 2,6-bis(1,1-dimethylethyl)-
7.96	749	541-01-5	Heptasiloxane, hexadecamethyl-
8.00	658	593-49-7	Heptacosane
8.22	872	96-76-4	Phenol, 2,4-bis(1,1-dimethylethyl)-
8.94	715	19095-24-0	Octasiloxane, 1,1,3,3,5,5,7,7,9,9,11,11,13,13,15,15-hexadecamethyl-
9.50	782	638-36-8	Hexadecane, 2,6,10,14-tetramethyl-
9.84	623	593-49-7	Heptacosane
10.66	628	55521-22-7	9,12,15-Octadecatrienoic acid, 2,3-bis[(trimethylsilyl)oxy]propyl ester, (Z,Z,Z)-
10.71	719	1620-98-0	3,5-di-tert-Butyl-4-hydroxybenzaldehyde
10.86	773	629-99-2	Pentacosane
11.78	877	82304-66-3	7,9-Di-tert-butyl-1-oxaspiro(4,5)deca-6,9-diene-2,8-dione

12.85	628	55521-22-7	9,12,15-Octadecatrienoic acid, 2,3-bis[(trimethylsilyl)oxy]propyl ester, (Z,Z,Z)-
13.25	687	7098-22-8	Tetratetracontane
13.53	636	55282-12-7	Octadecane, 3-ethyl-5-(2-ethylbutyl)-
22.66	589	0	Formic acid, 2-bromomethyl-4,4-dimethyl-3-(3-oxobut-1-enyl)cyclohex-2-enyl ester
24.35	565	55125-23-0	Benzoic acid, 3,5-dicyclohexyl-4-hydroxy-, methyl ester

APPENDIX B - Supplementary information of section 4

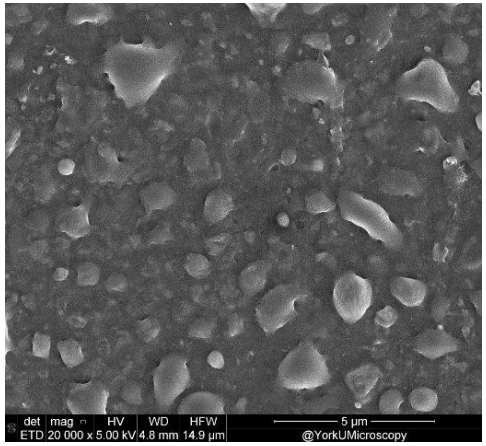
Before developing the chitosan scaffold in this study, this thesis attempted to synthesize chitosan microspheres without success. The table below summarizes the trials conducted in 2023.

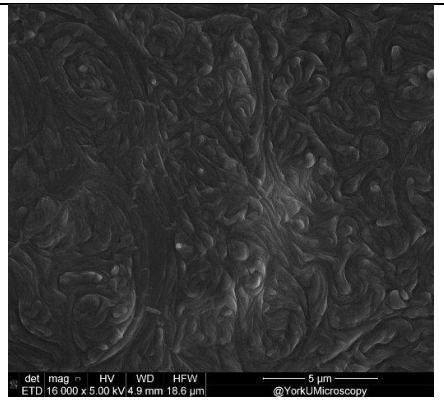
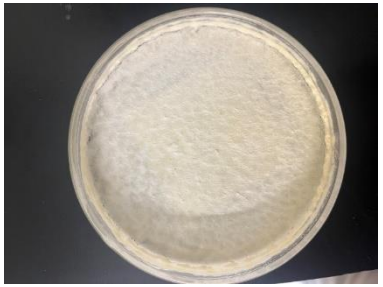
Tentative	Description
01	 The trials began with the deviation of a micro-emulsion and a thermally induced phase separation method. The chitosan solution is emulsified within the oil phase, resulting in a bluish-white emulsion. This emulsion is then rapidly cooled to -20°C for a duration of 3.5 hours, causing the dispersed water droplets containing dissolved chitosan to freeze and transform into ice particles. This freezing process effectively halts the movement of the chitosan polymer chains. When in room temperature, the ice begins to melt, and ethanol is introduced to expedite this melting process. Ethanol also acts as a dehydrating agent, extracting water molecules from the polymeric network and generating pores within the material. Additionally, ethanol serves as a co-surfactant. The role of phase inversion liquid - NaOH (sodium hydroxide) is to adjust the pH of the aqueous phase from acidic to basic. This change in pH leads to the deprotonation of the amino and hydroxyl groups present in chitosan molecules, rendering them insoluble. Consequently, the addition of NaOH results in the solidification and hardening of the porous polymeric microparticles composed of chitosan.

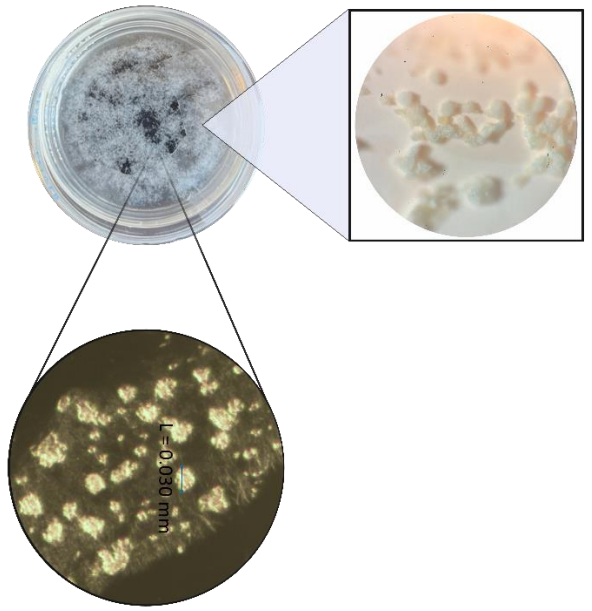
Tentative	Description	Outcome
02	 Conducted in becker according to literature conditions.	Evaporation of petroleum ether. Chitosan clumps.  
03	For the mixing of Span 80/Tween 60 prepare a 10x concentrated mixture to facilitate its addition to petroleum ether.	 Polymer still aggregating and not forming microspheres
04	Increased the stirring speed to 1200 rpm based on similar articles from the same research group	
05	Pre-cooled the phase inversion liquid at -20°C before pouring it into the quenched emulsion, based on similar articles from the same research group.	
06	Filtration and washing with water and ethanol.	
07	30 ml sealed serum bottles to reduce headspace/evaporation. Same conditions as step 2. Water bath for the flask to maintain 40º C.	

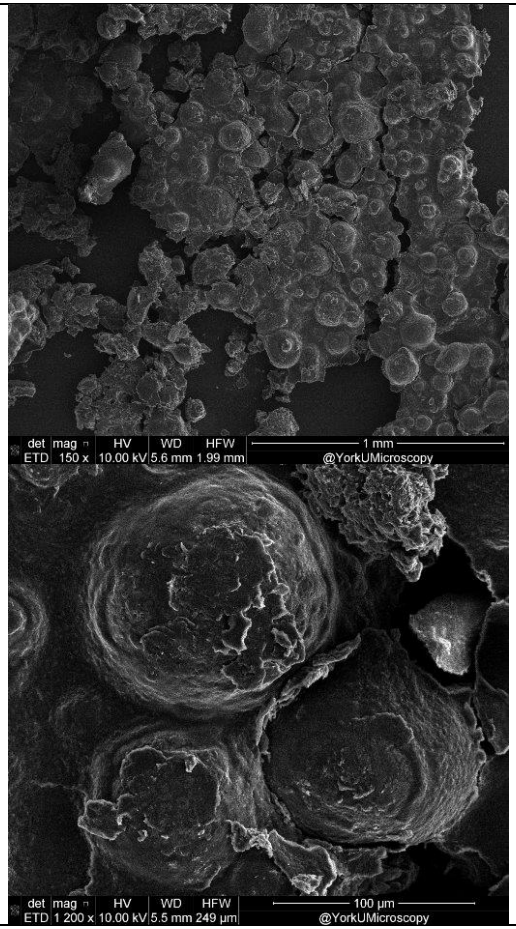
		
08	Tests with lower quenching temperature. Liquid nitrogen (-196 ºC).	
09	30 ml ethanol was added dropwise before the phase inversion liquid (expedite the melting process).	
10	Phase inversion liquid: instead of pouring dropwise (220 ml 1% (w/v) NaOH in 9% (v/v) ethanol in water solution)	
11	Stirring was continued under air-tight conditions overnight.	
12	Separation funnel overnight. Top layer: petroleum ether. The aqueous layer remains at the bottom 	
13	Centrifuge 5000 rpm for 5 min to separate the particles at the top	
14	Better control of the temperature in the water bath. consistent temperature throughout the water bath. Stirring water bath.	Evaporation of petroleum ether

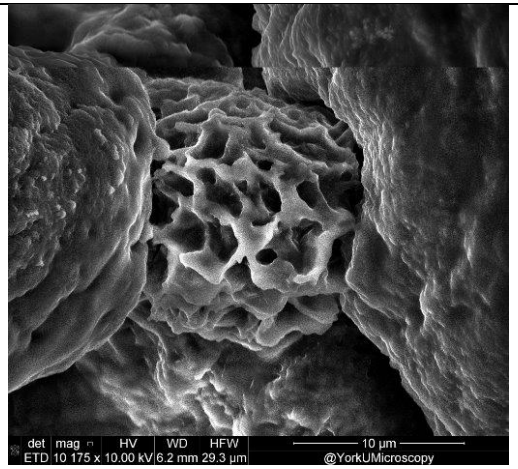
15	Use of a reflux condenser to avoid any type of evaporation. 	
16	Change in chitosan concentration 0.5% (w/v)	Gel-like chitosan formation. 

		
17	W/O emulsion ratio 1:5 W/O emulsion ratio 1:7 Following a three-hour emulsification process, a brief sonication for 5 minutes (40 kHz) was performed	**Ratio 1:5** Islands of particles inside a thin layer.  **Ratio 1:7** Rough and relatively continuous structure

		
18	Emulsification (3hr/40ºC/1200 rpm) → Quenching Liquid nitrogen (10 min) → Phase Inversion (NaOH) solution → Centrifugation → Drying	Formation of chitosan membranes **Ratio 1:5**  **Ratio 1:7** 
19	Emulsification (3hr/40ºC/1200 rpm) → Quenching Liquid nitrogen (10 min) → Phase Inversion (NaOH) solution →	Microscopy analysis confirms the formation of microspheres; however, gel-like chitosan is still

	Centrifugation → Drying	present, which entraps the microspheres. 
20	Emulsification (3hr/40ºC/1200 rpm) → Quenching Liquid nitrogen (10 min) → Phase Inversion (NaOH) solution → Centrifugation → Drying Using chitosan 95.6% DDA	SEM images show the formation of spherical shape particles with porous morphology in comparison with controls.

		det mag HV WD HFW ETD 150 x 10.00 kV 5.6 mm 1.99 mm 1 mm @YorkUMicroscopy det mag HV WD HFW ETD 1 200 x 10.00 kV 5.5 mm 249 µm 100 µm @YorkUMicroscopy	

		
Further research is required to explore the underlying cause of particle adhesion to the thin chitosan layer.		